LONDON WEATHER RADAR
LOCAL CALIBRATION STUDY

FINAL REPORT

LONDON WEATHER RADAR LOCAL CALIBRATION STUDY

FINAL REPORT

by

R. J. Moore, B. C. Watson, D. A. Jones and K. B. Black

This report is prepared for the National Rivers Authority

Thames Region

Institute of Hydrology

September 1989

Executive Summary

A once-in-50-year flood in the London area can cause damage to residential properties approaching £17m. Substantial potential savings exist if timely and accurate warning of imminent flooding can be given. The London Weather Radar Local Calibration Study was initiated in recognition that weather radar data from the Chenies radar serving the London area can contribute to the realisation of these potential savings. Chenies weather radar provides a unique source of information on rainfall variations over London and its surrounding area. This information can be especially valuable for localised summer convective storms which can cause substantial damage but still remain undetected by a conventional raingauge network. However, two serious shortcomings of the Chenies weather radar are that it is calibrated using only 5 raingauges and that the synoptic type dependent domain procedure used introduces temporal and spatial discontinuities in the rainfall estimates supplied.

The main aim of the Study was to use the 30 telemetering raingauges available for the London and Lee Valley area as the basis of a regional recalibration procedure. This would provide more accurate and reliable estimates of spatial rainfall variations, in particular to assist in flood warning operations. Procedures have been developed for the calibration of weather radar based on fitting surfaces to the calibration factor values, conventionally defined as the ratio of raingauge to coincident weather radar grid-square estimates of rainfall. Consideration was given to a wide range of recalibration procedures. A comprehensive program for the assessment of the different calibration methods was developed as the major data-analytic tool for the Study.

The results of the assessment using data from 23 rainfall events are used in this report to recommend procedures for recalibration and raingauge-only rainfall estimation. The recommended recalibration method provides a 22% improvement in accuracy relative to that obtained by the radar without calibration. An additional finding of the Study is a tendency for rainfall estimated by the Chenies radar to decrease by about 50% of its mean intensity as the range from the radar increases from 6 to 70 km: this report recommends that the at-site range correction be reviewed. Despite this failing, the radar even without raingauge calibration is shown to provide better spatial rainfall estimates than can be obtained using the very dense network of raingauges available in the Study area.

The main product of the Study is an operational system for recalibration of Chenies weather radar. The prototype system went operational on 14 March 1989 and has been used in support of flood warning activities since this time. A further procedure for estimating spatial rainfall using raingauges only was implemented in September 1989 to complement the recalibrated product and to replace it in the event that the radar malfunctions.

Acknowledgements

The members of the Steering Committee of the London Weather Radar Calibration Study - Peter Borrows and Chris Haggett (NRA Thames Region) and Chris Collier (Meteorological Office) - are thanked for their varied contributions. In particular, the Study owes a great debt to Chris Haggett who recognised the great potential to be gained from a local radar calibration facility which incorporated raingauge data derived from a regional telemetry network. Peter Borrows, as Chairman of the committee, provided sound advice and encouragement throughout the Study. Chris Collier contributed invaluable technical guidance at Steering Committee meetings as well as supplying internal Meteorological Office material relevant to the Study. Peter Larke, also of the Meteorological Office, has provided much detailed information relating to Chenies radar along with radar data for some early events. Martin Creese and Chris Richards (NRA Thames Region) provided invaluable support to the Study, particularly through supplying radar data and in integrating the calibration software into the NRA Thames Region's operational system for flood warning.

The Study was funded primarily by the NRA Thames Region (originally Thames Water Authority) but enjoyed the benefit of additional support from the Flood Protection Commission of the Ministry of Agriculture, Fisheries and Food via the Institute of Hydrology's strategic research programme on Real-time Flow Forecasting. The Study also forms a contribution to the CEC Project "Applications of Weather Radar for the Alleviation of Climatic Hazards".

Contents

1. Introduction

This document is the final report of a two year study concerned with developing local weather radar calibration procedures for use within the Thames region. The London Weather Radar Local Calibration Study was motivated by the recognition that the weather radar at Chenies which serves the NRA Thames Region is calibrated using only five raingauges. For the London and Lee Valley areas alone, the NRA Thames Region have as many as 35 telemetering raingauges and these could be used at a regional centre to recalibrate the radar to obtain a more accurate and reliable estimate of spatial rainfall variations, in particular to assist in flood warning operations.

An assessment of flood damage suffered by residential properties in the London area alone approaches £17m for floods occuring on average once every 50 years. Substantial savings are possible if timely and accurate warnings of flooding can be made. Such warnings must rely strongly on estimates of rainfall and of its variation over the London area, both now and for a short time in the future. Rainfall's variation over space is particularly important for summer convective storms which can cause highly localised flooding: such storms can remain largely undetected by a conventional network of raingauges but cause much damage. It is in just such situations that weather radar scores highly in providing a complete areal picture of the rainfall field. However, there is a need to make the weather radar product more accurate and reliable through improved calibration using the NRA Thames Region's own network of telemetering raingauges.

This report considers first the data management aspects of the Study which are not inconsiderable given its dependence on weather radar and telemetered raingauge data. The need for quality control of data is emphasised and the effects of blockages in the radar field and range from the radar are identified and discussed (Section 2). Section 3 deals with the general approach adopted in the Study for local calibration and focusses on the use of a calibration factor surface fitting method. A major component of the Study is the formulation of a computer program to rigorously assess the different calibration methods considered: this is described in Section 4. The results of this assessment are presented in Section 5. Transfer of the techniques developed to run operationally within the NRA Thames Region's regional flood warning centre was an essential objective of the Study. The final procedures recommended for operational implementation are also presented in Section 6 together with the major conclusions of the Study.

Three appendices provide details of the site descriptions of the calibration raingauges, the synoptic conditions associated with the storm events and the multiquadric surface fitting techniques used in the Study.

2. Data Management

2.1 RAINGAUGE AND RIVER LEVEL DATA

A total of 35 raingauges in the London area and the Lee Valley are available to form the basis for an operational system for calibrating radar data derived from the Chenies radar installation (Figure 2.1.1). Appendix I provides details of the raingauge sites concerned. The network of telemetering raingauges transmit rainfall counts every 15 minutes with a resolution of 0.2 mm. In addition, river flows are estimated at 38 locations from measurements of river level also transmitted at intervals of 15 minutes. These data are archived on the VAX 11/750 minicomputer at the Thames Barrier and are sent routinely to IH on magnetic tape along with weather radar data.

Data from the 20 London raingauges date back to late 1985 but data from the Lee Valley raingauges are only available from 12 October 1987 via the VAX.

A change in operating procedure has meant that the the two London gauges at Oakwood Park and Green Lanes have now been designated as Lee Valley gauges. Originally 0.5 mm tipping-bucket raingauges were deployed but now these have all been changed to have a 0.2 mm bucket. The problem of timing errors associated with these raingauge data is discussed later in Section 2.4.3. Missing data are infilled where possible by the NRA Thames Region's data acquisition system using the number of tips recorded at the start and end of a day.

2.2 WEATHER RADAR DATA

Weather radar data along with calibration information are received by the VAX computer at the Thames Barrier in real-time. These data have a 5 minute 2 km resolution out to a range of 76 km from the Chenies weather radar installation. They are archived and sent routinely once a month to IH on magnetic tape. IH has developed software to read these data and to remove the at-site calibration using the calibration information provided. Similar software has been developed to read the Meteorological Office's own at-site radar tapes and to store them on disk in the format in use by the NRA Thames Region.

The calibration information provided includes the one hour total rainfall for each of the 5 at-site calibration raingauges. These are provided every 15 minutes and relate to the previous hour's rainfall. Use of these data in the Local Calibration Study has been avoided because of problems of data transmission to Chenies radar site via the NRA Thames Region's Ferranti Argus at Reading.

During the first year of this Study, the Meteorological Office became aware of a consistent bias in the Chenies weather radar measurent of rainfall prior to

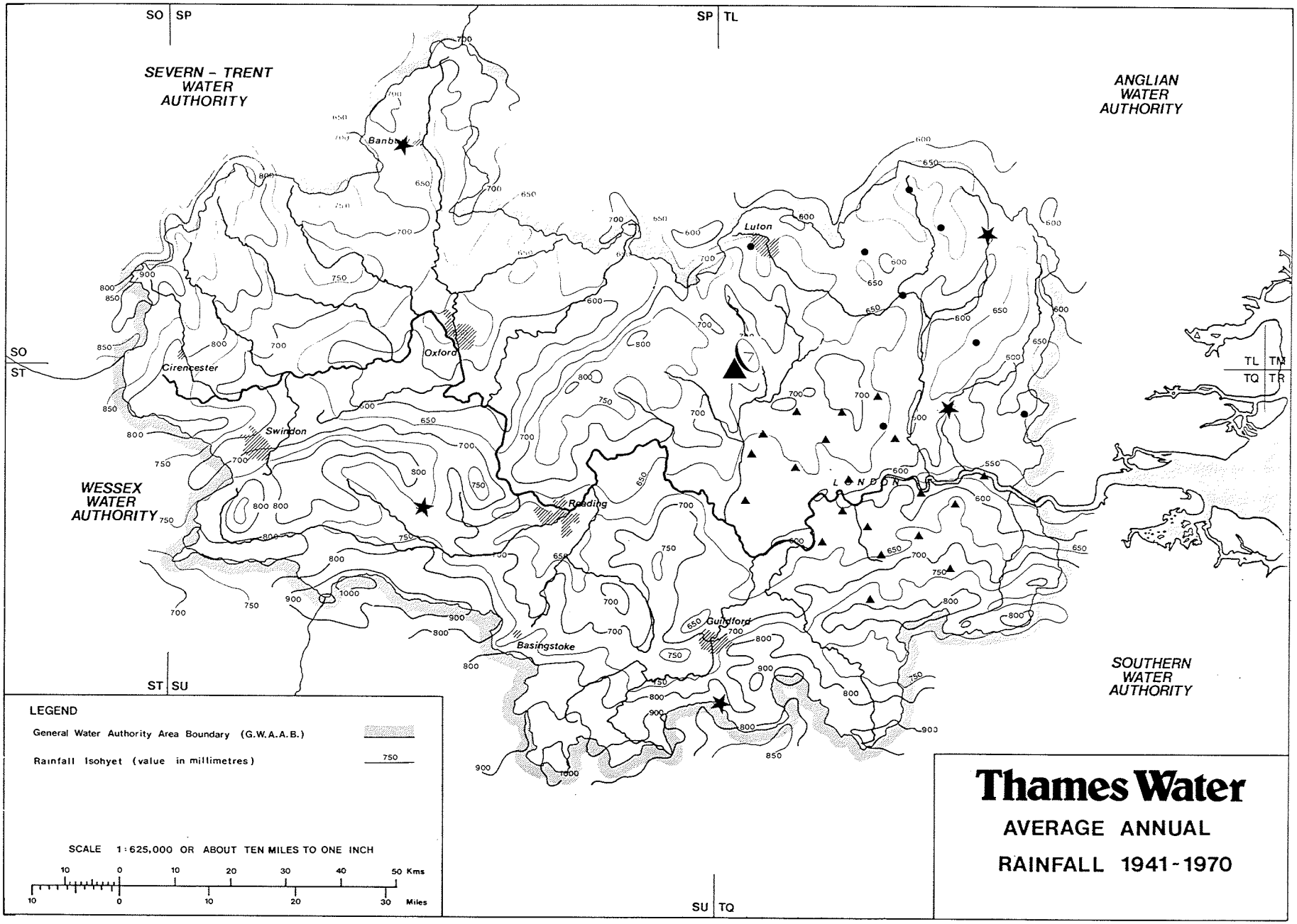

Based upon the Ordnance Survey 1:625,000 map with the permission of the Controller of Her Majesty's Stationery Office. Crown Copyright Reserved.

Prepared by Thames Water, Cartographic Services, Reading, 1986.

*Figure 2.1.1 Raingauge locations and average annual rainfall for the Thames Water study region (Δ London raingauges; ● Lee Valley raingauges; * Meteorological office raingauges).*

raingauge calibration. Following studies by the Meteorological Office and IH (at the request of NRA Thames Region) a decision was made to apply a factor of 2 to the radar rainfall measurement prior to at-site calibration: this was implemented at 10.30 23 February 1988. To ensure consistency across data sets a factor of 2 is applied to the "decalibrated" radar fields for all radar data held at IH prior to this time.

2.3 EVENT SELECTION

A database suitable for developing calibration procedures has been constructed from data for a number of storm events. Events were first identified using river level records in conjunction with raingauge data. A criterion was later introduced to help event identification: this highlights events for which at least one of the raingauges records more than 30 mm in a day (9 am to 9 am). A further four events were selected in 1989 based on selecting the time-frames giving the highest 15 minute average rainfall as computed from the raingauge data: this was intended to identify events with more widespread rainfall. Radar and raingauge data have been used to define the beginning and end of each event. The 32 storm events held in the database are summarised in Table 2.3.1. Of these events 23 (Table 2.3.2) have been chosen for inclusion for developing calibration procedures: these are mainly later events for which more raingauge data are available and where timing errors are less. Daily Weather Summaries supplied by the Meteorological Office have been used to describe the events: these synoptic descriptions are included as Appendix II to this report.

A special database has been set up in order to use data across a large number of events for a single analysis in a compact and efficient way. This contains only data for 15 minute intervals for each raingauge, and radar data for its coincident radar grid square, either as the value for that square or averages for its neighbourhood (see Section 3.3).

2.4 DATA QUALITY ASSURANCE

2.4.1 Introduction

As an essential first step of the study, careful consideration was given to quality control of data prior to analysis. Two main procedures were developed to reveal anomalies in the data, one based on identifying anomalies over space by forming a time-averaged radar rainfall field and the other based on identifying anomalies within shorter time periods by comparison of raingauge and radar time series. These procedures are described below. The section ends with an investigation of the effects of range from the radar on measured rainfall amounts.

Table 2.3.1 Events used to form an overall radar average rainfall field

Event Number	Start Time		End Time	
1	11.05	29 March 1986	22.45	29 March 1986
2	02.20	20 May 1986	20.00	20 May 1986
3	13.35	08 July 1986	21.30	08 July 1986
4	09.05	03 August 1986	22.45	03 August 1986
5	18.35	10 August 1986	23.00	10 August 1986
6	10.05	25 August 1986	09.00	26 August 1986
7	05.50	04 January 1987	21.30	04 January 1987
8	23.50	07 June 1987	09.00	09 June 1987
9	09.15	06 October 1987	09.00	10 October 1987
10	18.15	20 October 1987	02.00	21 October 1987
11	10.00	11 November 1987	06.00	12 November 1987
12	10.50	15 March 1988	20.45	15 March 1988
13	13.20	20 March 1988	04.00	21 March 1988
14	08.05	29 March 1988	10.00	30 March 1988
15	19.05	18 April 1988	23.45	18 April 1988
16	01.20	08 May 1988	23.45	08 May 1988
17	16.05	08 June 1988	09.00	09 June 1988
18	10.15	30 June 1988	16.45	30 June 1988
19	08.05	02 July 1988	21.00	02 July 1988
20	08.05	03 July 1988	22.00	03 July 1988
21	00.05	04 July 1988	21.45	04 July 1988
22	07.05	06 July 1988	14.00	06 July 1988
23	15.35	16 July 1988	08.30	17 July 1988
24	17.05	21 July 1988	23.45	21 July 1988
25	21.05	22 July 1988	03.15	23 July 1988
26	01.45	31 August 1988	13.15	31 August 1988
27	22.15	31 August 1988	14.30	01 September 1988
28	04.00	17 February 1989	15.30	17 February 1989
29	14.15	26 February 1989	22.00	26 February 1989
30	08.30	14 March 1989	23.00	14 March 1989
31	16.15	20 March 1989	00.45	21 March 1989
32	11.00	24 May 1989	23.00	24 May 1989

Table 2.3.2 Events used for calibration and evaluation

Event Number	Start Time		End Time	
9	09.15	06 October 1988	09.00	10 October 1987
10	18.15	20 October 1988	02.00	21 October 1987
11	10.00	11 November 1987	06.00	12 November 1987
12	10.50	15 March 1988	20.45	15 March 1988
13	13.20	20 March 1988	04.00	21 March 1988
14	08.05	29 March 1988	10.00	30 March 1988
15	19.05	18 April 1988	23.45	18 April 1988
16	01.20	08 May 1988	23.45	08 May 1988
17	16.05	08 June 1988	09.00	09 June 1988
18	10.15	30 June 1988	16.45	30 June 1988
19	08.05	02 July 1988	21.00	02 July 1988
20	08.05	03 July 1988	22.00	03 July 1988
21	00.05	04 July 1988	21.45	04 July 1988
22	07.05	06 July 1988	14.00	06 July 1988
23	15.35	16 July 1988	08.30	17 July 1988
24	17.05	21 July 1988	23.45	21 July 1988
25	21.05	22 July 1988	03.15	23 July 1988
26	01.45	31 August 1988	13.15	31 August 1988
27	22.15	31 August 1988	14.30	01 September 1988
29	14.15	26 February 1989	22.00	26 February 1989
30	08.30	14 March 1989	23.00	14 March 1989
31	16.15	20 March 1989	00.45	21 March 1989
32	11.00	24 May 1989	23.00	24 May 1989

2.4.2 Time-average radar rainfall fields

Average rainfalls during the course of an event, and averaged across all (32) events, were calculated from the decalibrated radar data and used to obtain time-average radar rainfall fields. Examples of these are shown in Figure 2.4.1. Several features are present in more than one event, suggesting that they are connected with permanent echoes caused by the beam intercepting an object or high ground. Any blockage in the beam will cause a decrease in the beam width and a reduction in inferred rainfall intensity will result. This constrasts with clutter caused by obstructions which will increase the returned signal. Corrections for blockages and clutter are made at the radar site but the anomalies shown in Figure 2.4.1 indicate that the adjustment is not perfect. Figure 2.4.2, provided by the Meteorological Office, provides an explanation for these anomalies in terms of masts, pylons and cables. Cables between pylons when wet will cause the sector of the radar field affected to overestimate rainfall. Rainfall intensities are also higher in the vicinity of the radar due to infilling of the 0.5 degree beam data with data from the 1.5 degree beam; at short range physical properties of the radar and its antenna also affect the return signal and there is no range correction. Anomalies in the south-east corner of the field arise from interference from a second radar located in France.

(a) 9:15 19 May 1986 to 9:00 21 May 1986

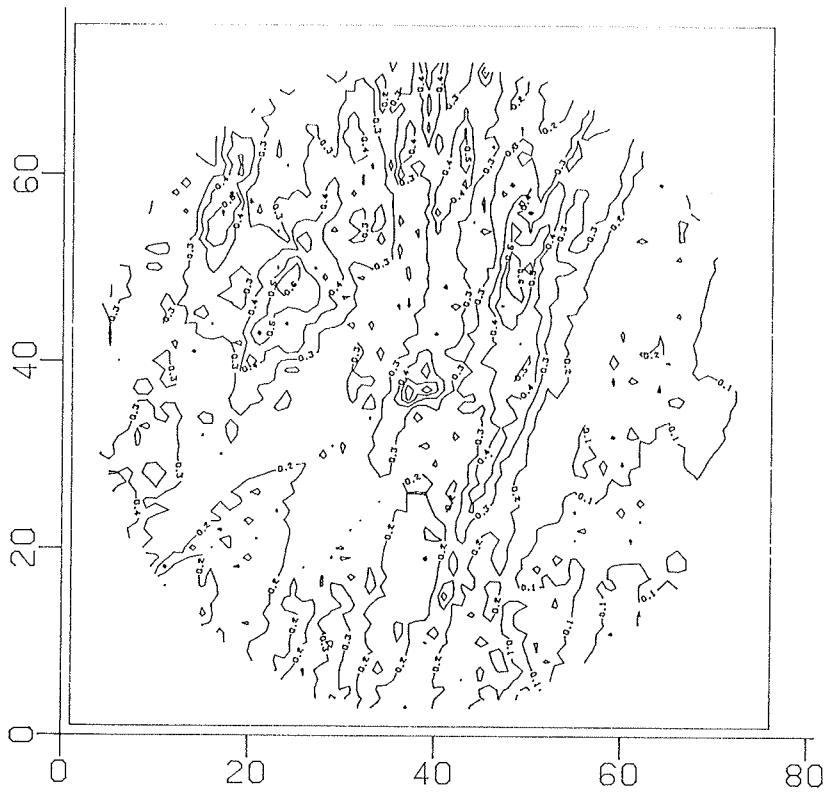

(b) 9:30 25 August 1986 to 0:15 26 August 1986

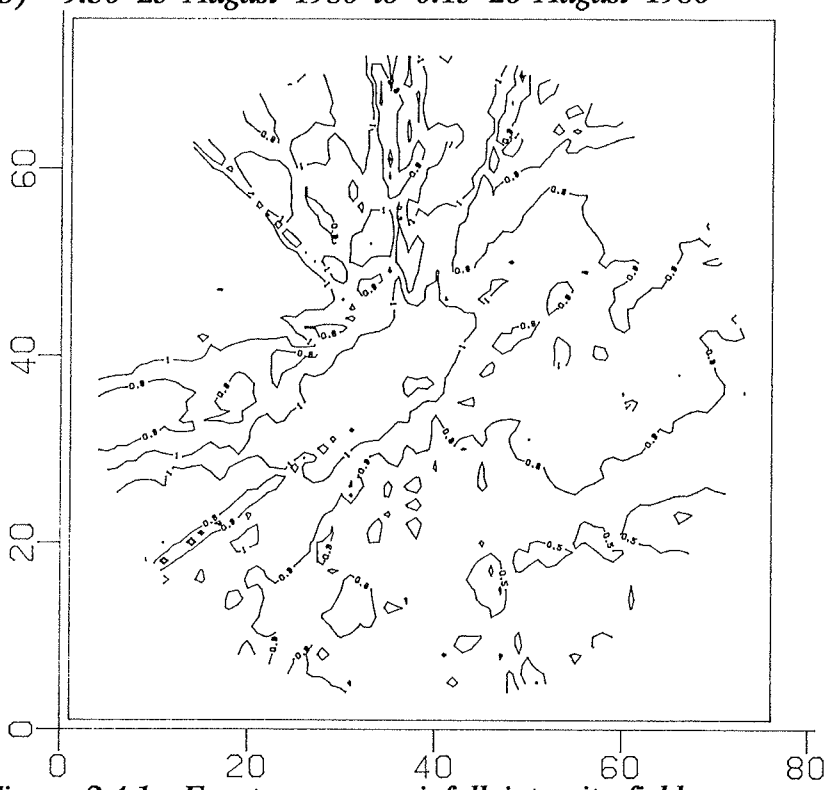

Figure 2.4.1 Event average rainfall intensity fields

(c) 9:15 3 January 1987 to 9:00 5 January 1987

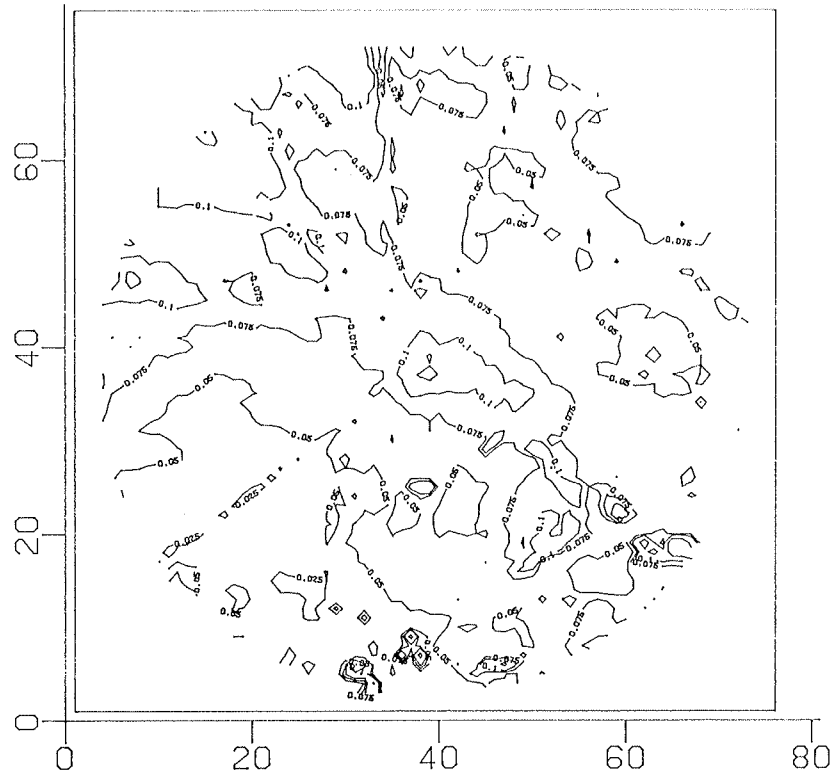

(d) 9:05 7 June 1987 to 9:00 9 June 1987

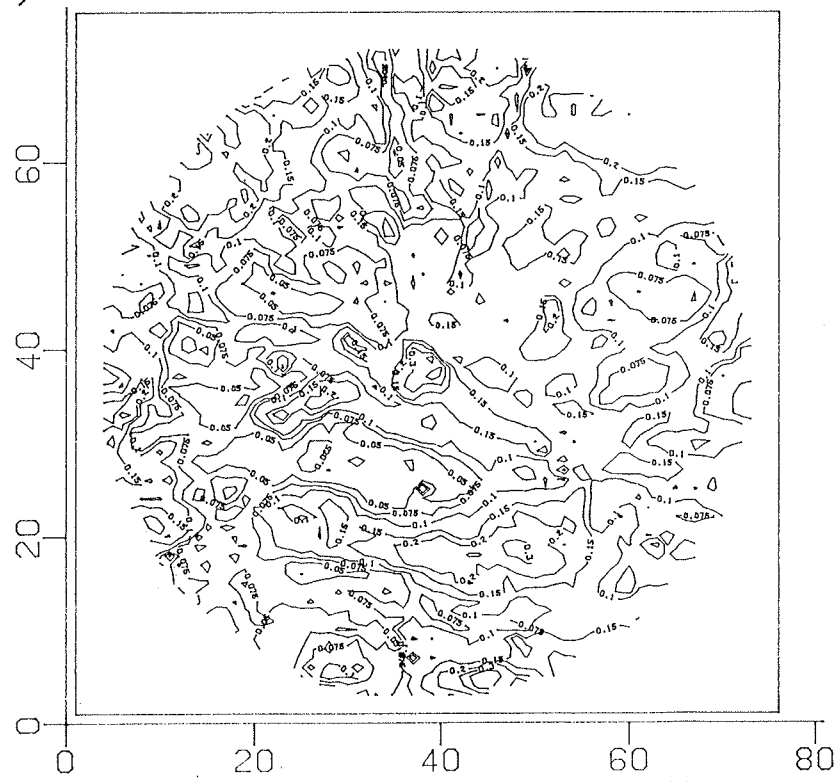

Figure 2.4.1 Event average rainfall intensity fields

(e) 00.00 20 March 1988 to 23:55 20 March 1988

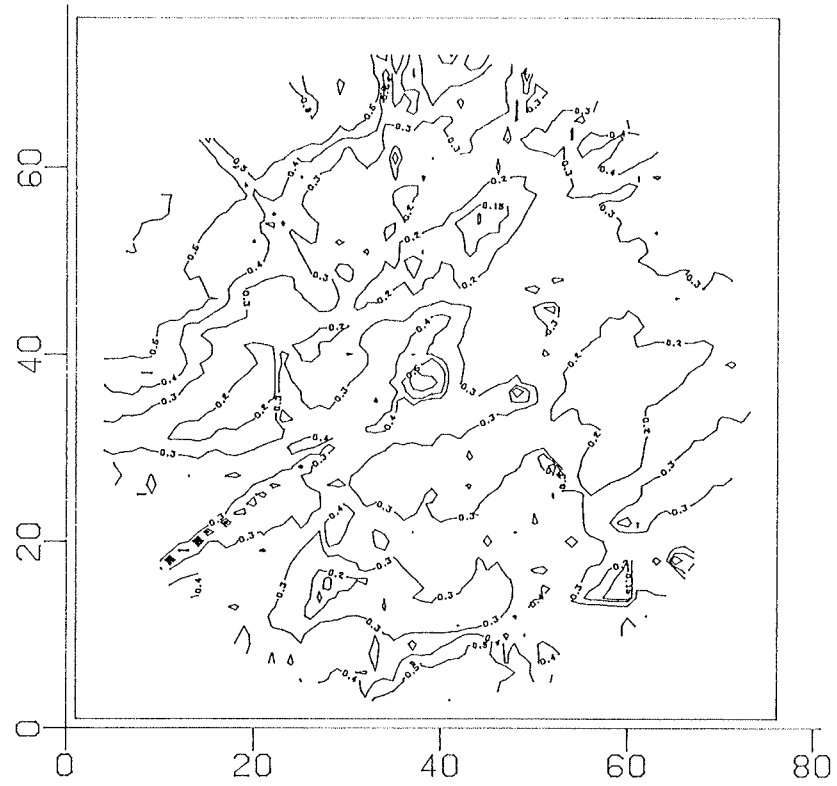

(f) 00:00 8 May 1988 to 23:45 8 May 1988

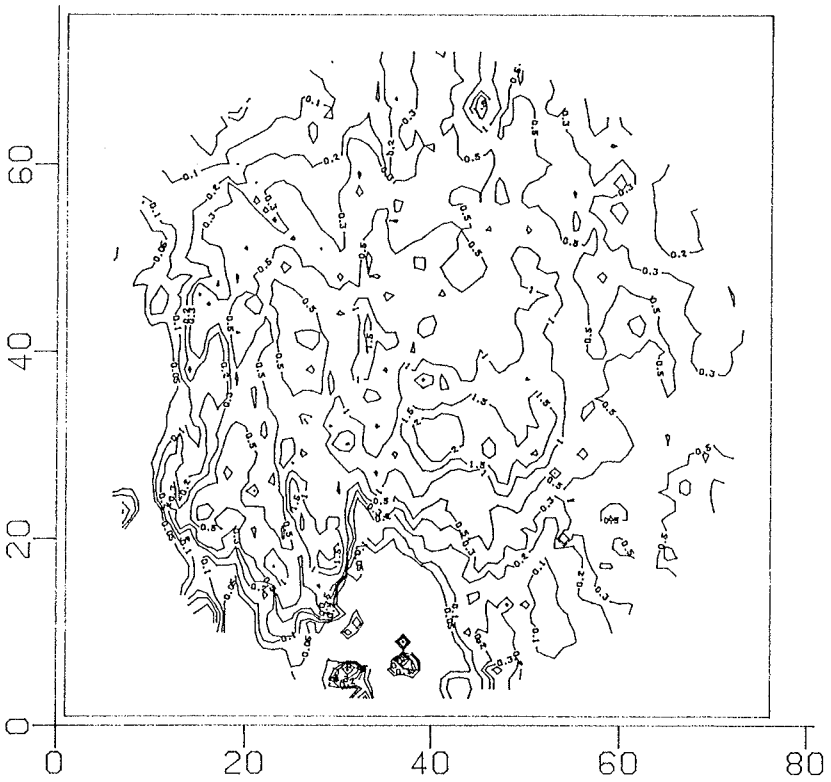

Figure 2.4.1 Event average rainfall intensity fields

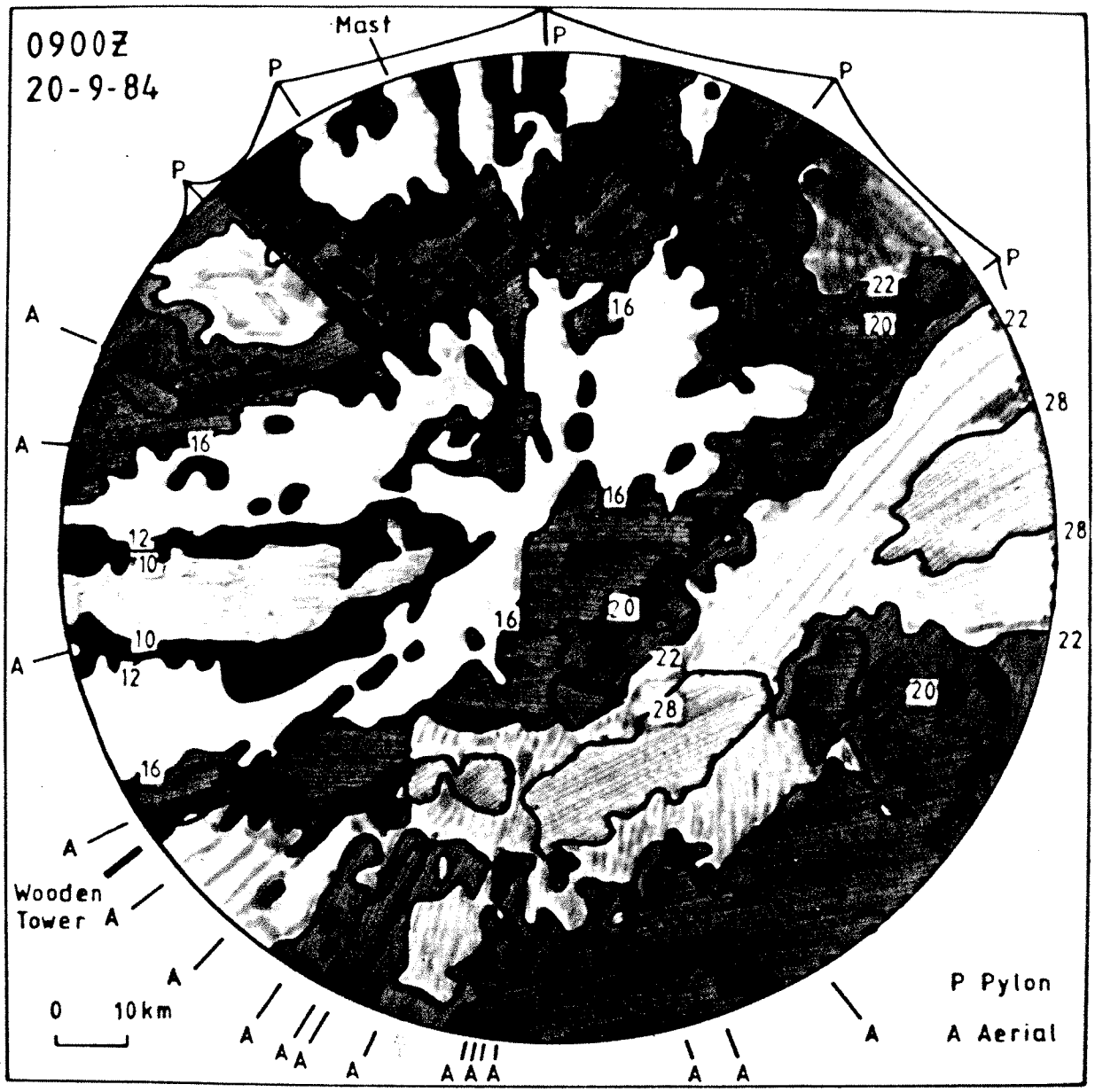

Figure 2.4.2 Average rainfall intensity field for the day ending 09.00 hr 20 September 1984 provided by the Meteorological Office indicating causes of anomalies

The locations of the anomalous spokes and other features have been looked at in relation to the location of the 35 raingauges to be used for local calibration. A time-average rainfall field obtained from radar data across all 32 events is shown in Figure 2.4.3. Fortunately none of the raingauge sites are located in a significantly anomalous area and therefore all raingauges can be safely used for local calibration.

2.4.3 Comparison of raingauge and radar rainfall values

Simple time series plots of raingauge and coincident radar data were used to validate the relative timing of these data. Unfortunately these revealed timing errors between the two data sets (Figure 2.4.4). The cause of this is attributed principally to the Dynamic Logic raingauge telemetering outstations: some outstations are more reliable than others at different times. Replacement of outstations occurred during the Study and is now complete with the new equipment supplying more reliable data.

The main error identified is a 30 minute shift in all values recorded between 09.00 hr and 01.30 hr the following day. Whilst a correction has been correctly applied by NRA Thames Region in some cases this has not always been the case. Clock drift by up to 3 minutes in a day can also cause rainfall to be assigned to the wrong timeframe.

Another source of timing error arises from the mode of retrieval of data at the end of a day. Normally raingauge data for a day starts to be retrieved at 09.18 hr following logging of the raingauge count for 09.15 hr. Sometimes the daily retrieval occurs before the 09.15 hr gauge reading is complete and then data for the day will be stored 15 minutes out of phase. This problem is less likely to arise from the new outstations.

Software was specially developed to detect these discrepancies and correct for them. Plots of the raingauge and coincident radar data presented as time series, cross-correlation functions, and scatter plots at different timestep lags were used to identify the time shifts required. The nature of the timing errors described above meant that two separate assessments per day had to be made for every raingauge.

Table 2.4.1 provides an indication of the reliability of raingauge data and how this has changed over time. Information relating to which gauges failed to operate or for which data from them are suspect is presented in Table 2.4.2 for the events used for assessment.

2.4.4 Range studies

Time-average rainfall fields were found in Section 2.4.2 to be very useful in drawing out anomalies in the weather radar data field. Another way of revealing anomalies using the average properties of a rainfall intensity field is to focus on the variation in the mean and variance of the grid cell values as the range from the radar site is increased.

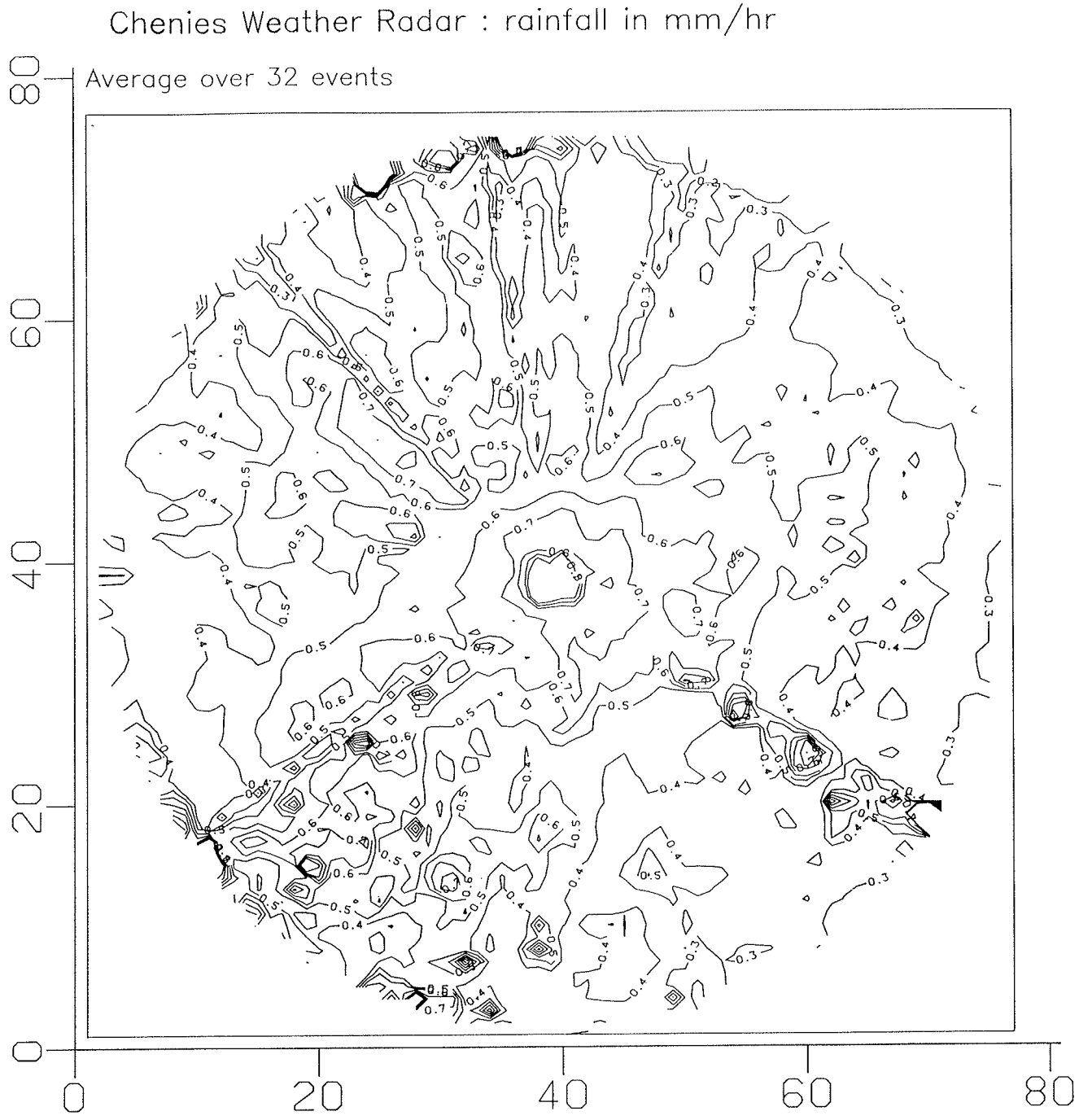

Figure 2.4.3 Average rainfall intensity field averaged across 32 events

(a) Eltham High Street 11.00 to 20.45 hr 15 March 1988

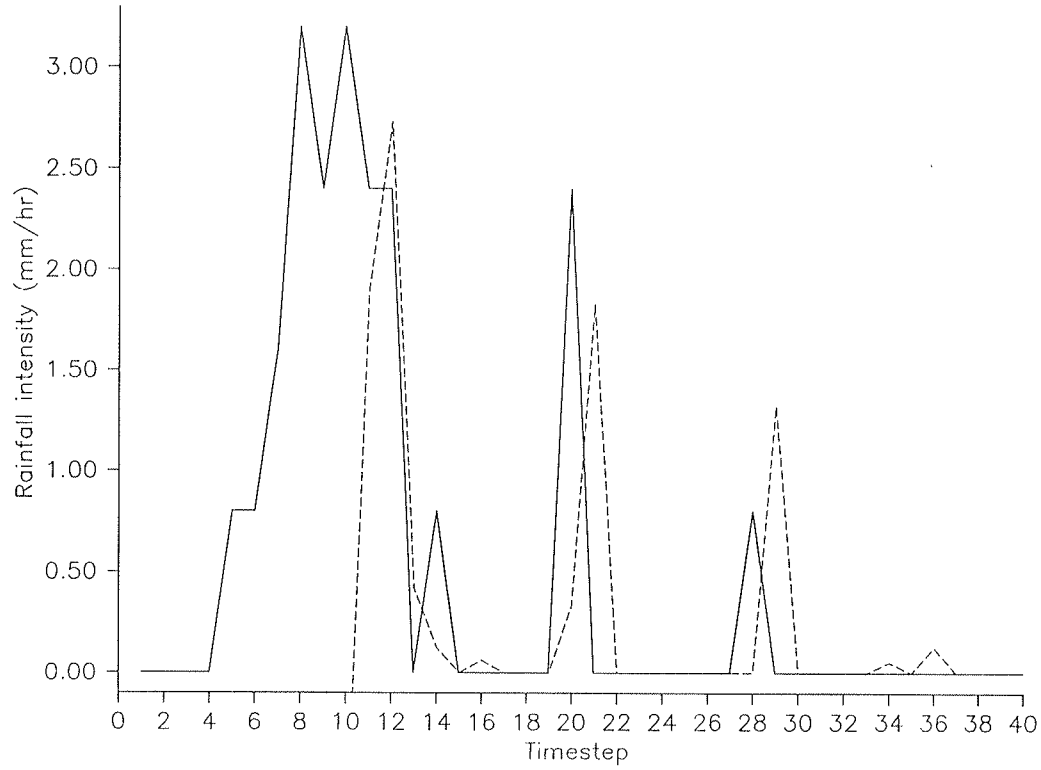

(b) Brent Reservoir 17.15 to 23.45 hr 21 July 1988

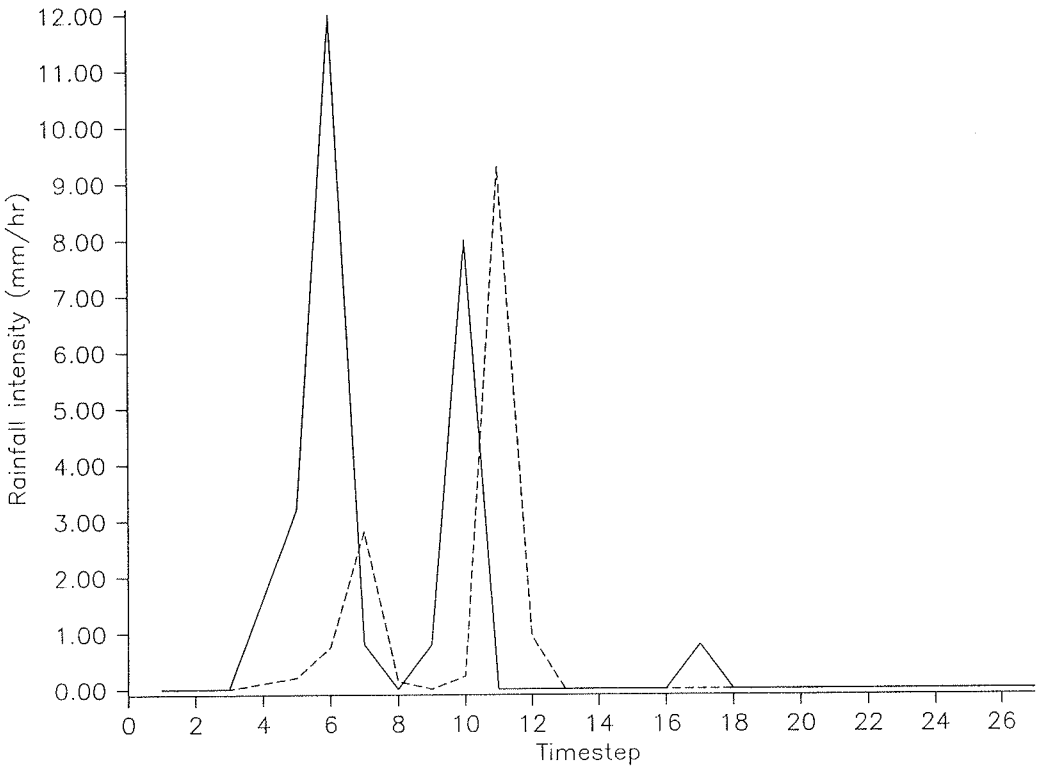

Figure 2.4.4 Time series plots of raingauge and radar rainfall values showing timing errors

Table 2.4.1 Raingauges used in the study and inventory of changes to outstations

Gauge	30 min. shift necessary	Outstation modified	New outstation installed
1 Crossness STW	Until Nov. 1987	November 1987	by April 1989
2 Eltham High Street	"	"	"
3 Deptford PS	"	"	"
4 Keston	"	"	"
5 Kelsey Park	"	"	"
6 Beddington STW	Until Dec 1988	-	December 1988
7 Putney Heath Reservoir	"	-	"
8 Furzedown Rec.	"	-	"
9 How Green Reservoir	"	-	"
10 Hogsmill Valley STW	"	-	"
11 Perry Oaks	"	-	"
12 Uxbridge (Hillingdon Court Park)	"	-	"
13 Ruislip Manor	Until April 1989	-	by April 1989
14 Harrow Weald Cemetery	Until Dec. 1988	-	December 1988
15 Mill Hill Cemetery	"	-	"
16 Green Lanes	"	-	"
17 Holland Park	"	-	"
18 Greenford Cemetery (Ealing)	"	-	"
19 Oakwood Park	"	-	"
20 Brent Reservoir	Until Nov. 1987	November 1987	by April 1989
21-30 Lee Valley Gauges	All data should be reliable		

If x_{ijt} denotes the radar value for the (i,j) grid cell at timeframe t then the mean $\bar{x}(d)$ and variance $\sigma^2(d)$ at a given distance d averaged over an event can be computed from the grid cell radar values $\{x_{ijt}$, i=1,2,...,m; j=1,2,...,n; t=1,2,...,T$\}$ as follows:

$$x_{ij} = \frac{\sum_{t=1}^{T} x_{ijt}}{T} \qquad (2.4.1a)$$

$$\bar{x}(d) = \frac{\sum_{i,j \in d}^{N_d} x_{ij}}{N_d} \qquad (2.4.1b)$$

$$\sigma^2(d) = \frac{\sum_{i,j \in d}^{N_d} (x_{ij} - \bar{x}(d))^2}{N_d} \qquad (2.4.1c)$$

Table 2.4.2 Missing and suspect raingauge data

	Event	Period			Gauges for which no data are available	Gauges for which data are suspect
1	Oct 1987a	09.15 6/10/87	- 09.00	10/10/87	15,21-30	16
2	Oct 1987b	18.15 20/10/87	- 02.00	21/10/87	15,17,18,21-30	16
3	Nov 1987b	10.00 11/11/87	- 06.00	12/11/87	15,17,20,21-30	14
4	Mar 1988a	11.00 15/3/88	- 20.45	15/3/88	15,17,21,23,25,26,27,29	-
5	Mar 1988b	13.30 20/3/88	- 04.00	21/3/88	15,17,21,23,25,26,27,29	20
6	Mar 1988c	08.15 29/3/88	- 10.00	30/3/88	10,15,17,21,23,26,27,29	-
7	Apr 1988a	17.00 18/4/88	- 23.45	18/4/88	8,15,17,21,23,26,27,29	-
8	May 1988	01.30 8/5/88	- 23.45	8/5/88	12,15,21,23,26,29	30
9	Jun 1988a	16.15 8/6/88	- 09.00	9/6/88	15,21,23,26,29	30
10	Jun 1988b	10.15 30/6/88	- 16.45	30/6/88	15,18,21,23,26,29	-
11	July 1988a	08.15 2/7/88	- 21.00	2/7/88	15,21,23,26,29	-
12	July 1988b	08.15 3/7/88	- 22.00	3/7/88	15,21,23,26,29	-
13	July 1988c	00.15 4/7/88	- 21.45	4/7/88	15,21,23,26,29	-
14	July 1988d	07.15 6/7/88	- 14.00	6/7/88	3,15,21,23,26,29	-
15	July 1988e	15.45 16/7/88	- 08.30	17/7/88	2,15,21,23,26,29	-
16	July 1988f	17.15 21/7/88	- 23.45	21/7/88	2,15,21,23	-
17	July 1988g	19.15 22/7/88	- 03.15	23/7/88	2,15,21,23	-
18	Aug 1988a	01.45 31/8/88	- 13.15	31/8/88	15,21,23,25	-
19	Aug 1988b	22.15 31/8/88	- 14.30	1/9/88	15,21,23,25	-
20	Feb 1989b	14.15 26/2/89	- 22.00	26/2/89	15	-
21	Mar 1989a	08.30 14/3/89	- 23.00	14/3/89	15	-
22	Mar 1989b	16.15 20/3/89	- 00.45	21/3/89	15	-
23	May 1989a	11.00 24/5/89	- 23.00	24/5/89	-	-

where N_d is the number of grid cells at a distance d from the radar site.

The mean and standard deviation of the radar rainfall at given distances from the radar have been computed using the above formulae for a selection of events: these are displayed in Figure 2.4.5. Figure 2.4.6 shows the result when the formulae are applied across all 32 events in the database. Mean rainfall is seen generally to decrease with increasing distance from the radar whilst the standard deviation shows little consistent pattern. There is also a tendency for rainfall to increase again beyond about 70 km and this effect is also discernible around the edge of the average rainfall intensity field shown in Figure 2.4.3. This increase is due to only the last few events in 1989 having data out to this range, as a result of a modification to the at-site software, and is best ignored.

(a) 02.20 to 20.00 20th May 1988

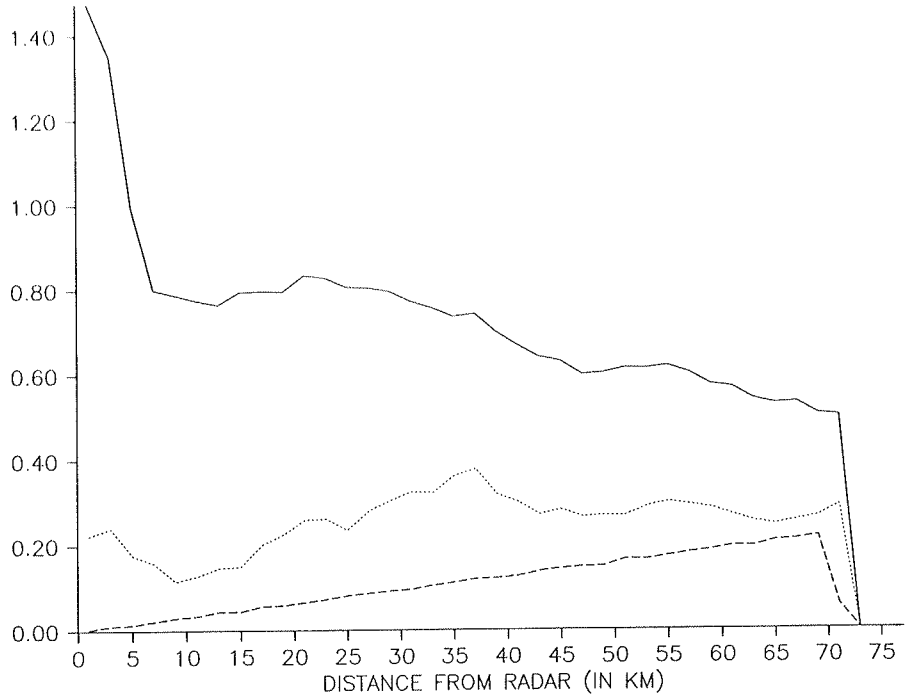

(b) 01.20 to 23.45 8 May 1988

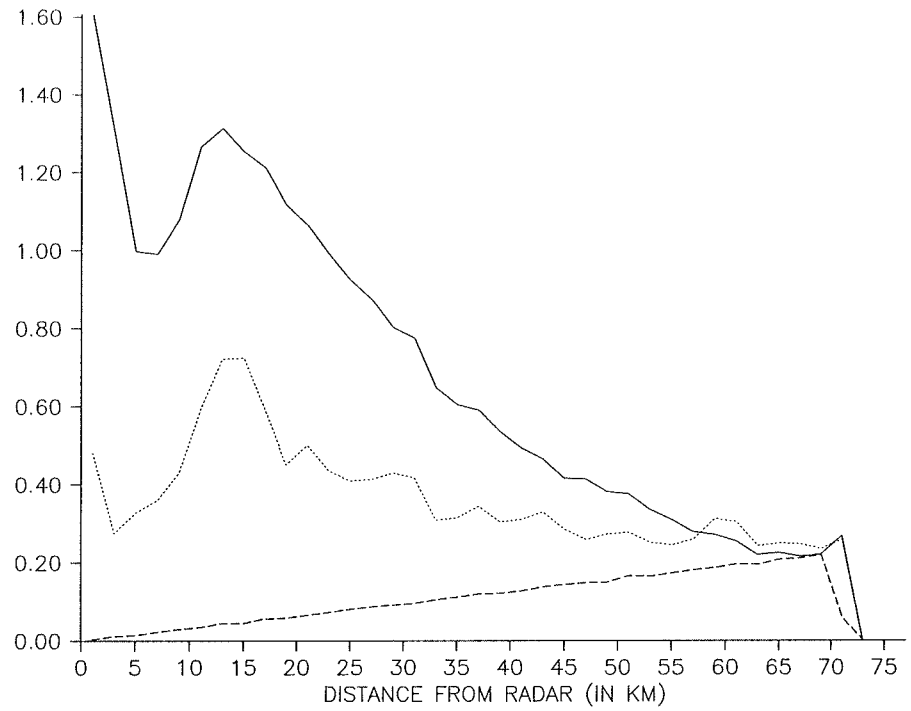

Figure 2.4.5 Event average radar fields as a function of distance (solid line: average rainfall (mm/hr); short dashes: standard deviation between cells at same distance; long dashes: number of contributing cells divided by 1000).

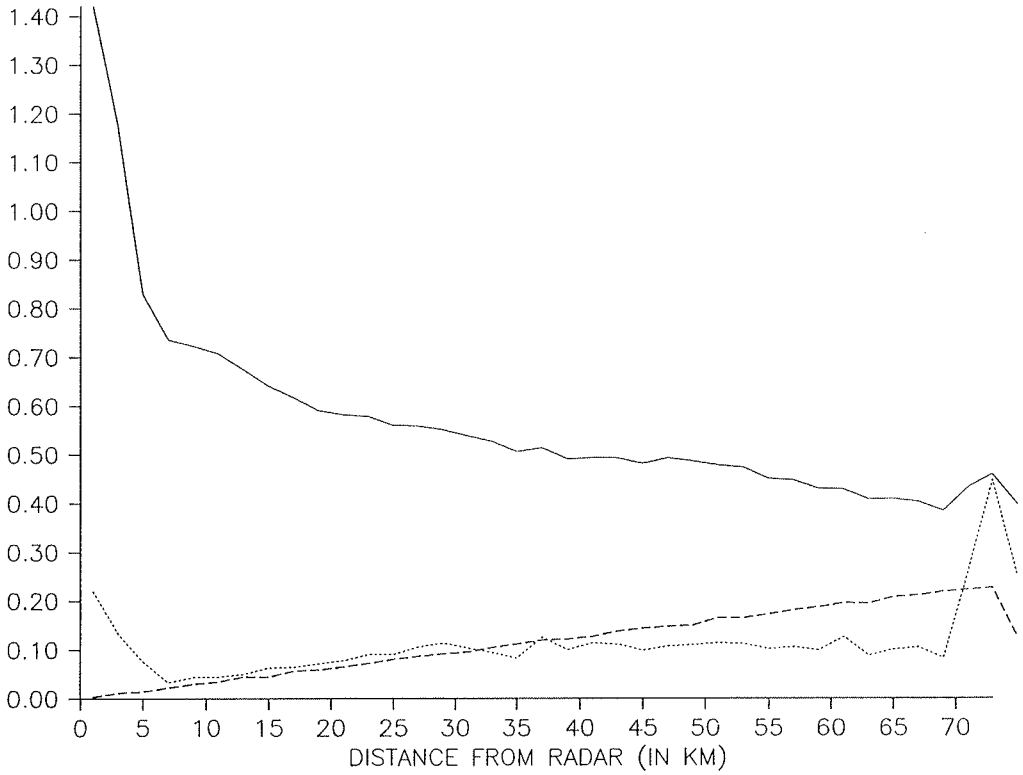

Figure 2.4.6 Radar rainfall as a function of distance from radar averaged over 32 events (solid line: average rainfall (mm/hr); short dashes: standard deviation between cells at same distance; long dashes: number of contributing cells divided by 1000).

Note that the abrupt increase in both mean and standard deviation at a distance of 6 km in Figure 2.4.5b indicates that a small number of grid cells are responsible for the peak in the mean intensity, indicating an isolated peak in the average radar field. This is consistent with a stationary convective cell observed for this particular storm event. A dominant feature in all the plots is the abrupt increase in mean rainfall within about 6 km of the radar, which is consistent with the overestimation of rainfall observed in the time-average rainfall intensity fields (Section 2.4.2). The number of grid cell values used to estimate the mean and standard deviation statistics at each distance are displayed in the figures to provide an indication of the relative accuracy of these sample statistics.

Whilst a correction for range is made at the radar site these results indicate substantial scope for improvement. The introduction of range as an explanatory variable in the multiquadric surface fitting method is discussed in Sections 3.5.3 and 5.2.4.

3. Weather Radar Calibration Methods

3.1 INTRODUCTION

The problem of weather radar calibration is essentially to develop a procedure to merge grid-square radar estimates of rainfall with a set of point estimates obtained from a raingauge network to obtain a better estimate of spatial rainfall than can be provided by either raingauges or radar used alone. This problem is being tackled by first forming calibration factors from raingauge and coincident radar grid values of rainfall and then fitting a smooth surface to these factors. The calibration factor field can then be applied to the radar rainfall field to derive a calibrated rainfall field which effectively combines raingauge and radar data. This approach has meant consideration of the following sub-problems:

(i) calibration factor definition;

(ii) location error adjustment;

(iii) raingauge quantisation error; and

(iv) calibration factor surface fitting techniques.

These are discussed in turn in this section whilst a framework for assessing the different procedures presented is outlined in Section 4.

3.2 CALIBRATION FACTOR DEFINITION

The calibration factor may be defined in the conventional manner as the ratio of the raingauge total over an interval of time, R_g, to the radar total, R_r, for the radar grid-square coincident with the gauge location; that is

$$c = R_g/R_r. \qquad (3.2.1)$$

However, this is undefined when R_r is zero and $R_g>0$. This can be a commonplace occurrence when dealing with data at 15 minute intervals. Several new definitions of the calibration factor have been developed to overcome this problem. They are

(i) Standard calibration factor

$$c = (R_g + \epsilon_g)/(R_r + \epsilon_r) \qquad (3.2.2)$$

where ϵ_g and ϵ_r are constants;

(ii) Reciprocal calibration factor

$$c = (R_r + \epsilon_r)/(R_g + \epsilon_g) \tag{3.2.3}$$

where ϵ_r and ϵ_g are constants;

(iii) Difference calibration factor

$$c = R_g - R_r ; \tag{3.2.4}$$

(iv) Trimmed standard ratio calibration factor

$$c = \begin{cases} u & R_r = 0 \text{ or } R_g/R_r > u \\ R_g/R_r & \text{elsewhere} \\ \ell & R_g/R_r < \ell \end{cases} \tag{3.2.5}$$

where ℓ and u are the lower and upper trimming limits;

(v) Trimmed reciprocal ratio calibration factor

$$c = \begin{cases} u & R_g = 0 \text{ or } R_r/R_g > u \\ R_r/R_g & \text{elsewhere} \\ \ell & R_r/R_g < \ell \end{cases} \tag{3.2.6}$$

where ℓ and u are the lower and upper trimming limits;

(vi) Logarithmic calibration factor

$$c = \log\{(\epsilon_g + R_g)/(\epsilon_r + R_r)\} \tag{3.2.7}$$

where ϵ_g and ϵ_r are constants;

(vii) Modified logarithmic calibration factor

$$c = \begin{cases} \log(R_g/r_0) + 1 - R_r/r_0 & R_g > r_0 \text{ and } R_r \leq r_0 \\ \log(R_r/r_0) - 1 + R_g/r_0 & R_r > r_0 \text{ and } R_g \leq r_0 \\ \log(R_g/R_r) & R_g, R_r > r_0 \\ R_g/r_0 - R_r/r_0 & R_g, R_r \leq r_0 \end{cases} \tag{3.2.8}$$

where r_0 is a non-zero constant. This formulation is based on a modified form of the logarithmic curve which, as well as being defined for all values of R_g and R_r, behaves smoothly, each section of the curve having the same slope, $1/r_0$, at the point of intersection $R. = r_0$. When both R_g and R_r are greater than r_0 the calibration factor has the straightforward form of being the

logarithm of the ratio of R_g to R_r.

The values for the constants involved in the above expressions are obtained by optimisation using the assessment of calibration performance set out in Section 4.

3.3 LOCATION ERROR ADJUSTMENT

Radar grid-square averaging procedures have been developed to compensate for a raingauge not being representative of the coincident radar grid square, for example due to wind drift or a location towards the edge of the square. Averages of the radar values for squares in the neighbourhood of the gauge are used in place of the coincident grid-square value when forming the calibration factors. Four methods are considered:

(i) **one-grid method**: use of the radar value for the grid-square coincident with the raingauge;

(ii) **nine-grid selected neighbours method**: use of the average of one, two or four grid-square values in the neighbourhood of the raingauge depending on the location of the gauge in the grid-square (Figure 3.3.1a);

(iii) **four-grid selected neighbours method**: use of four grid-square values in the neighbourhood of the gauge, which four depending on which quadrant of the square the gauge is located (Figure 3.3.1b); and

(iv) **nine-grid method**: use of the average of all nine radar rainfall values for the grid-squares containing the gauge and surrounding it.

3.4 RAINGAUGE QUANTISATION ERROR ADJUSTMENT

Raingauge values derive from a count of the number of tips of a tipping-bucket made over an interval of 15 minutes. Consequently values may be in error by ± 2mm/hr if a bucket size of 0.5mm is used or ± 0.8mm/hr for a 0.2 mm capacity bucket. Both sizes of bucket have been used in the study area in the past but now all gauges use the higher resolution bucket. In order to compensate for the quantisation error introduced by this form of recording the raingauge values are rounded towards the radar value, by an amount equal to the bucket size, prior to forming the calibration factor. Formally, given δ_g = (bucket size in mm)/(time interval in hrs) is the rainfall intensity quantisation error for the time interval considered, then the quantisation error adjusted rainfall intensity in mm/hr is

$$R_g^* = \begin{cases} R_r & |R_g - R_r| \leq \delta_g \\ R_g + \mathrm{sgn}(R_r - R_g).\,\delta_g & |R_g - R_r| > \delta_g . \end{cases} \qquad (3.4.1)$$

(a) nine-grid selected neighbours method

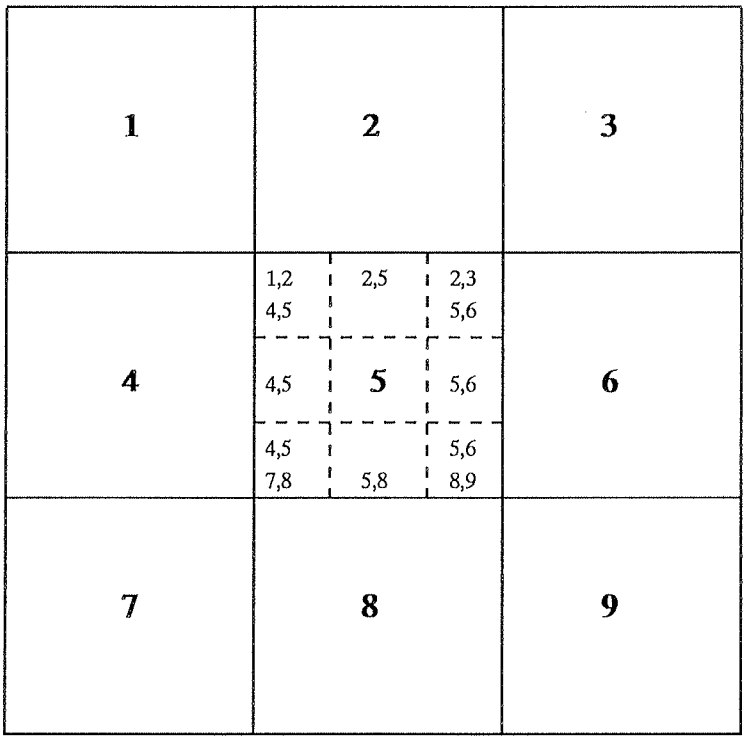

(b) four-grid selected neighbours method

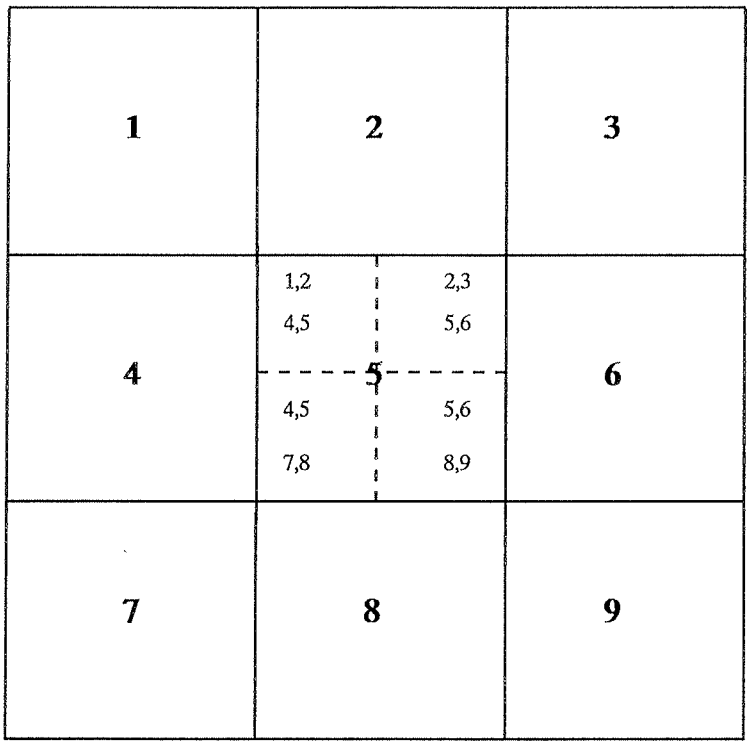

Figure 3.3.1 Radar grid squares indicating the associated neighbouring squares used to form domain averages in forming calibration factors for a gauge sited within square 5.

Calibration factors formed using this quantisation error adjusted rainfall are clearly conservative in terms of modifying the radar data field.

3.5 CALIBRATION FACTOR SURFACE FITTING TECHNIQUES

3.5.1 Multiquadric surface fitting

The form of surface adopted to represent the calibration factor field is an extended form of the multiquadric defined as

$$z_i = a_0 + a_1 d_{i1} + a_2 d_{i2} + \ldots + a_N d_{iN} \qquad i = 1,2,\ldots,N \qquad (3.5.1)$$

where z_i is the data value of the ith point, $\{a_i, i=0,1,2,\ldots,N\}$ are coefficients, and d_{ij} is the "distance" between points i and j. In this case the data values $\{z_i, i=1,2,\ldots,N\}$ would be the calibration factors for the N raingauge locations. Normally d_{ij} would be the Euclidean distance

$$d_{ij} = \sqrt{x_{ij}^2 + y_{ij}^2} \qquad (3.5.2)$$

where x_{ij} and y_{ij} are the distances in the x and y co-ordinate directions. Extensions and alternatives that have been considered include:

(i) smoothed Euclidean distance

$$d_{ij} = \sqrt{x_{ij}^2 + y_{ij}^2 + c^2} - c$$

where c is a smoothing parameter;

(ii) exponential form of Euclidean distance

$$\exp(-d_{ij}/\ell)$$

where ℓ is a scaling length parameter:

(iii) inverse distance

$$1/(1 + d_{ij}/\ell) \ .$$

In each of these cases the surface would normally be fitted to pass exactly through the N calibration factor data values. The resulting fitted surface is then used to calculate the calibration factors at other points in the radar field. These can then be used to factor the radar rainfall field to obtain the required calibrated rainfall field.

3.5.2 Extensions to surface fitting procedures

A number of modifications to the straightforward procedure of fitting a multiquadric surface to the calibration factor values have been considered. As a consequence three methods of fitting a multiquadric surface to pass exactly through the calibration factor values have been developed. Each one differs in terms of the conditions assumed in specifying the surface fitting procedure. They are:

(i) the surface passes exactly through the points;

(ii) in addition to (i), that the surface tends to flatten away from the surface fitting points;

(iii) in addition to (i), that the surface is constrained to reduce its roughness.

A further variant of each of the above three cases allows the surface not to pass exactly through the calibration factor values, thereby producing a smoother surface. This is achieved by replacing the Euclidean distance, $d_{ij}=0$ when i=j (ie at the data point) in equation (3.5.1) by a constant value -K. This has the effect of allowing the surface to pass within a distance $a_i K$ of the i'th data value. Appendix III provides a more detailed review of multiquadric surface fitting procedures of the above types.

3.5.3 Extension to include explanatory variables

A natural extension of the multiquadric surface fitting method is the inclusion of explanatory variables. Thus the linear dependence function involving Euclidean distances may be extended to include explanatory variables such as:

(i) distance from radar;

(ii) height of radar beam above the ground; and

(iii) altitude of the ground level.

This dependence may be introduced in the straightforward way as follows for a single explanatory variable $\{h_i, i=1,2,...,N\}$:

$$z_i = b_1 + b_2 h_i + a_1 d_{i1} + a_2 d_{i2} + ... + a_N d_{iN} \qquad (3.5.3)$$

where $b_1, b_2, a_1, a_2, ..., a_N$ are coefficients defining the form of the surface. Extension to include more than one type of explanatory variable is obvious.

Estimation of the new coefficients, b_1 and b_2, may be achieved by using simple least squares regression of calibration factors on the explanatory variable. The residuals from this regression can then be used as the z_i data values and the multiquadric surface fitted in the normal way. Alternative estimation methods have been developed in line with those which minimise roughness or ensure surface flatness away from the gauge locations.

3.5.4 Derivation of explanatory variables

Automatic procedures have been implemented to calculate the radar beam height for any point, taking into account the use of beam 1 (1.5 degree elevation) data to infill areas for which beam 0 (0.5 degree elevation) is affected by permanent clutter echoes. Figure 3.5.1 shows this infill area in relation to the raingauges. Table 3.5.1 presents for each gauge the raingauge-to-radar distance, the beam elevation used, and the height of the radar beam above the radar and above the raingauge. In computing the height of the beam at a given range (along the earth), r, the "four-thirds earth approximation" is used; that is

$$h(r, \theta) = r \left[\frac{3r}{8R} \cos\theta + \sin\theta \right] \qquad (3.5.4)$$

where θ is the radar beam elevation in degrees and R is the radius of the earth. This approximation for the path of a radiowave through the atmosphere accounts for both the earth's curvature and refraction of the ray by the atmosphere. In practice the bending of the beam due to refraction will vary as a function of the atmospheric conditions (eg. humidity, temperature), and will affect the approximation which assumes a standard atmosphere with a vertical gradient of the index of refraction of about -4 x 10^{-8} m^{-1}.

3.6 EXAMPLES OF SURFACE FITTING

3.6.1 Introduction

Examples of fitting multiquadric surfaces are presented in this section, first to a simple one-dimensional case and second to actual calibration factor values obtained for a storm event over London. The one-dimensional case has been used to gain an understanding of the behaviour of different forms of surface, whilst the real example, at this stage, focusses on graphical tools developed for displaying the surfaces produced in three dimensions.

3.6.2 A simple one-dimensional example

Figures 3.6.1 and 3.6.2 give some examples of how the parameters of the multiquadric surface fitting techniques affect the surfaces produced. Since it is easier to assess what is going on in one dimension rather than in two, a simple one-dimensional function interpolation problem provides a good way of visualising the surfaces being fitted to the calibration factors. Figure 3.6.1 shows the effect of varying the parameter c in the distance function used within the multiquadric surface fitting technique: in one dimension this distance is

$$d = \sqrt{(x_1 - x_2)^2 + c^2} - c.$$

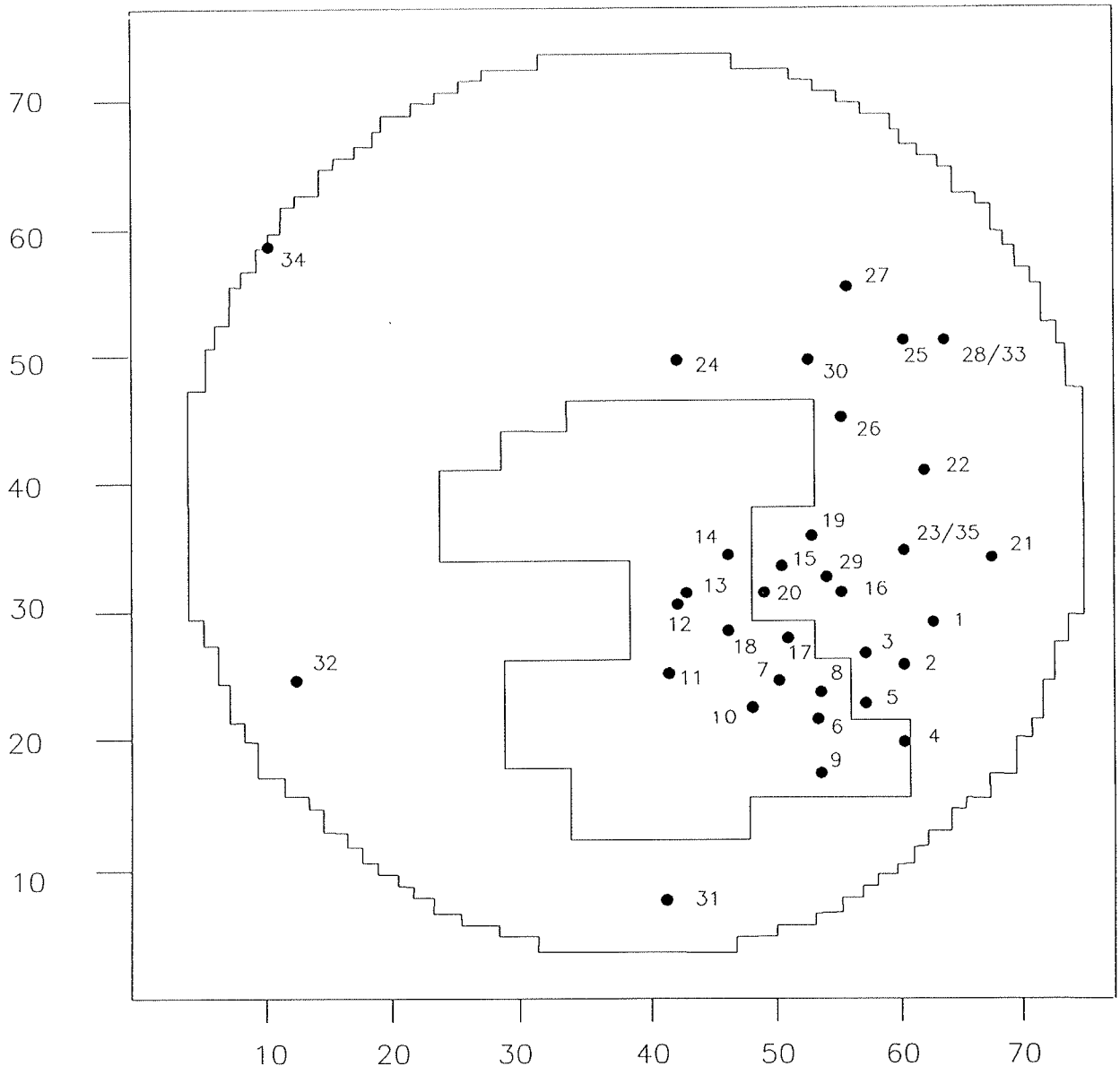

Figure 3.5.1 Infill area where beam 0 (0.5° elevation) data is replaced by beam 1 (1.5° elevation) data; also shown are the locations of the raingauges used in the study.

Table 3.5.1 Distances of raingauges from Chenies radar and height of radar beam above the raingauge.

	Raingauge	Distance to Radar (km)	Beam Elevation (°)	Height of radar beam above radar (m)	Height of radar beam above raingauge (m)
1	Crossness STW	50.85	0.5	596	738
2	Eltham High Street	48.83	0.5	567	642
3	Deptford PS	42.70	0.5	480	625
4	Keston	54.46	1.5	1600	1578
5	Kelsey Park	47.24	0.5	544	659
6	Beddington STW	44.08	1.5	1268	1383
7	Putney Heath Reservoir	34.08	1.5	960	1054
8	Furzedown Recreation Ground	39.40	1.5	1123	1233
9	How Green Reservoir	49.60	1.5	1443	1432
10	Hogsmill Valley STW	36.36	1.5	1030	1168
11	Perry Oaks	24.40	1.5	674	801
12	Uxbridge (Hillingdon Court Park)	16.96	1.5	461	571
13	Ruislip Manor	14.27	1.5	386	491
14	Harrow Weald Cemetery	15.82	1.5	419	471
15	Mill Hill Cemetery	23.01	0.5	232	304
16	Green Lanes	33.10	0.5	353	472
17	Holland Park	30.61	1.5	856	985
18	Greenford Cemetery (Ealing)	22.24	1.5	611	738
19	Oakwood Park	28.69	0.5	299	382
20	Brent Reservoir	23.13	0.5	233	341
21	Nags Head Lane	55.55	0.5	666	776
22	Thornwood	46.26	0.5	530	604
23	Chigwell	41.45	0.5	463	594
24	Runley Wood	22.32	0.5	224	237
25	Braughing Friars	47.30	0.5	545	579
26	Hertford	34.92	0.5	377	490
27	Chipping	47.04	0.5	541	587
28	Stansted	54.56	0.5	651	722
29	Hornsey	31.03	0.5	328	445
30	Stevenage	33.39	0.5	357	437
31	Cranleigh (Guildford)	60.75	0.5	747	850
32	Chieveley (Newbury)	60.57	0.5	745	791
33	Stansted (Met. Office)	54.47	0.5	650	721
34	Bretch Hill (Banbury)	62.07	0.5	768	766
35	Chigwell (Met. Office)	41.35	0.5	462	597

It was thought that, as c moves away from zero, the surface fitted would become smoother since the sharpness of the gradient-change in the region of each point is reduced. This is so, but, as can be seen, the surface (or function in this case) becomes more widely, even wildly, varying as c increases. This effect appears to explain the results found in exploratory trials of the re-calibration process that the best value of c is in fact zero.

Figure 3.6.2 shows the way in which the fitted surface changes as the offset parameter K varies. When K is non-zero the surface no longer exactly interpolates the given points but provides an approximating surface. The plot shows how the fitted function relates to the given data points: those points which agree well with adjacent points are approximated closely, while those associated with rapid changes in data values lie somewhat further from the fitted function. As expected, as K increases the surface does become smoother, but also the departures from the data points become larger.

3.6.3 Surface fitting applied to calibration factors

Tools have been developed to produce three dimensional displays of the calibration factor surfaces and the associated decalibrated and calibrated radar rainfall fields. Figure 3.6.3 shows the multiquadric surface fitted to pass exactly through the calibration factors evaluated at the 19 operational (out of 20) raingauge locations in the London area for the 15 minute time frame ending at 21.30 hr 25 August 1986. The calibration factors are defined in their modified logarithmic form: zero corresponds to no change in the radar field and positive values indicate that an increase in the radar value would result from an application of the calibration surface values to the radar data. The surface is fitted so that it becomes flat with increasing distance from the gauge locations. The surface is very rough so that extrapolation of calibration factor values away from the gauge locations will be unreliable. Also the form of the surface changes markedly from time frame to time frame. Consequently the surface, rather than providing a conservative means of adjusting the radar field, will result in a rather radical and transient adjustment.

In order to achieve a more conservative adjustment of the radar field using the raingauge information, the multiquadric surface has been fitted so that the surface is not constrained to pass exactly through the calibration factor values at the gauge locations. This results in the smoother, less extreme surface shown in Figure 3.6.4 Figure 3.6.5 shows the same surface when viewed from below the surface from its south-west corner; the actual calibration factor values at the gauge locations are shown superimposed in this figure. This position of view reveals the negative undulations in the surface in regions where the calibration factor surface indicates overestimation of rainfall by the radar when judged with respect to the gauge values. Finally Figures 3.6.6a and 3.6.6b show the radar rainfall field in its original uncalibrated form and after the calibration factor surface adjustment has been applied.

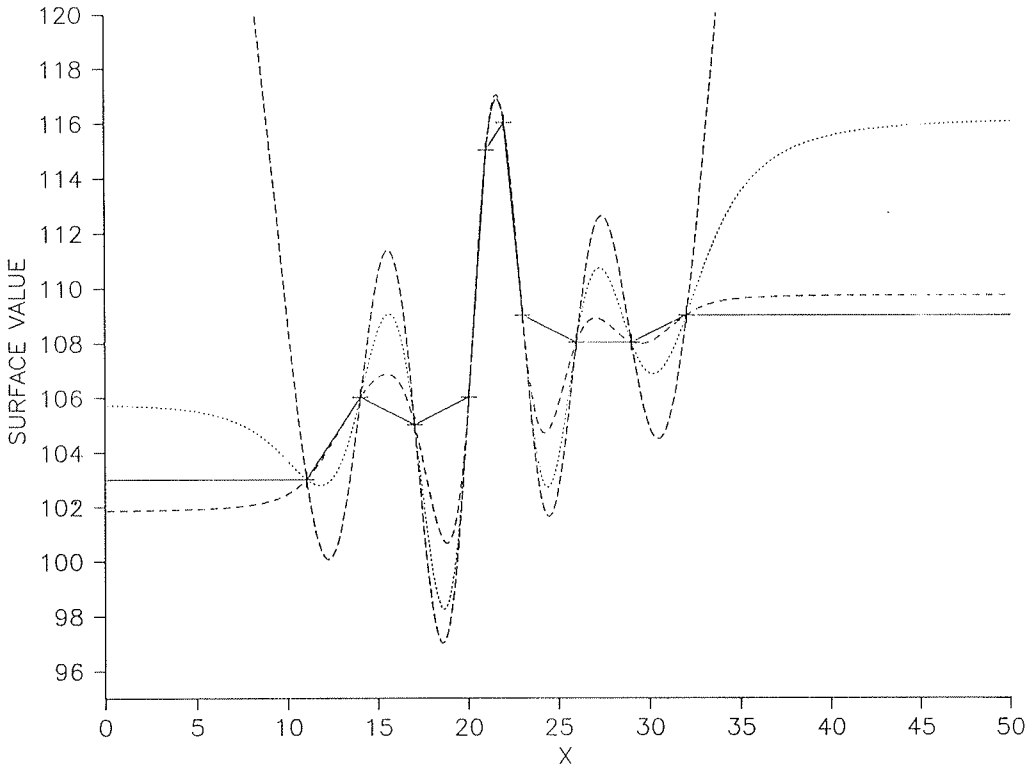

Figure 3.6.1 Affect of varying the parameter c of the multiquadric surface in a simple one-dimensional example (solid line: c=0; medium dashes: c=2; short dashes: c=4; long dashes: c=6).

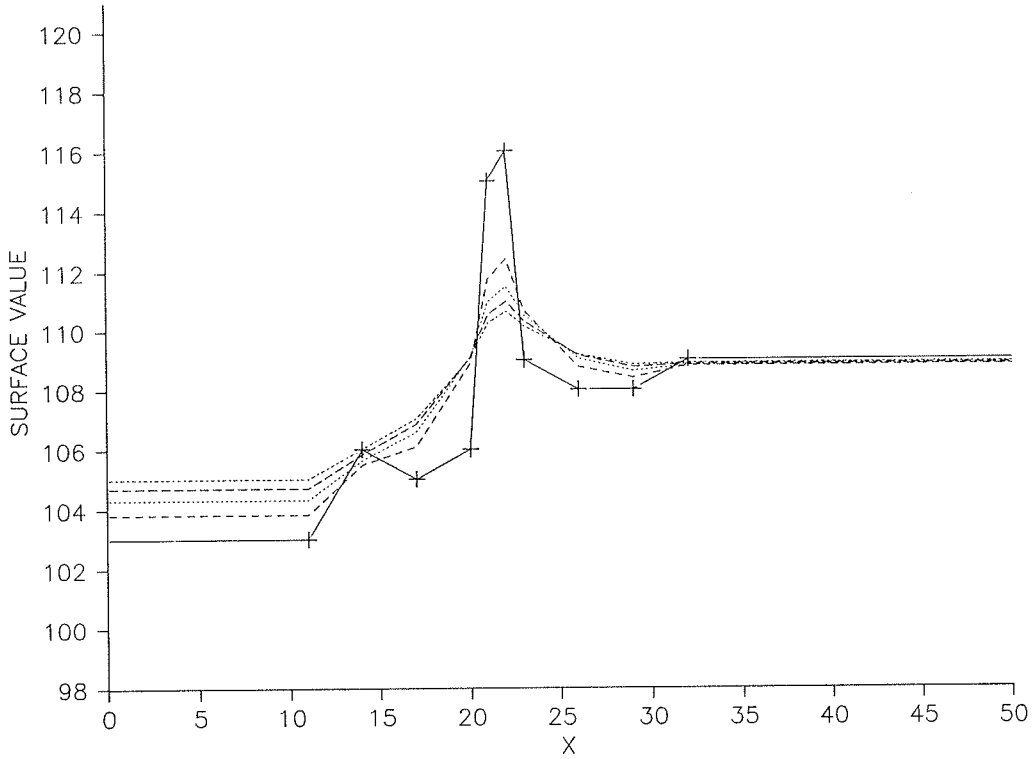

Figure 3.6.2 Affect of varying the parameter K of the multiquadric surface for a simple one-dimensional example (solid line: K=0; medium dashes: K=3; short dashes: K=6; long dashes: K=9; mixed dashes: K=12.

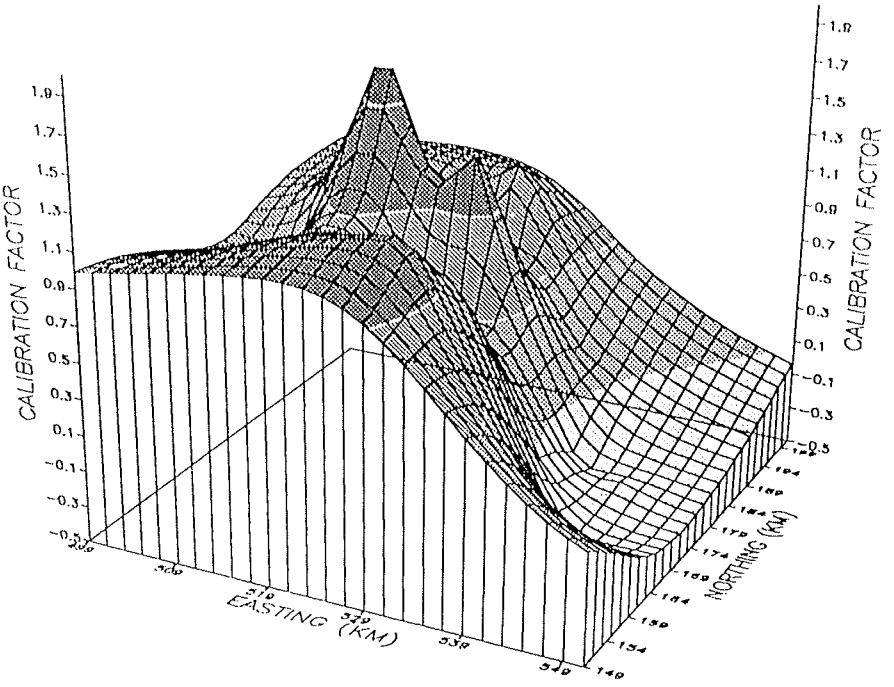

Figure 3.6.3 Multiquadric surface fitted to pass exactly through the calibration factors evaluated for the network of 20 raingauges located in the London area for the 15 minute time-frame ending 21:30 hr 25 August 1986.

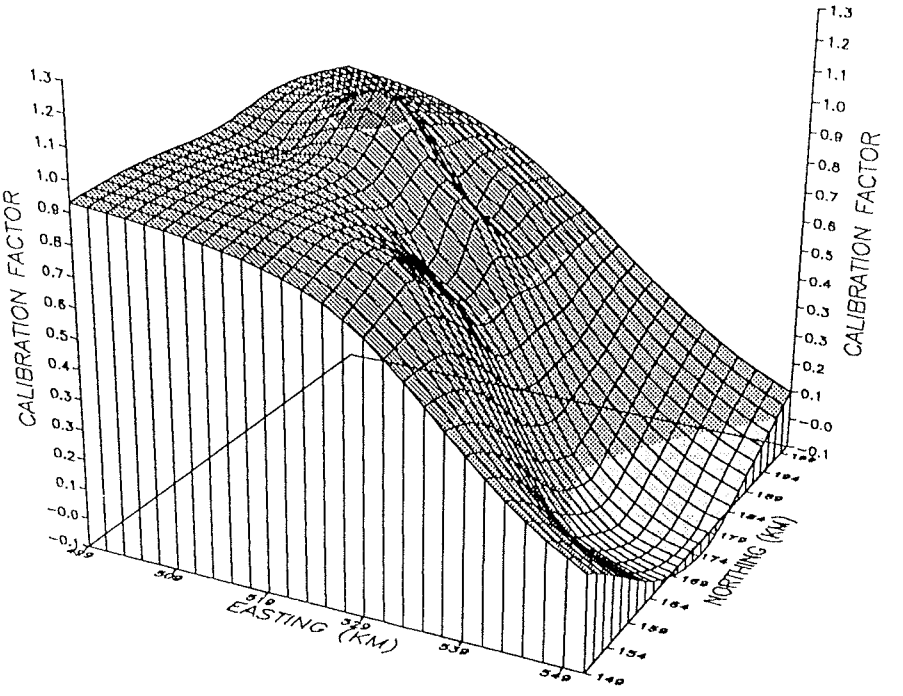

Figure 3.6.4 Multiquadric surface not constrained to pass exactly through the calibration factors evaluated for the network of 20 raingauges located in the London area for the 15 minute time-frame ending 21:30 hr 25 August 1986.

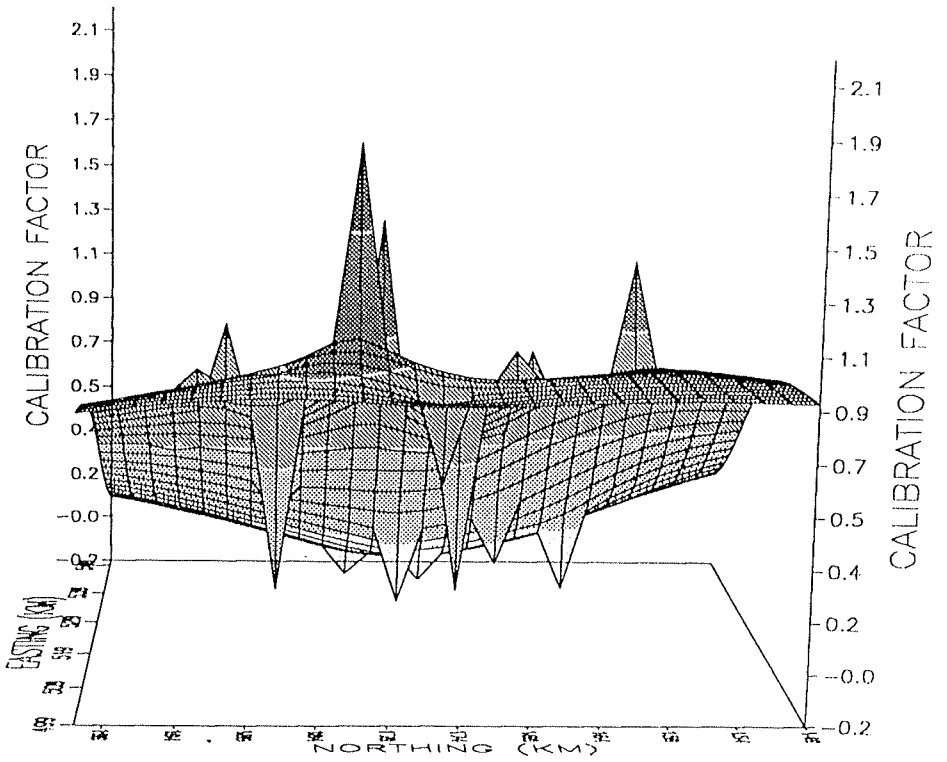

Figure 3.6.5 Multiquadric surface shown in Figure 3.6.4 viewed from its south west corner with actual calibration factor values at the gauge locations superimposed.

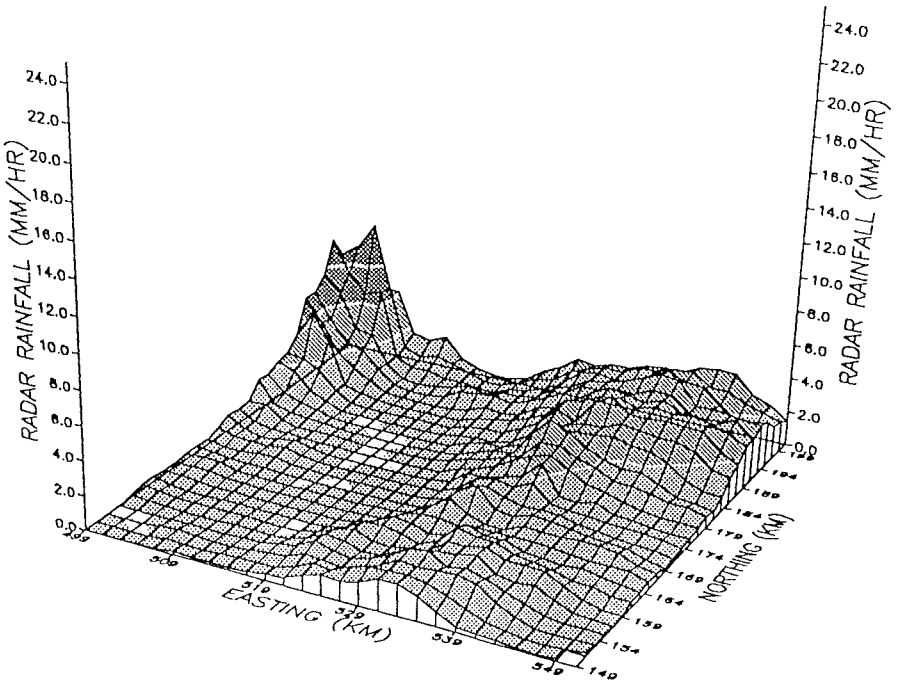

Figure 3.6.6a Radar rainfall field in its original uncalibrated form.

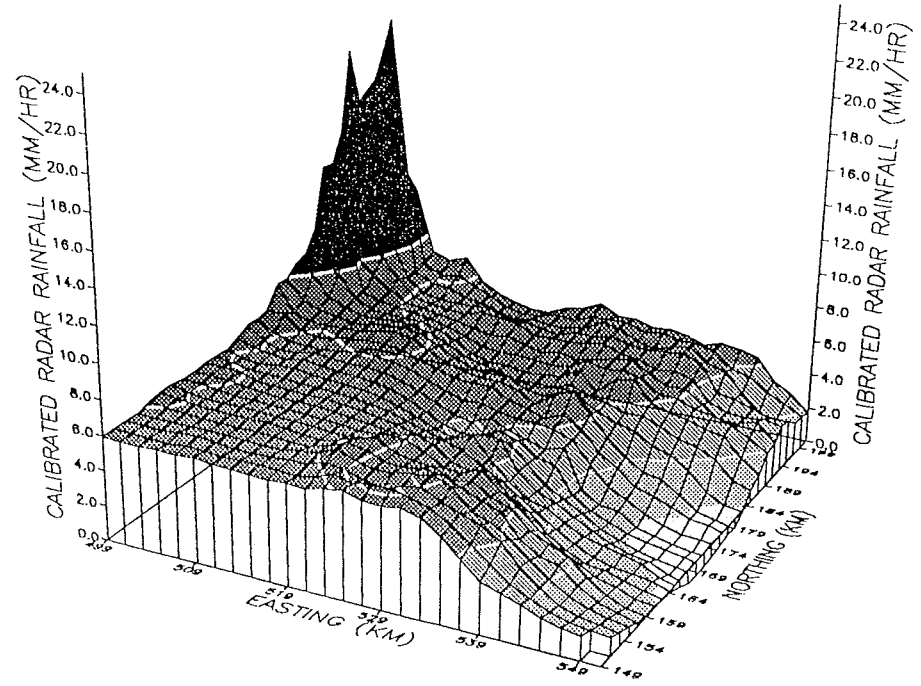

Figure 3.6.6b Radar rainfall field after the calibration factor surface adjustment has been applied.

4. Calibration Assessment Methods

4.1 INTRODUCTION

The conclusions of the Local Calibration of Weather Radar Study will be based on an objective comparison of the performance of candidate techniques when applied to previous rainfall events. To this end, a flexible computer program has been developed which will compute appropriate statistics of calibration performance: it will calculate performance statistics for individual rainfall events and will combine together results for any selection of events. In addition, the performance statistics can be calculated simultaneously for a wide choice of different calibration procedures or, more generally, for any methods of estimating rainfall at "ungauged sites". This computer program forms the major data-analytic tool for the project. Section 4.2 describes the way in which the performance statistics are calculated and then Section 4.3 expands on the above outline of the capabilities of the program.

4.2 CALCULATION OF PERFORMANCE STATISTICS

4.2.1 Gauges for Calibration and for Validation

The program distinguishes between raingauges to be used for calibrating the radar data and raingauges to be used for validating the calibration, and allows these to be chosen independently. Base sets of gauges of each type are accepted as data input, but these are subject to variation for each time frame because of the possibility of data being missing. For each time frame (normally 15 minutes), estimates are formed according to the rules designated for each of the validation gauges for which data exists: the estimates are calculated from as many as possible of the "calibration" base set, excluding the current validation gauge, for which both raingauge and radar data exist. If too many of the calibration base gauges have missing data then the time frame is omitted entirely.

Use of the facilities provided by this feature will enable a number of questions to be examined: for example;

(a) the effect of local calibration procedures on the estimated field outside the immediate region of the calibration gauges,

(b) the improvement of estimation performance as the number of gauges used for calibration increases,

(c) the possible improvement to the calibration procedures if the set of five widely spread raingauges used in the standard calibration are included with the local network in an overall calibration.

4.2.2 Statistics of Performance

The comparison between different methods of calibration will be based on one or more statistics summarising the performance of each method across all validation gauges and over all time frames of all events. For example, 12 events may consist of 600 time frames which, for 20 validation gauges, would provide 12,000 pairs of calibrated-estimate and raingauge-observation values. Four variations of the usual root mean square error measure of estimation performance have been included in the computer program: these are based on the following four ways of defining "error". Let r be the calibrated-estimate and R_g be the corresponding raingauge observation. Then "errors" E_1, E_2, E_3 and E_4 are defined as follows:

$$E_1 = R_g - r,$$

$$E_2 = \begin{cases} E_1 - \delta_g & E_1 > \delta_g, \\ 0 & |E_1| \leq \delta_g, \\ E_1 + \delta_g & E_1 < -\delta_g, \end{cases} \qquad (4.2.1)$$

$$E_3 = \log\{(10 + R_g)/(10 + r)\} = \log\{1 + E_1/(10 + r)\}$$

$$E_4 = \log\{1 + E_2/(10 + r)\}.$$

Here data units are millimetres per hour and δ_g is the rainfall intensity corresponding to one tip of the raingauge in the time-frame period. Thus E_1 is the ordinary error, E_2 is the quantisation-adjusted error, while E_3 and E_4 are versions of E_1 and E_2 which deflate the effect of an error of a given size when the "true" rainfall is large. For convenience errors of the types E_3 and E_4 will be called the log-error and quantised-adjusted log-error: they are discussed further in the following subsection. As an indicator of bias, the mean error as well as the root mean square error is calculated for each of the four definitions of error.

4.2.3 The log-error performance criterion

Some reconsideration has been given to the way in which different rainfall estimation procedures should be compared. This followed from two somewhat different points which arose during the Study: namely that

(a) "recalibrated" radar values would be used not only as input data for rainfall-runoff modelling, but also for the display of spatial rainfall patterns;

(b) there was the potential that the comparison was placing too much emphasis on the performance of the procedures on those few occasions when very high rainfall was observed.

For point (a) above, the use of the derived data as input for rainfall-runoff

models suggests that equal weights should be given to estimation errors in all parts of the observation range, whereas comments relating to use of the prototype procedure for display purposes have emphasised the importance of distinguishing zero rainfall from non-zero rainfall. To a large extent, this reconsideration has been prompted by the Study's investigation of procedures for estimating spatial rainfall fields from telemetered raingauge data only: here errors are rather larger than when radar data are incorporated into the procedure.

Although the intention is to arrive at an overall measure of estimation performance for use in an objective comparison of candidate procedures, there is inevitably a degree of subjective assessment within the way in which the performance measure is constructed from individual pairs of "observation" and "estimated value". Types of assessment entailed are for example:

(i) if the observed (i.e. true) value is 4 mm/hr, is an estimated value of 2 mm/hr as good (or bad) as one of 6 mm/hr?

(ii) is the error incurred in estimating a value of 4 mm when the true value is 2 mm/hr about the same as estimating a value of 22 mm/hr when the true value is 20 mm/hr?

The measure of performance provided by E_1 and E_2 in the previous sub-section is such that the answers in both cases would be "yes". They both lead to root mean square error (rmse) criteria based on an error defined as

$$\text{"error"} = \text{"observed"} - \text{"predicted"}. \qquad (4.2.2)$$

A subjective assessment of possible error criteria has been made by using an intuitive assessment of when pairs of estimates and observations might be judged equally good. This led to the rmse criterion based on errors defined as

$$\text{"error"} = \log(10 + \text{"observed"}) - \log(10 + \text{"predicted"}) \qquad (4.2.3)$$

where "observed" and "predicted" are quarter-hourly values of rainfall in units of mm/hr. Table 4.1 shows a selection of groups of observed and predicted values which are judged to have equivalent errors using this criterion.

An assessment of the performance of recalibration procedures for rainfall estimation using radar data indicated that the use of this criteria had little effect on which procedure was judged "best". However, on account of the intuitively desirable properties of the log-error this criterion has been adopted as the main performance criterion for assessment.

4.3 VARIETIES OF CALIBRATION

The program allows comparisons to be made between rainfall estimation techniques of a very large range of types. Besides the different types of multiquadric surfaces already outlined, the program allows the following

Table 4.1 Groups of observed and predicted values having equivalent errors using the log-error criterion of equation (4.2.3)

Group	Observed	Predicted	Error
1	0	0	0
	10	10	
	30	30	
	50	50	
2	0	-	0.05
	10	9.02	
	30	28.05	
	50	47.07	
	0	0.51	-0.05
	10	11.03	
	30	32.05	
	50	53.08	
3	0	-	0.20
	10	6.4	
	30	22.7	
	50	39.1	
	0	2.2	-0.20
	10	14.4	
	30	38.9	
	50	63.3	
4	0	-	0.50
	10	2.1	
	30	14.3	
	50	26.4	
	0	6.5	-0.50
	10	23.0	
	30	55.9	
	50	88.9	

different aspects to be selected independently.

Time-averaging for calibration

The calibration factors may be derived from radar and gauge rainfall intensities averaged over a specified number of previous time frames. Where missing values exist, the averages are defined so as to include values for a previous time frame only if both radar and gauge values are present. For the purposes of the performance assessment program only, the calibration factor is taken to be undefinable if either the radar or gauge value for the "present" time frame is missing: this is to facilitate the comparison of estimators based on different amounts of time-averaging for calibration since the measures of performance are then based on estimates for exactly the same set of "true" rainfalls.

Space-averaging for calibration

For each estimator to be compared, the calibration factor may be selected to be derived from a different one of the four types of spatial averaging of the radar intensity field (Section 3.3). That is, for each gauge site, the corresponding radar value will be one of: the value from the radar grid square in which the gauge is sited; two possible ways of specifying up to 4 of the 9 neighbouring grid-squares; or all of the 9 neighbouring grid-squares.

Space-averaging for estimation

Each estimator may be obtained by applying the interpolated calibration factor for the validation site to either the radar rainfall value from the grid-square in which the gauge is sited or to an average radar intensity value formed from all of the 9 neighbouring grid-squares. This is equivalent to options (i) and (iv) in Section 3.3

Selection of estimator type

The program allows five different types of estimates of rainfall intensity to be compared. Each estimator may be selected to estimate rainfall at a validation site by one of

(a) the average of the raingauge values at the calibration sites;

(b) the interpolated values from a multiquadric surface applied to the raingauge values;

(c) the result of applying an estimated calibration factor to the radar intensity field, where the calibration factor is defined as the average of the calibration factors at the calibration sites.

(d) as for (c) except that the calibration factor applied is obtained as the interpolated value obtained from a multiquadric surface applied to the calibration factors.

(e) the radar value corresponding to the estimation site, without applying any calibration technique.

In cases (a) and (b), the raingauge values concerned are potentially time-averaged and transformed values, with the appropriate back-transformation following averaging or surface fitting. For (e), the radar value may be derived from one of the methods of space-averaging for estimation.

Selection of calibration factor type

Each estimator may be derived from one of the seven types of calibration factor discussed in Section 3.2.

Selection of calibration factor parameters

The calibration factor selected for each estimator is further defined by specifying values for the parameters (for example ϵ_g, ϵ_r) for that calibration factor type.

Quantisation adjustments in calibration

Each estimator may be chosen to be based on the original raingauge values or on quantisation-adjusted raingauge values. For the latter, the possible effects of the data quantisation induced by the counting of raingauge bucket tips is allowed for by a preliminary adjustment of the raingauge values towards the radar values, the amount of adjustment being limited to that corresponding to one fewer or one extra bucket tip.

Elimination of negative rainfall estimates

Many of the calibration factor types and surface fitting techniques are potentially capable of resulting in negative estimates of rainfall. In practice, these negative values would be set to zero. The program allows a selection to be made for each estimator of whether or not this zero-truncation is applied.

Constraining zero rainfall amounts in original field to remain zero

It is possible that some of the calibration factor surface methods may result in zero radar rainfall values in the original field being re-estimated as non-zero values in the recalibrated field. In practice, these non-zero values may be reset to zero. The program allows a selection to be made for each estimator of whether or not this zero-value protection is applied.

Application of calibration to a later time-frame

In the operational system the same calibration factor surface requires to be applied to the present 5 minute radar image and then to two subsequent ones. The off-line assessment framework departs from the operational system by applying the present 15 minute average calibration factor surface to the present 15 minute average radar image. In order to simulate the operational environment more closely, and having access only to 15 minute raingauge rainfall totals, it is possible to apply the 15 minute average calibration factor surface to the 15 minute average radar image, one 15 minute time-frame later. This will give a conservative indication of how the calibration method's performance will degrade operationally at the 5 and 10 minute time steps within a 15 minute time-frame.

5. Assessment of Methods

5.1 INTRODUCTION

The results obtained by applying the calibration assessment methods described in Section 4 were obtained in two stages. The first stage employed data from 19 rainfall events and led to the recommendation of a prototype calibration procedure: this has been running as an operational system at the Waltham Cross Flood Warning Centre since 20 March 1989. A second stage of assessment employed data from the 23 rainfall events presented in Table 2.3.2: it is the results of this assessment which are presented in this section and which have led to the final recommendations for implementation made in this report. The error criterion used througout for assessment was the root mean square of the quantisation-adjusted log-error described in Section 4.2.2: this error definition makes an allowance for errors in the tipping-bucket raingauge as well as deflating the influence of an error occurring when estimating a relatively high rainfall intensity.

Two forms of estimator of spatial rainfall amount are considered for operational implementation. The main form is the use of a calibration factor surface to recalibrate the weather radar data field and the assessment of the best form for this is discussed in Section 5.2. It is also useful to fit a surface to the raingauge values only, in order to provide an estimate of spatial rainfall in the abscence of radar data: the choice of an appropriate method is discussed in Section 5.3. Simpler estimators of the rainfall field, such as the raingauge average, are compared with these two estimators in Section 5.4. Finally the conclusions and recommendations for operational implementation are presented in Section 5.5.

5.2 SURFACE FITTING TO CALIBRATION FACTORS

5.2.1 Effect of calibration factor definition

The various forms of multiquadric surface described in Section 3.5 together with the alternative calibration factor definitions presented in Section 3.2 have been assessed in stages. As a preliminary evaluation of the different calibration factor definitions, results were obtained using the simple surface type based on the Euclidean distance and flatness constraint (Table 5.2.1). With the values of the smoothing parameter, c, and the offset parameter, K, fixed at zero and 15 km, the incidental parameters of the calibration factor definitions were optimised using data from all 23 events (column 3 of Table 5.2.1). The smallest rmse value is obtained using the logarithmic calibration factor defined as $\log\{(R_g + 5)/(R_r + 7)\}$ where R_g and R_r are the raingauge and radar rainfall intensities in mm/hr respectively. However the rmse for the simpler standard calibration definition, $(R_g + 3)/(R_r + 5)$, is only 0.4% greater.

The sensitivity of these results to c and K was explored. For the logarithmic

Table 5.2.1 Effect of calibration factor definition (multiquadric with c = 0 and K = 15 km)

Calibration factor definition	rmse	Incidental parameters
1. Reciprocal	.0543	ϵ_g = 11, ϵ_r = 15 mm/hr
2. Standard	.0539	ϵ_g = 3, ϵ_r = 5 mm/hr
3. Difference	.0585	no parameters
4. Trimmed standard ratio	.0608	ℓ = .2, u = 1.75
5. Trimmed reciprocal ratio	.0596	ℓ = .3, u = 2.0
6. Logarithmic	.0537	ϵ_g = 5, ϵ_r = 7 mm/hr
7. Modified logarithmic	.0551	r_o = 3.5 mm/hr

calibration factor definition no reduction in rmse resulted and for the standard definition an increase in K from 15 to 25 km only reduced the rmse by 0.2% to .0538.

The results reported in the following sections all relate to the "standard" form of calibration factor, although corresponding results have also been obtained for the "logarithmic" form. These results did not suggest that changing the calibration factor would be valuable.

5.2.2 Effect of surface form

Table 5.2.2 presents the results of a comparison of the different forms of surface obtained through the use of the three different types of distance measure (Section 3.5.1) and the three constraint conditions (Section 3.5.2 and Appendix III). The better results were obtained when the surface was constrained to flatten away from the raingauge sites and the standard calibration factor definition with ϵ_g=3 and ϵ_r=5 mm/hr was used. The exponential of the Euclidean distance and the inverse of the Euclidean distance performed equally well as distance measures. Note that the rmse of .05344 obtained from the transformation of the Euclidean distance is less than 0.5% smaller than that obtained without transformation, and demands more computing resources. However the use of transformed distance measures in the multiquadric surface definition will allow the influence of calibration factor values to be more localised: this may prove to be a beneficial characteristic in practice.

Figure 5.2.1 shows the calibration factor surfaces formed using the simple Euclidean distance and using the inverse distance for the time-frame 16.30 14 March 1949 (Event 30). It is clear that using the inverse distance measure causes the surface to be more 'peaky', so that each individual calibration factor value has less influence on the surface away from its location. The decalibrated radar rainfall field for this time-frame is shown in Figure 5.2.2. Figure 5.2.3 indicates the effect of applying the calibration factor surfaces in

Table 5.2.2 Effect of distance measure and surface type on calibration factor surface estimation of rainfall

Distance measure	Surface type	rmse	incidental parameters
Euclidean distance	flatness constraint	.05378	ϵ_g=3, ϵ_r=5 mm/hr c=0, K=25 km
Exponential form of Euclidean distance	no recalibration at large distance	.05578	ϵ_r=ϵ_g=4 mm/hr c=0, ℓ=210 km; K=.1
"	flatness constraint	.05344	ϵ_g=3, ϵ_r=5 mm/hr c=0, ℓ=30 km; K=.5
"	roughness constraint	.05375	ϵ_g=4, ϵ_r=6 mm/hr c=0, ℓ=10 km; K=.55
Inverse distance	no recalibration at large distance	.05569	ϵ_g=ϵ_r=4 mm/hr c=0, ℓ=180 km; K=.1
"	flatness constraint	.05344	ϵ_g=3, ϵ_r=5 mm/hr c=0, ℓ=30 km; K=.35
"	roughness constraint	.05377	ϵ_g=3, ϵ_r=5 mm/hr c=0, ℓ=10 km; K=.35

Figure 5.2.1 to this radar field.

5.2.3 Assessment of varieties of calibration

The varieties of calibration outlined in Section 4.3 are evaluated here using the form for the calibration factor surface selected above: this uses an inverse distance measure and flatness constraint.

Time-averaging for calibration

Table 5.2.3 summarises the effect on the root mean square error criterion of using calibration factors calculated using raingauge and radar data averaged over 15, 30, 45 and 60 minute periods. The surface is applied to each 15 minute average radar rainfall field within the period to obtain the recalibrated fields from which the errors are derived. The offset parameter, K, has been optimised for each time-average and is seen to decrease with increased time-averaging: less smoothing via K is needed since surface smoothing results from the time-averaging operation. The smallest rmse is obtained by averaging over 30 minutes but the reduction is only 0.6% of that for the one 15 minute time-frame.

(a) Euclidean distances

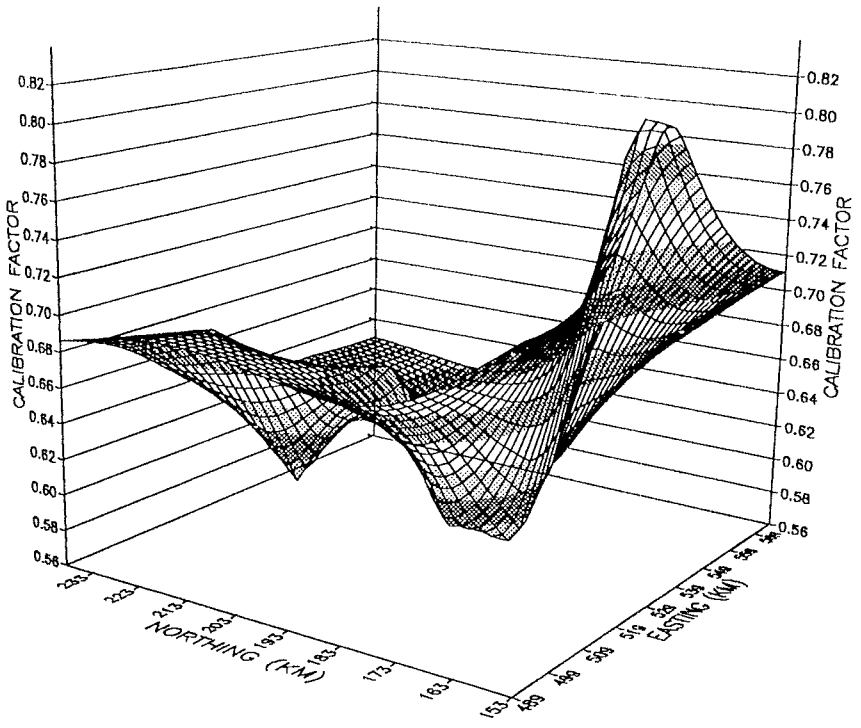

(b) Inverse distance

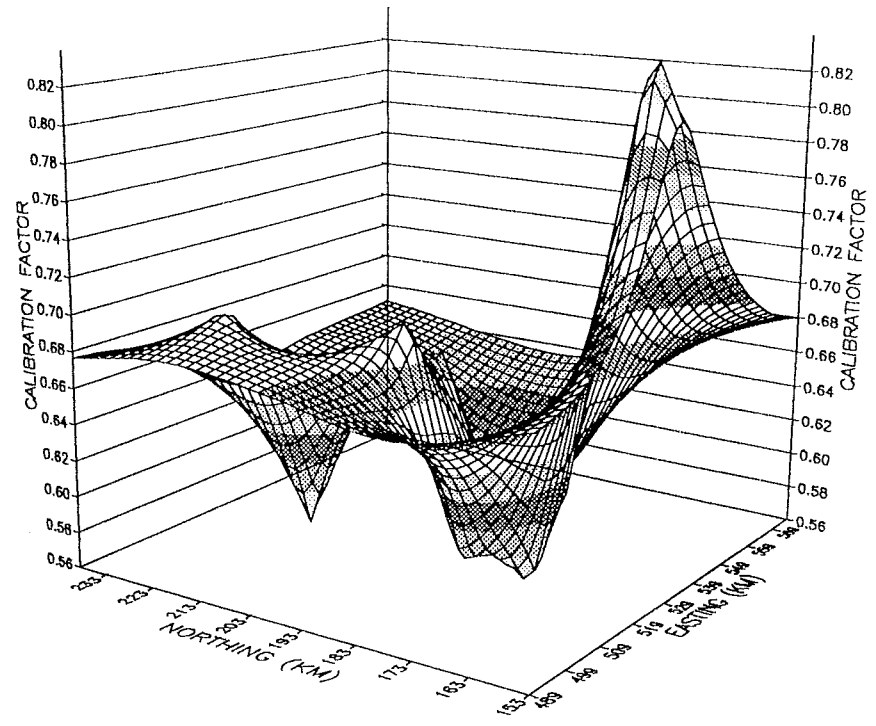

Figure 5.2.1 Calibration factor surfaces for 16.30 14 March 1989 obtained using different distance measures.

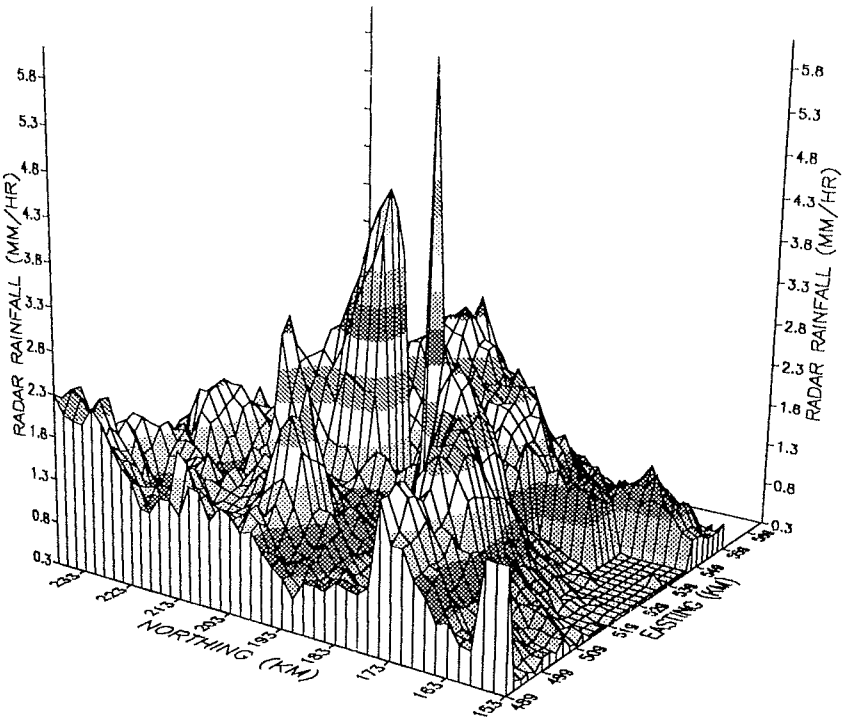

Figure 5.2.2 Decalibrated radar field for 16.30 14 March 1989

Space-averaging for calibration

Table 5.2.4 presents the effect of using the 4 forms of spatial averaging of the radar rainfall grid values described in Section 3.3. The method which performs best averages the radar values for one, two or four grid squares selected from the 9 grid squares depending on the position of the gauge within its radar grid square. However the improvement obtained from space-averaging is small.

Space-averaging for estimation

Table 5.2.4 also assesses how a calibration surface applied to a 9-grid space-averaged field compares with the normal application to the one-grid field as an estimator of rainfall. A reduction of only 0.2% results from using the 9-grid average.

Quantisation adjustments in calibration

This adjustment, based on the bucket size of a recording raingauge (Section 3.4), produced a 4% deterioration in performance.

Elimination of negative rainfall estimates

Any negative estimates of rainfall obtained from the calibration procedures are set to zero prior to forming the errors for evaluation. The effect of allowing the negative estimates to remain was found to have little effect on the rmse

(a) Euclidean distance

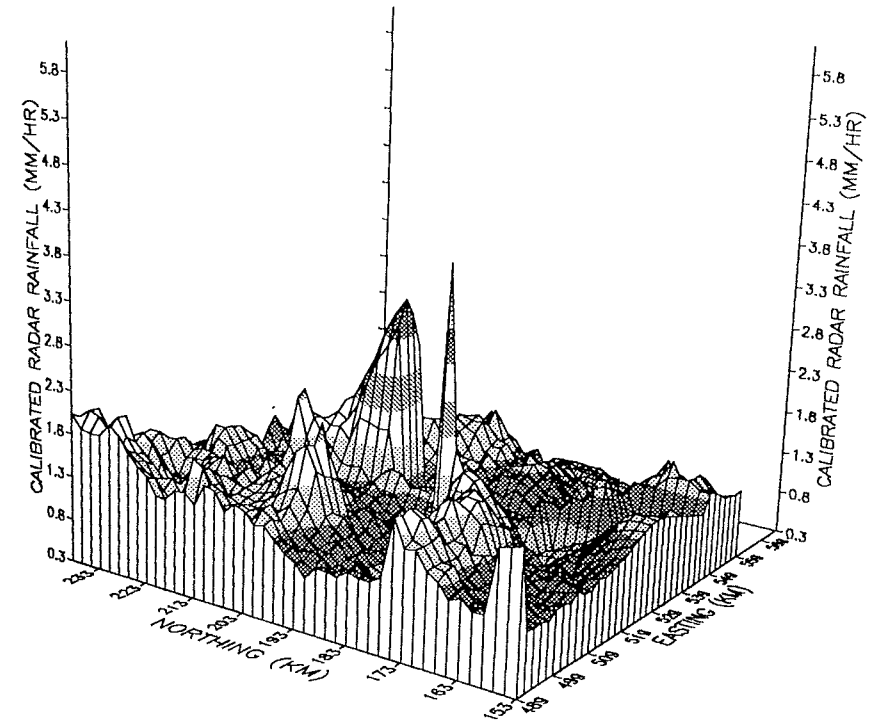

(b) Inverse distance

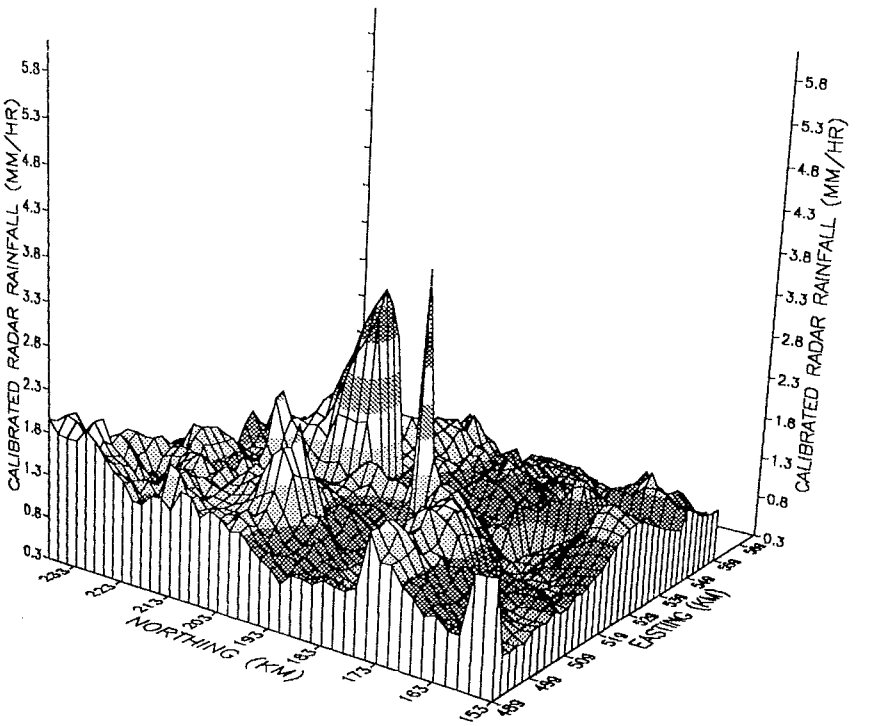

Figure 5.2.3 Recalibrated radar fields for 16.30 14 March 1989 obtained using the calibration surfaces in Figure 5.2.1 and based on different distance measures.

Table 5.2.3 Effect of time-averaging

Number of time-frames averaged (15 min time-frames)	Offset parameter, K km	rmse
1	.3	.0534
2	.2	.0531
3	.1	.0536
4	.1	.0543

Table 5.2.4 Effect of space-averaging

Method of space-averaging in calculation	in evaluation	rmse
One-grid	One-grid	.05344
	Nine-grid	.05337
Nine-grid selected neighbours	One-grid	.05340
	Nine-grid	.05332
Four-grid selected neighbours	One-grid	.05362
	Nine-grid	.05346
Nine-grid	One-grid	.05351
	Nine-grid	.05338

performance criterion.

Constraining zeros in original field to remain zero

Zero rainfall values in a decalibrated radar rainfall field may be replaced by non-zero values as a result of recalibration. The effect of resetting these values to zero was found to have little effect on the rmse performance criterion.

Application of calibration to a later time-frame

A requirement of the operational recalibration system is that each 5 minute radar-rainfall field should be recalibrated. However, since raingauge data are only available every 15 minutes calibration factor surfaces can only be fitted at this interval. This means that a fitted surface is used for the current radar time-frame and for the next 5 and 10 minute frames before a new surface is fitted. To assess the degradation in performance, the effect of using a surface for the time-frame 15 minutes after that to which it was fitted was examined. The rmse increased by 10% and the degradation in performance over the 10 minute interval of the operational system will not be expected to be worse than this.

5.2.4 Use of explanatory variables

An extension of the multiquadric surface fitting method to include explanatory variables was described in Section 3.5.3. Table 5.2.5 presents the results obtained by introducing the following explanatory variables: height of the raingauge above Ordnance Datum, the range of the raingauge from the radar, and the height of the radar beam above the raingauge. Rather than resulting in an improvement in performance there was a slight deterioration in all cases with the range from the radar causing the least harm.

Table 5.2.5 Evaluation of multiquadric surface fitting using explanatory variables

Explanatory variable	rmse
None	.0534
Height of gauge AOD	.0544
Range of gauge from radar	.0538
Height from gauge to beam	.0543

5.2.5 Calibration factor statistics

It is of interest to examine the statistics of the calibration factor values themselves in addition to the rmse performance statistics arising from the different rainfall estimation methods. Table 5.2.6 provides a summary of the mean and standard deviation of the calibration factor, $(R_g + 3)/(R_r + 5)$, computed for each raingauge site using data from the 23 rainfall events. This analysis was expected to reveal any anomalous raingauges. However, the results indicate that the differences between average values of the calibration factors at the different raingauge sites are small. The values range from 0.64 to 0.71 across the 27 gauges that operate for more than 300 time-frames. Raingauges 4 and 9 have the highest mean calibration factors: these gauges are located at relatively large distances from the radar and also lie within the 1.5 degree elevation beam infill area (Figure 3.5.1). Possibly as important, if not more, is that the two gauges are also the highest at 172 and 161 m AOD respectively (Table I.1). The raingauge site descriptions in Appendix I indicate that these two raingauges are in good gauge locations and hence the radar and altitude influences appear to provide the most plausible explanation for these differences.

Table 5.2.6 Analysis of standard calibration factor values (ϵ_g = 3, ϵ_r = 5 mm/hr) for each raingauge

Raingauge Number	Mean	Standard deviation	Number of time-frames
1	.64	.16	1213
2	.65	.16	1000
3	.65	.17	1096
4	.71	.26	1211
5	.66	.17	1214
6	.68	.23	1216
7	.65	.16	1213
8	.67	.18	1189
9	.70	.20	1212
10	.66	.24	1115
11	.65	.18	1211
12	.68	.24	1129
13	.67	.21	1215
14	.67	.20	1141
15	.52	.10	45
16	.65	.14	1003
17	.66	.14	820
18	.65	.15	1166
19	.67	.20	1210
20	.65	.17	1031
21	.64	.15	169
22	.65	.15	937
23	.62	.12	169
24	.65	.15	937
25	.66	.21	744
26	.66	.17	332
27	.67	.27	728
28	.67	.19	936
29	.66	.18	332
30	.64	.15	794
Overall mean	.66		
Overall standard deviation	.19		

5.3 SURFACE FITTING TO RAINGAUGE VALUES ONLY

A useful facility is to be able to estimate the rainfall field from raingauge data only: this estimate can serve to both complement the recalibrated radar field and to replace it in the event that the radar malfunctions. The properties of a surface fitted to raingauge data are likely to differ from those fitted to calibration factor values. In particular a rainfall surface would be expected, on the basis of radar evidence, to display sharp peaks, as opposed to the smoother behaviour of a calibration factor surface. It is therefore likely that

surfaces constrained to have zero rainfall at large distances will prove more appropriate.

A summary of the results obtained using the different distance measures and surface constraints, and after optimising the incidental parameters, are presented in Table 5.3.1. The form of surface that performs best employs the exponential of the Euclidean distance and is constrained to be flat away from the raingauge locations. However, the improvement relative to the simple surface formed using the Euclidean distance without transformation is 0.7%. Transforming the raingauge values before fitting the surface improved the performance by 3.6% and the results in Table 5.3.1 relate to this case. The transformation found to be best was of the modified logarithmic form: $\log(R_g)$ for R_g>4.5 mm/hr and $(R_g/4.5) + \log(4.5) - 1$ otherwise.

Table 5.3.1 Effect of distance measure and surface type on raingauge-only estimation of rainfall.

Distance measure	Surface type	rmse	incidental parameters
Euclidean distance	flatness constraint	.07248	r_o=3.5 mm/hr; c=0, K=5 km
Exponential form of Euclidean distance	zero rainfall at large distance	.07233	r_o=3.5 mm/hr; c=0, ℓ=80 km K=.05
"	flatness constraint	.07194	r_o=4.5 mm/hr; c=0, ℓ=20 km K=.15
"	roughness constraint	.07240	r_o=4.5 mm/hr; c=0, ℓ=20 km K=.2
Inverse distance	zero rainfall at large distance	.07222	r_o=3.5 mm/hr; c=0, ℓ=80 km K=.04
"	flatness constraint	.07196	r_o=4.5 mm/hr; c=0, ℓ=20 km K=.05
"	roughness constraint	.07244	r_o=4.5 mm/hr; c=0, ℓ=20 km K=.1

5.4 COMPARISON OF ALTERNATIVE RAINFALL ESTIMATORS

As a comparative indicator of performance it is useful to compare the performance of the rainfall estimator derived by calibration surface fitting with other simpler estimators including the at-site calibrated and decalibrated radar estimators. Table 5.4.1 summarises the performance of different estimators after first optimising the incidental parameters involved. The root mean square error statistic is presented in the standard form with units of mm/hr, as well as the quantisation-adjusted log-error used throughout the assessment, to give a direct impression of the error involved. The final column of the table gives the

Table 5.4.1 Evaluation of alternative rainfall estimation techniques

Technique	Root mean square error		% improvement	
	log-error	standard	log-error	standard
At-site radar	.073	1.636	0	0
Decalibrated radar	.068	1.527	7	7
Raingauge average	.084	1.826	- 15	- 12
Surface fitting to raingauges	.072	1.645	1	- 1
Calibration factor average	.058	1.394	21	15
Surface fitting to calibration factors	.053	1.303	27	20

improvement in accuracy relative to the at-site calibration estimator.

Note that the decalibrated radar performs better than the at-site calibrated radar. One reason for the poor performance of the at-site radar calibration, identified during the Study, derives from problems with transmission of the calibration raingauge data via the Ferranti-Argus computer at Reading. It is particularly relevant to observe that the uncalibrated radar outperforms the raingauge network by 6%, even after using a sophisticated surface fitting technique. This result is a persuasive argument in favour of radar, particularly since the raingauge network is so dense over the London and Lee Valley region. The best technique, surface fitting to the calibration factors, is seen to be 27% more accurate than the at-site radar and 22% better than the decalibrated radar data.

Table 5.4.2 provides a summary of the biases associated with the errors derived from the alternative rainfall estimation techniques. The biases are notably small from all techniques with the preferred "surface fitting to calibration factors" estimator providing the smallest log-error bias apart from the at-site radar estimator. These small biases also lend support to the overall assessment scheme used in the Study. The use of raingauges as the ground "truth" introduces a complication since they are point measurements and not the grid-square average measurements of rainfall that are provided by radar. These 15 minute rainfall totals at a point will be more variable than

Table 5.4.2 Bias statistics of alternative rainfall estimation techniques

Technique	Bias	
	log-error	standard
At-site radar	.0003	.0316
Decalibrated radar	.0069	.1856
Raingauge average	.0072	.0367
Surface fitting to raingauges	.0052	.0504
Calibration factor average	.0033	- .0012
Surface fitting to calibration factors	.0024	.0035

the corresponding radar grid values (averages of three, almost instantaneous, values made at 5 minute intervals) although when averaged over time the point measurements will provide unbiased estimates of the grid values. It is therefore comforting to observe that the errors from the rainfall estimation techniques, when averaged over all 23 events in time (and across 30 raingauges in space), do not display any substantial bias.

Table 5.4.3 provides a breakdown of the performance criterion into the contribution from each of the 23 events. Surface fitting to the calibration factors is the best estimator for 16 of the 23 events. The decalibrated radar data provides better performance than the at-site calibrated data in all but four of the 23 storm events. Also, the simple average of the raingauge values outperforms the at-site calibrated radar data for about half of the events. As previously mentioned, one reason for the poor performance of the at-site calibration is related to calibration raingauge data transmission problems.

Table 5.4.3 Event evaluation of alternative rainfall estimation techniques

Event	At-site radar	Decalibrated radar	Average of raingauge values	Surface fitting to raingauge values	Average of calibration factors	Surface fitting to calibration factors
1 Oct 1987a	0.056^{+}	0.053	0.051	0.043	0.038	0.036*
2 Oct 1987b	0.115	0.148^{+}	0.112	0.098	0.099	0.088*
3 Nov 1987b	0.077	0.089	0.090^{+}	0.075	0.076	0.068*
4 Mar 1988a	0.036	0.036	0.040^{+}	0.033	0.031	0.030*
5 Mar 1988b	0.044^{+}	0.031	0.033	0.025	0.024	0.022*
6 Mar 1988c	0.025^{+}	0.018	0.015	0.013	0.014	0.012*
7 Apr 1988a	0.054	0.051	0.079^{+}	0.065	0.049	0.048*
8 May 1988	0.067	0.064*	0.170^{+}	0.146	0.071	0.066
9 Jun 1988a	0.039	0.038	0.057^{+}	0.045	0.035	0.032*
10 Jun 1988b	0.110*	0.115	0.171^{+}	0.158	0.121	0.118
11 July 1988a	0.039	0.030	0.041^{+}	0.040	0.028*	0.029
12 July 1988b	0.057^{+}	0.044	0.055	0.050	0.037	0.036*
13 July 1988c	0.056^{+}	0.042	0.051	0.047	0.041	0.040*
14 July 1988d	0.096	0.064	0.096^{+}	0.090	0.063*	0.066
15 July 1988e	0.054	0.051	0.066^{+}	0.051	0.040	0.035*
16 July 1988f	0.112	0.108	0.128^{+}	0.110	0.093	0.086*
17 July 1988g	0.070	0.091	0.096^{+}	0.066	0.069	0.056*
18 Aug 1988a	0.152	0.128	0.170^{+}	0.148	0.123	0.117*
19 Aug 1988b	0.063	0.063	0.070^{+}	0.053	0.048	0.042*
20 Feb 1989b	0.090^{+}	0.081	0.062	0.043*	0.069	0.061
21 Mar 1989a	0.060^{+}	0.041	0.019	0.018*	0.030	0.023
22 Mar 1989b	0.104^{+}	0.095	0.052	0.036*	0.078	0.052
23 May 1989a	0.093^{+}	0.093	0.060	0.061	0.061	0.056*
Average across events	0.073	0.068	0.084^{+}	0.072	0.058	0.053*

* best method for event

\+ worst method for event

6. Conclusions and Recommendations

6.1 INTRODUCTION

The London Weather Radar Local Calibration Study has indicated that an improvement in the accuracy of radar estimates of spatial rainfall amounts of 27% can be achieved over the London and Lee Valley area. This increase in accuracy is obtained by replacing the at-site radar estimate in current use by a calibration factor surface estimate which merges the uncalibrated radar data with raingauge measurements from 30 sites. The procedure recommended does not introduce discontinuities into the radar rainfall field in time and space. These are undesirable features of the at-site calibration method and result from the use of calibration domains (within which typically one raingauge is used for calibration) which change with synoptic type (identified through the variability of the factors used for calibration).

This final section presents the recommended methods to be used for operational implementation. Two methods are suggested for consideration in local calibration of weather radar, the one recommended being simple but the one suggested for trial being more complex but possibly having more desirable characteristics. A method for estimating spatial rainfall amounts using raingauges only is also recommended. This will serve as a useful complement to the recalibrated product and can replace it if the radar malfunctions. The accuracies of the suggested techniques for rainfall estimation are also summarised. A recommendation is also made concerning the range correction currently used in the Chenies radar. Finally, some comments are made regarding the recalibration software now integrated and operational within the NRA Thames Region's Flood Warning System.

6.2 RADAR CALIBRATION TECHNIQUE

The recommended method for operational implementation, after taking into account both computing requirements and accuracy, has the following characteristics:

(i) a Euclidean distance function;
(ii) a flatness constraint;
(iii) a smoothing constant, c, equal to zero;
(iv) an offset parameter, K, equal to 25 km; and
(v) a calibration factor definition of the standard type with ϵ_g=3 and ϵ_r=5 mm/hr ie. $(R_g + 3)/(R_r + 5)$.

This method is of identical form to the prototype procedure previously recommended, based on a more restricted assessment using a smaller database, and in operational use since 20 March 1989. The only changes requiring to be made to implement this current recommendation are to reset the incidental parameters K=15 km, ϵ_g=4 and ϵ_r=5 mm/hr to those indicated above.

The recommended method, like the prototype, may lead to each individual raingauge value having too large an influence on the rainfall field away from the location of that gauge. If this proves to be of concern in the operational system then the more complex but more accurate "trial method" having the following characteristics could be evaluated in an operational context:

(i) an inverse distance function with a scaling length parameter, ℓ, equal to 30 km;
(ii) a flatness constraint;
(iii) a smoothing constant, c, equal to zero;
(iv) an offset parameter, K, equal to 0.35;
(v) a standard calibration factor definition with ϵ_g=3 and ϵ_r=5 mm/hr ie. $(R_g + 3)/(R_r + 5)$.

Again this is similar to the operational prototype but with the Euclidean distance, d_{ij}, replaced by $1/(1+d_{ij}/30)$, and the incidental parameters reset to K=0.35, ϵ_g=3 and ϵ_r=5 mm/hr.

6.3 RAINGAUGE-ONLY RAINFALL ESTIMATION TECHNIQUE

It is also recommended that a rainfall estimator be implemented that is based on raingauge values only, to both complement the recalibrated radar product and to replace it in the event that the radar data are unavailable. The recommended raingauge surface fitting method has the following characteristics:

(i) an exponential form of the Euclidean distance, $\exp(-d_{ij}/\ell)$, with a scaling length ℓ equal to 20 km;
(ii) a flatness constraint;
(iii) a smoothing constant, c, equal to zero;
(iv) an offset parameter, K, equal to 0.15; and
(v) transformation of the raingauge values prior to surface fitting using the transform $\log(R_g)$ for R_g>4.5 mm/hr and $(R_g/4.5) + \log(4.5) - 1$ otherwise (any negative values resulting from back-transformation are replaced by zero).

The method previously recommended, based on a more restricted analysis using fewer rainfall events, applied a zero rainfall at large distance constraint, and used the same distance measure, but with a scaling length of 50 km, and an offset parameter of 0.02. Note that the raingauge-only surface method of rainfall estimation is 14% more accurate than using the simple arithmetic average of the gauge values.

6.4 RELATIVE ACCURACY OF DIFFERENT RAINFALL ESTIMATION TECHNIQUES

As a summary of the performance of the selected methods their percentage increase in accuracy relative to the existing at-site radar calibration is presented below:

(i) recommended calibration factor surface method: 26%

(ii) trial calibration factor surface method: 27%

(iii) recommended raingauge-only surface method: 1%.

The poor performance of the at-site calibration, first recognised during this Study, has been identified as being at least in part due to faulty data transmission of the calibration raingauge data via the Ferranti Argus computer at Reading. Steps have been taken to halt the application of the at-site calibration until an improvement in data transmission can be guaranteed.

A particularly remarkable result of the Study is that the radar, even without raingauge calibration, can outperform the very dense network of raingauges (30 over an area of about 360 km^2) even when a sophisticated surface fitting method is used. However, when radar and raingauges are used in combination then an improvement of 22% is obtained, relative to the radar without raingauge calibration. Figures 6.1 and 6.2 show an example of the estimated rainfall field in mm/hr obtained using the recommended recalibration and the raingauge-only methods respectively. The additional information on the detailed structure of this convective event that radar provides, even given a rather dense raingauge network, provides a rather persuasive argument for the value of radar.

6.5 THE EFFECT OF RANGE FROM THE RADAR

Finally, the range correction used at the radar site has been found to be deficient. A tendency for rainfall intensity to decrease from .7 to .4 mm/hr, on average, with increasing range between 6 and 70 km from the radar has been observed (Figure 2.4.6). It is recommended that the at-site range correction be modified to correct for this tendency, ideally also taking into account the effects of the beam infill region (Figure 3.5.1) and the areas of radar anomaly (Figure 2.4.3).

6.6 THE OPERATIONAL SYSTEM

Software for radar decalibration, recalibration and raingauge-only rainfall estimation have been supplied to the NRA Thames Region as the final product of this Study. It should be noted that the calibration and performance assessment relate only to that part of the 2 km Chenies radar

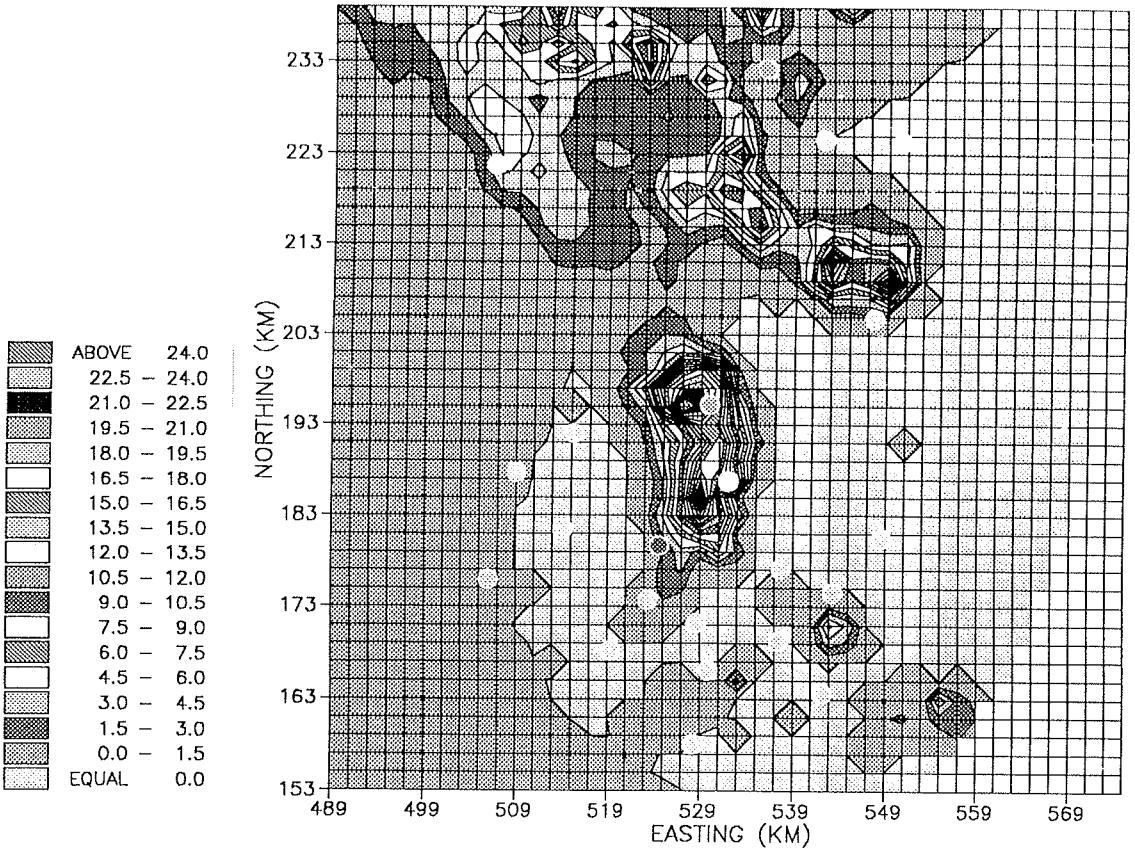

Figure 6.1 Recalibrated radar field: 19.15 8 May 1988

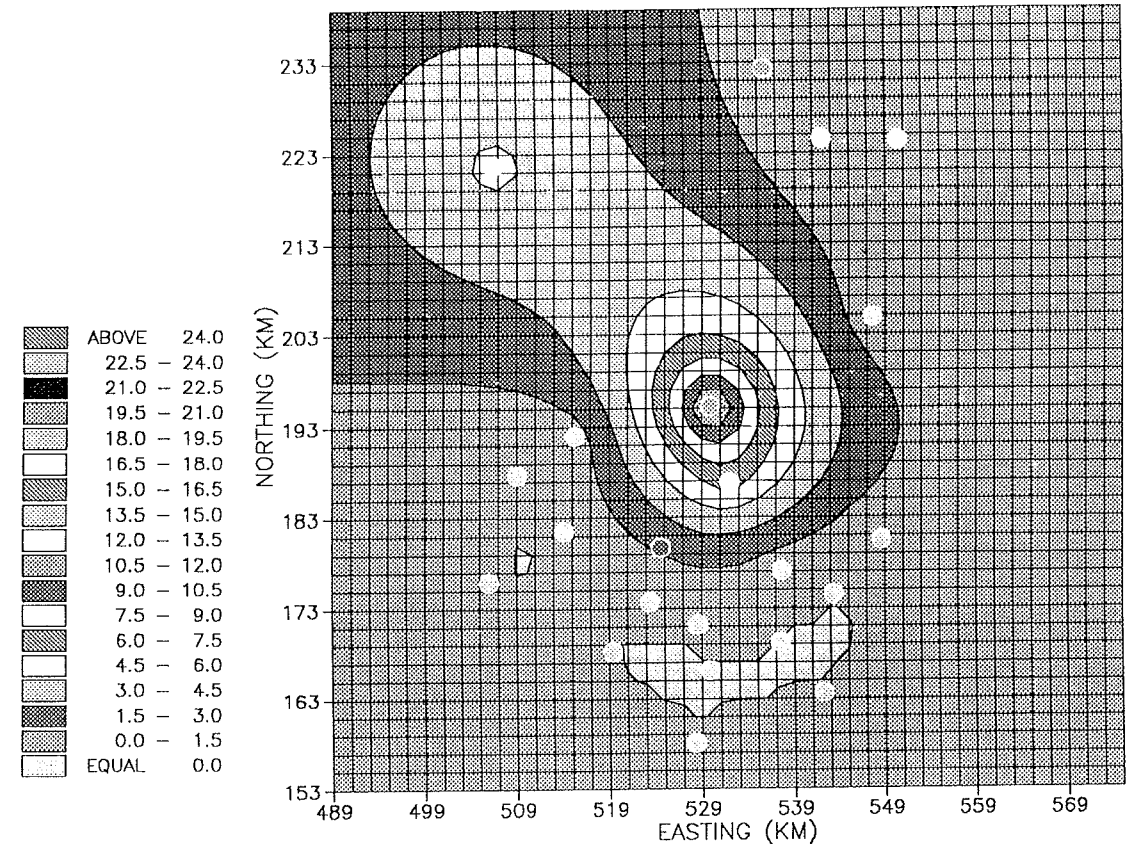

Figure 6.2 Raingauge-only rainfall field corresponding to Figure 6.1.

field which extends over the network of 30 raingauges in the London and Lee Valley area. The recalibration software has the capability to define a user-prescribed window within the radar field: this is used in the operational system to restrict the display to this area. In addition, the program is robust to any data loss caused by a failure to receive raingauge data, the procedure adapting automatically to perform recalibration using the reduced set of gauges. A further Study is required to investigate an appropriate recalibration method for use over the rest of the NRA Thames Region's area of responsibility.

The prototype recalibration system has been operating in support of the NRA Thames Region's flood warning service to the London and Lee Valley area since 14 March 1989, and the raingauge-only rainfall estimator became operational in September 1989. The revised procedures recommended here require only minor modification to the operational software. Finally, and of particular importance, is the speed of execution of the recommended procedures based on multiquadric surface fitting methods: it takes less than 25 seconds of central processor unit time on a VAX 11/750 to perform decalibration, surface fitting to the calibration factor values, and recalibration.

Appendix I: Site Description of Raingauges

Table I.1 provides a list of the recording raingauge sites used in the study together with their grid reference and altitude. The gauges employed are of the Didcot Tipping Bucket type with a tip interval of 0.2 mm. Descriptions of some of the sites have been supplied by Mr M.J. Hopper, Met 01e (Rainfall), of the Meteorological Office and these follow. Most of these sites telemeter data to the National Rivers Authority Thames Region offices at Waltham Cross via the VAX computer at the Thames Barrier: the exceptions are sites 31, 32 and 33 used for at-site radar calibration which are telemetered via the Ferranti Argus computer located at the NRA Thames Region offices in Reading.

1. Crossness S. Wks Stn. No. 290007

Over-shelter	from	trees	190-220	deg.	Max	elevation	40	deg.	at	210	deg.
"	"	"	220-240	"	"	"	30	"	"	230	"
"	"	"	280-330	"	"	"	43	"	"290-310		deg.

The site does suffer from a fair amount of over-shelter. The situation could be improved by the felling of one or two trees or by moving the gauge as there appears to be several possible locations in this very large works.

2. Eltham High Street Resr. (Unregistered)

Non-standard roof site
The gauge is located on the pump-house roof. This appears to be purely for convenience. A more satisfactory site - on the grass covered reservoir - would involve a cable run of about 100 feet.
The station is not registered with the Met. Office due to the unorthodox nature of the site. Gauges situated on flat roofs can be subject to varying degrees of turbulence which could affect the catch. However for flood control purposes the errors may not be significant, but it is difficult to be sure.

3. Greenwich (Deptford) P. Sta. Stn. No. 289101

Over-shelter	from	tree	340-050	deg.	Max	elevation	43	deg.	at	030 deg.
"	"	"	070-080	"		elevation	40	deg		
"	"	house	200-220	"		"	35	deg		
"	"	offices	020-070	"		"	28	deg		

Not a particularly good site; the gauge being situated in the grounds of a very small pumping station and surrounded on all sides by trees and buildings and therefore suffers from a fair amount of over-shelter. However this is to be expected in inner London and the site is therefore acceptable to the Met. Office.

Table I.1 Location and height of raingauges

	Station Name	Grid reference		Height of gauge AOD (m)
1	Crossness STW	5486	1805	8
2	Eltham High Street	5433	1745	75
3	Deptford PS	5377	1771	5
4	Keston	5422	1636	172
5	Kelsey Park	5375	1692	35
6	Beddington STW	5299	1661	35
7	Putney Heath Reservoir	5234	1737	56
8	Furzedown Recreation Ground	5286	1712	40
9	How Green Reservoir	5283	1581	161
10	Hogsmill Valley STW	5194	1682	12
11	Perry Oaks	5060	1759	23
12	Uxbridge (Hillingdon Court Park)	5075	1840	40
13	Ruislip Manor	5090	1877	45
14	Harrow Weald Cemetery	5153	1920	98
15	Mill Hill Cemetery	5231	1917	78
16	Green Lanes	5320	1868	31
17	Holland Park	5246	1797	21
18	Greenford Cemetery (Ealing)	5141	1815	23
19	Oakwood Park	5299	1952	67
20	Brent Reservoir	5208	1870	42
21	Nags Head Lane	5565	1914	40
22	Thornwood	5476	2048	76
23	Chigwell	5424	1926	19
24	Runley Wood	5064	2217	137
25	Braughing Friars	5420	2245	116
26	Hertford	5338	2134	37
27	Chipping	5357	2323	104
28	Stansted	5504	2243	79
29	Hornsey	5308	1894	33
30	Stevenage	5274	2211	70
31	Cranleigh (Guildford)	5041	1392	47
32	Chieveley (Newbury)	4469	1739	104
33	Stansted (Met. Office)	5503	2243	79
34	Bretch Hill (Banbury)	4444	2240	152
35	Chigwell (Met. Office)	5423	1926	15

4. **Holwood (Keston) Stn. No. 291210**

Over-shelter from tree 010-030 deg. azimuth & 35 deg. elevation.
Over-shelter from trees 050-100 deg. " & 35 deg. "

A secure site in an ornamental garden at the offices of a large company with some over-shelter but generally reasonably good exposure.

5. **Kelsey Park (Unregistered)**

Non-standard roof site.
Gauge is located on shed roof. A poor unorthodox site with considerable over-shelter from a line of tall trees from North North East to South South East and possible splash-in problems from a nearby sloping roof. There is no other site available in the immediate vicinity.

6. **Beddington New S. Sks. Stn. No. 287864**

Over-exposure to winds from 250-320 deg. azimuth.

A reasonably good site subject to some over-exposure and possible turbulence due to buildings scattered around this large sewage works.

7. **Putney Heath Resr. Stn. No. 287283**

A very good site with no exposure problems, the gauge being situated on a grass covered reservoir with trees at a distance on all sides.

8. **Streatham, Furzedown Rec. Grnd. Stn. No. 288020**

Over-shelter from conifer tree 270 deg. azimuth, elevation 30 deg.

A good site by the bowling green in a public park in suburbia with just a slight amount of over-shelter.
Vandalism or at least interference from the public is a possibility.

9. **How Green Resr. Stn. No. 287451**

A good site with no exposure problems.

The gauge is situated on a grass-covered reservoir belonging to the Sutton District Water Co. with trees and housing on all sides at a distance.

10. **Hogsmill Valley S. Wks. Stn. No. 286392**

A good site with no exposure problems.

11. Longford, Perry Oaks S. Wks. Stn. No. 247570

Slight over-shelter from tree 300-320 deg. elevation 30 deg.

Basically a good site with the gauge situated on a level area between two lagoons with sloping grass sides in a large sewage works at the western side of Heathrow Airport.

12. Uxbridge, Hillingdon Court Park Stn. No. 247337

Over-shelter from a tree 050-080 deg. Max elevation 40 deg. at 060 deg.
" " " 250-310 " " " 37 " " 260 "

An acceptable site suffering from some over-shelter from trees.
The gauge is situated in a small works compound at the side of a public park but it appears to be a reasonably secure site.

13. Ruislip, Manor Farm Bowling Green Stn. No. 279502

Over-shelter from tree 120-200 deg. Max elevation 57 deg. at 170 deg.

Although suffering from a considerable amount of over-shelter in the above sector this is not affecting the prevailing wind and the site is therefore considered to be a reasonable one.
The gauge is situated at the side of the bowling green and is fairly secure. There are indications that the groundsman may be somewhat careless with his water sprinklers in warm weather. Spurious results could arise from this and I intend to warn him about it.

14. Harrow Weald Cemetery (Unregistered)

Non-standard roof site
Gauge is located on office roof. Again an unorthodox site and the same objections apply as shown.

17. Holland Park (Unregistered)

Non-standard roof site.
Gauge is located at the edge of a sloping shed roof. A poor unorthodox site with possible splash-in problems from the sloping roof in addition to the usual problems with turbulence. There is no obvious alternative site in the congested nursery compound which is full of sheds and glasshouses.

20. Brent Resr. Stn. No. 246847

Over-shelter from tree 240-320 deg. max elevation 60 deg. at 270-290 deg.

A reasonable site despite some over-shelter from a small tree.

31. Cranleigh S. Wks. Stn. No. 282289

A very good site with no exposure problems.
Gauge located on small grass area at side of sewage works.

32. Chieveley S. Wks. Stn. No. 268851

Over-exposure to winds from most directions.

An acceptable site but not particularly good.

33. Stansted Mountfitchett S. Wks. Stn. No. 243131

Over-exposure to winds from 150-260 deg.
" " " " 300-330 "

A reasonably good site despite some slight over-exposure.
Gauge located at side of small works and surrounded by open fields.

Appendix II: Synoptic conditions for the events

This Appendix provides a brief synoptic description of the 32 rainfall events used in the Study. A midday synoptic chart for each event, taken from the Meteorological Office Daily Weather Summary, is included at the end of the Appendix (Figure II.1). The synoptic summaries follow.

Event 1: 11.05 29 March 1986 to 22.45 29 March 1986

A low of 986 mb was situated off North West Scotland during the day. In central and southern counties of England and Wales many places had several heavy showers with hail and sleet and there were a few thunderstorms. Temperatures were near or rather above normal in Eastern parts of Britain.

Event 2: 2.20 20 May 1986 to 20.00 20 May 1986

A high was situated over Eastern Europe. A cold front passed across Britain approaching from the west, occluding to the North as it did so. Thunderstorms over central southern England and the Midlands gave heavy rain in many places overnight, reaching the Vale of York by dawn. Severe flooding was reported from places in the Midlands. The thunderstorms continued to move north into the rest of Northern England and Southern Scotland in the morning with numerous reports of heavy rain and further storms over southern Britain. Drier conditions slowly moved across England from the west during the afternoon and early evening but the warm, humid air over eastern areas served to generate widespread showers and thunderstorms for the rest of the day. It became warm or very warm over southeast England and East Anglia.

Event 3: 13.35 08 July 1986 to 21.30 08 July 1986

A high of 1030 mb was fairly static out in the Atlantic. Mostly cloudy weather with patchy rain spread across the country overnight. During the morning the cloud became more broken generally with sunny spells developing. There were still some showers, however, and during the afternoon quite a few heavy showers and scattered thunderstorms developed over central, eastern and southern England. Some very heavy downpours occurred locally, and flooding was reported in the Maidstone area of Kent. Most places became fine during the evening. Temperatures were near normal in the south.

Event 4: 09.05 03 August 1986 to 22.45 03 August 1986

During the morning, a depression moved northeast from the Bay of Biscay into northern France. On its northern side rain, sometimes heavy and thundery, spread northwards into southern England, and the cloud covering and freshening northeast wind kept the weather very cool for the time of

year. Rain reached the Channel Islands around daybreak and spread northwards to much of England and Wales during the day. There was a lot of heavy rain in central southern and southeast England and East Anglia with quite a few thunderstorms in the afternoon.

Event 5. 18.35 10 August 1986 to 23 00 10 August 1986

A low situated to the southwest brought thunderstorms to some southern areas, especially in the afternoon and evening. Great Malvern, Hereford and Worcester recorded 41.4 mm in the 24 hours ending 09.00 GMT on 11 August 1986.
Temperatures over much of Britain were close or a little below normal but East Anglia, southeast and central southern England became warm or very warm.

Event 6. 10.05 25 August 1986 to 09.00 26 August 1986

A very vigorous depression (ex-tropical depression Charley) moved into south-west Britain bringing rain and gales to most parts of the country. The low had a central pressure of 981 mb as it sat off the southwest of Wales at 24.00 25 August 1989.
A lot of the rain was quite heavy and prolonged but during the evening it began to ease off in the Channel Islands and southwest England as the depression moved across England.
It was a cool day over the whole of the British Isles, and quite windy too for much of England. Lizard (Cornwall) reported a gust of 61 knots during the early evening.

Event 7. 05.50 04 January 1987 to 21.30 04 January 1987

Atlantic fronts moved across the country as a deep depression moved towards Iceland bringing wet weather to much of Britain.
Central and southern areas of England and southwest Wales had a cloudy night and day, with a little rain or sleet overnight, and dawn temperatures near freezing in the extreme east. During the day, the rain turned heavy and persistent before clearing southward in the evening.

Event 8. 23.50 07 June 1987 to 09.00 09 June 1987

A low of 995 mb was situated in the North Sea on 7 June 1987 and slowly moved off into Scandinavia on 8 June 1987.
On 7 June 1987 it became mostly cloudy in the afternoon with a wet afternoon in the Channel Islands: this rain spread to east Sussex and Kent in the evening. It remained very unsettled across the whole of the UK on the 8th with showers and longer spells of rain.
Rain was more persistent down the eastern half of the UK with heavy bursts in places and some thunderstorms were reported in the Midlands and southeast England during the day. Temperatures generally stayed well below normal.
The rain died out from the south and west during the 9th June, often

turning to showers first.

Event 9. 09.30 06 October 1987 to 09.00 10 October 1987

On the 5th and 6th a cold front moved east across the country accompanied by heavy rain. A deepening depression moved northeast near north Scotland on the 7th and 8th bringing rain and strong winds to most places, followed by showers and it was cold enough for some of these to fall as snow on the Scottish mountains. However, the south was affected by more fronts and it became very wet. In some parts of southern England more than 50 mm of rain fell in 24 hours on the 9th: 53.1 mm was recorded at Heathrow, London in the 24 hours ending 09.00 10.10.87.

Event 10. 18.15 20 October 1987 to 02.00 21 October 1987

A depression developed to the southwest of England and then proceeded to move up the Irish Sea with its associated frontal system.
The most persistent rain moved north from southwest England across Wales and northwest England, and into southern and eastern Scotland during the early hours of 20th October 1987. A further area of often heavy rain moved north from France into central southern and southeast England, London and the Midlands. The effect of this was that by midnight quite a few places in the south had had their wettest October of the century. The most rain recorded in the 24 hours ending 09.00 21st October 1987 was 41.3 mm at Bedford. Temperatures remained on the warm side of normal.

Event 11. 10.00 11 November 1987 to 06.00 12 November 1987

On the 11th and 12th, a deepening depression moved east from the Atlantic towards western Scotland and it brought strong winds and heavy rain to much of the country. At Guernsey 59.6 mm of rain fell on the 11th.
At daybreak on the 11th persistent and heavy rain reached Cornwall and this spread northwards and eastwards during the day, affecting Shetland in the evening. There was heavy rain and gales, particularly in the south.
The rain turned showery during the night petering out before dawn.

Event 12. 10.50 15 March 1988 to 20.45 15 March 1988

A deepening depression (975 mb at midday) moved up from the southwest causing rain to become heavy and widespread across the country. There were gales in places in the south. Brighter showery and still very windy weather spread east across Wales and much of England in the afternoon. There were heavy showers with hail in places, and also isolated thunderstorms.

Event 13. 13.20 20 March 1988 to 04.00 21 March 1988

A low moved from the south west across southern England during 20th March 1988. During the morning, cloud thickened quickly from the south, bringing outbreaks of heavy rain to the far southwest by midday. Some of

the heaviest rain fell in south coastal areas, and later more generally in the south eastern area of Britain.
Temperatures were well above normal in most places. In south coastal regions of England though, persistent low cloud, mist and fog, together with heavy rain, held temperatures around normal.

Event 14. 08.05 29 March 1988 to 10.00 30 March 1988

A double low structure was present over Great Britain, one low centred to the northwest of Scotland, the other over northern France. The Scottish low petered out late on 30 March, and the French low moved eastwards into the North Sea.
On the 29th, most places in England had rain, with persistent rain in central and southern England. In southwest and central southern England and East Anglia most places had a wet night, but much of England and Wales were clear and cold. The weather turned drier from the west during the afternoon and evening.

Event 15. 19.05 18 April 1988 to 23.45 18 April 1988

Late in the day areas of heavy rain and some thunderstorms spread northwards from France, while a cold front, moving slowly eastwards on the 19th, brought further showers. Outbreaks of rain spread slowly east into central and eastern England during the day, though many eastern, and particularly southeastern, districts were sunny for a time. There were scattered thunderstorms in northeast England in the afternoon and the southeast of England in the evening. Eastern and southeast England were very warm.

Event 16. 01.20 08 May 1988 to 23.45 08 May 1988

A depression and frontal system moved from the southwest across southern England into eastern France.
Thundery outbreaks of rain extended into East Anglia and the southeast overnight with some heavy thunderstorms in parts of west and northwest London but over the rest of the UK it was a mostly cloudy night.
The southern half of England and Wales became dry in the morning and brighter with some sunny spells. Further outbreaks of rain developed over East Anglia during the afternoon and in the late afternoon some severe thunderstorms formed over the Thames Valley from north Hampshire and Berkshire to west London; these moved north across the east Midlands during the evening before dying out before midnight. Uxbridge in northwest London received over 88 mm (3.47") of rain between midnight and midnight.
It was a very warm day over much of southern England.

Event 17. 16.05 08 June 1988 to 09.00 09 June 1988

A high pressure area was situated in the North Atlantic, whilst an area of low pressure was developing over Spain. An occluded front extended over Northern Europe bringing cool northeast winds and spells of rain to much of central and southern Britain. Some of the rain was heavy and thundery;

Stansted in Essex received a total of 26.2 mm in the 24 hours ending 09.00 09 June 1988.
An area of quite heavy rain moved west-southwest from Suffolk and Essex across the South Midlands to South Wales overnight which turned to drizzle during the morning, slowly becoming very light.

Event 18. 10.15 30 June 1988 to 16.45 30 June 1988

A depression formed to the west of Ireland and an associated front began to move slowly east across the country. This brought periods of rain to many parts and thunderstorms to some places. There was generally a lot of cloud over the country during the day, but it was bright at times in most places and became very warm and humid. From early afternoon, thunderstorms became widespread (moving north-north-east) over central, eastern and northern England. Very heavy rain occurred in some of the storms.

Event 19. 08.05 02 July 1988 to 21.00 02 July 1988

A double low structure was situated over Ireland and Scotland. Through the morning, showers quickly developed, with heavy, thundery showers reported, together with hail in places. It was a cool day in most places.

Event 20. 08.05 03 July 1988 to 22.00 03 July 1988

The northern of the double low systems moved away towards Scandinavia, whilst the southern low pressure centre moved eastwards across southern Britain and deepened. It produced the lowest July pressure in England since 1956. In its circulation, areas of rain moved northeast across the country. Brighter weather but still with showers reached southern counties in the late afternoon. There were some isolated reports of thunder in the extreme east of England.

Event 21. 00.05 04 July 1988 to 21.45 04 July 1988

The area of low pressure persisted over Britain slowly moving north. Many places had frequent heavy showers with some more persistent rain in northern England. Thunderstorms became widespread over central southern England, the Midlands, East Anglia, Lincolnshire and parts of Essex and north London from late morning to early evening, and hail was also reported.

Event 22. 07.05 06 July 1988 to 14.00 06 July 1988

An area of heavy rain moved north-east across England and Wales associated with a depression centred in western Scotland. Many places in southern England were sunny for a good part of the day, but most places had heavy showers and in central southern, southeast and eastern England along with East Anglia there were thunderstorms.

Event 23. 15.35 16 July 1988 to 08.30 17 July 1988

A complex frontal system existed over Britain associated with a depression centred south of Iceland. It turned cloudy during the 16th July and outbreaks of rain spread slowly eastwards. Overnight, it remained cloudy with rain and drizzle, some of the rain being heavy in places. The rain died out during the morning of the 17th.

Event 24. 17.05 21 July 1988 to 23.45 21 July 1988

A depression moved east across central Britain, bringing rain, and a number of thunderstorms to most places. Norwich Weather Centre, Norfolk recorded 42.0 mm of rain in the 24 hours ending at 09.00 22nd July 1988.

Event 25. 21.05 22 July 1988 to 03.15 23 July 1988

Very humid air affected much of England and Wales and there were periods of rain in most places. A warm front extended across far southern England associated with a low to the south of Ireland. During the evening, rain in the southwest moved northeast across England and Wales, the rain heavy in places.

Event 26. 01.45 31 August 1988 to 13.15 31 August 1988

A warm front moved eastwards across England. Central and eastern districts of England had heavy rain in the morning with quite a few thunderstorms, but by early afternoon the weather had brightened up.

Event 27. 22.15 31 August 1988 to 14.30 01 September 1988

A deep depression moved north across Ireland bringing strong winds and heavy rain to most of the country. The rain was accompanied by a strengthening southeasterly wind. By midday, it had brightened up over parts of Northern Ireland, Wales and the Midlands, this brighter weather spreading to other parts of England during the afternoon.

Event 28. 04.00 17 February 1989 to 15.30 17 February 1989

Frontal systems moved northeast across the country with rain which was preceded by snow in places. Rain over Cornwall spread steadily northeast reaching much of the southern half of England and Wales by dawn. The rain was heavy for a time in the south and turned to snow over the Midlands giving a few cms in places for a while. Brighter weather with a few showers spread to much of southern England during the afternoon.

Event 29. 14.15 26 February 1989 to 22.00 26 February 1989

A depression, which on the 25th had a central pressure of below 950 mbar

and in southern England brought the lowest recorded pressure since before 1870, moved away into the North Sea. During the day there was some sunshine everywhere and some places had a sunny day, but there were showers, most frequent in Wales and central and southern England, where they were heavy with hail and thunder and in places sleet or snow. In the late afternoon and evening there was a longer spell of rain, sleet or snow.

Event 30. 08.30 14 March 1989 to 23.00 14 March 1989

A depression moved quickly east across central Britain. It was cloudy and wet with heavy rain spreading to many places by early afternoon. In south Wales and southern England there was a lot of heavy rain and it turned windy here as well, with severe gales on coasts.

Event 31. 16.15 20 March 1989 to 00.45 21 March 1989

An area of low pressure in the English Channel brought rain to the south of the country. Wet weather reached west Wales around midday and spread across Wales, central and southern England and more southern parts of northern England. There was a lot of heavy rain and some sleet and snow too for a time in many places, especially over high ground in the Midlands.

Event 32. 11.00 24 May 1989 to 23.00 24 May 1989

An anticyclone over the Atlantic and a frontal system moving slowly down across the country from Scotland brought thunderstorms to many inland areas of England and Wales, which were locally severe with large hailstones, and caused flash flooding.
One or two isolated thunderstorms affected the Midlands, central southern England and North Wales during the morning. In the afternoon thunderstorms became more widespread with heavy rain and flooding across central southern England, the Midlands and parts of northern England. Some places had well over an inch of rain under the heaviest storms. During the evening the thundery activity became more confined to the East Midlands and northeast England.

Event 1

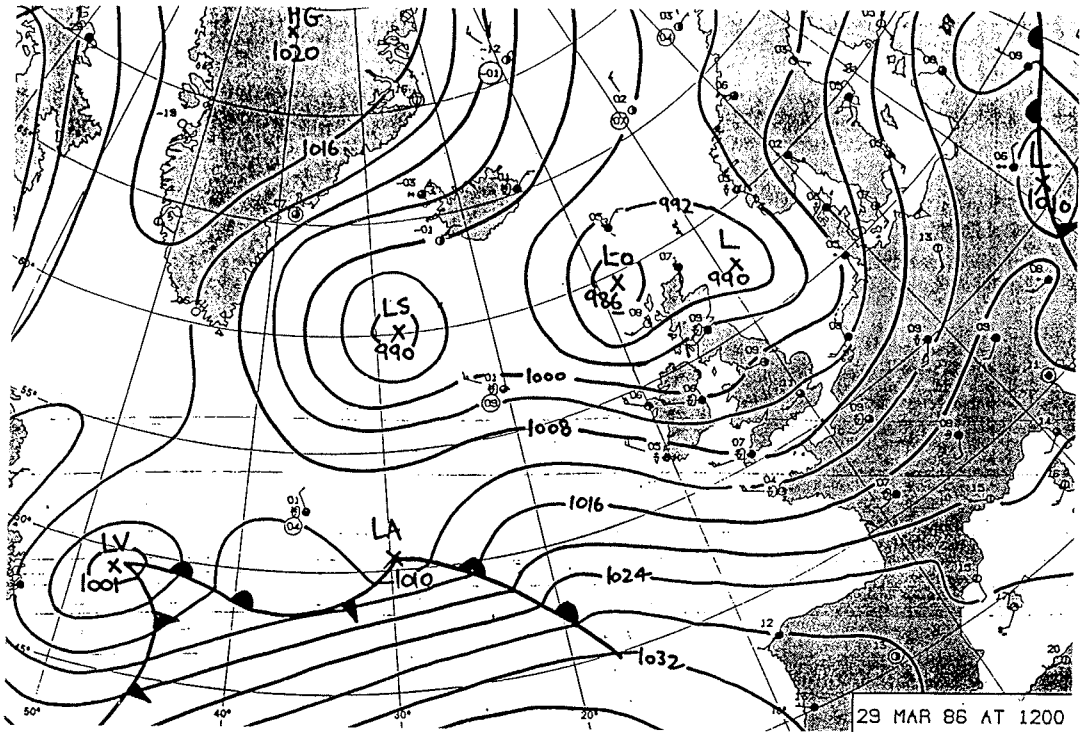

Event 2

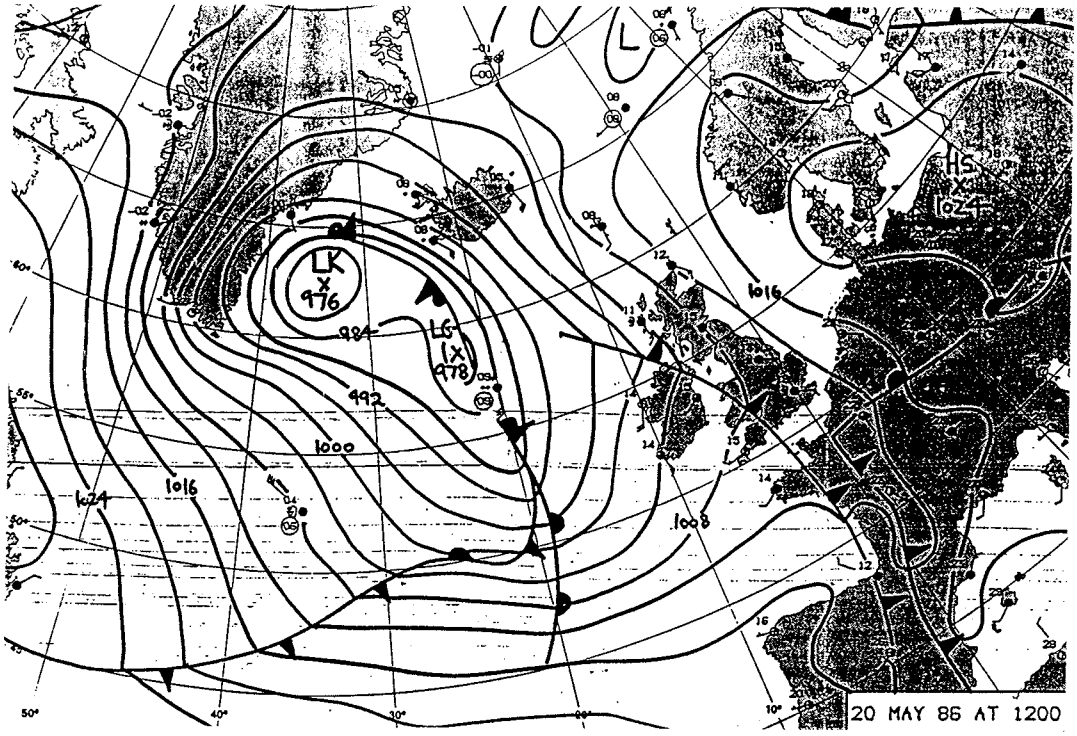

Figure II.1 Midday synoptic chart for each rainfall event

Event 3

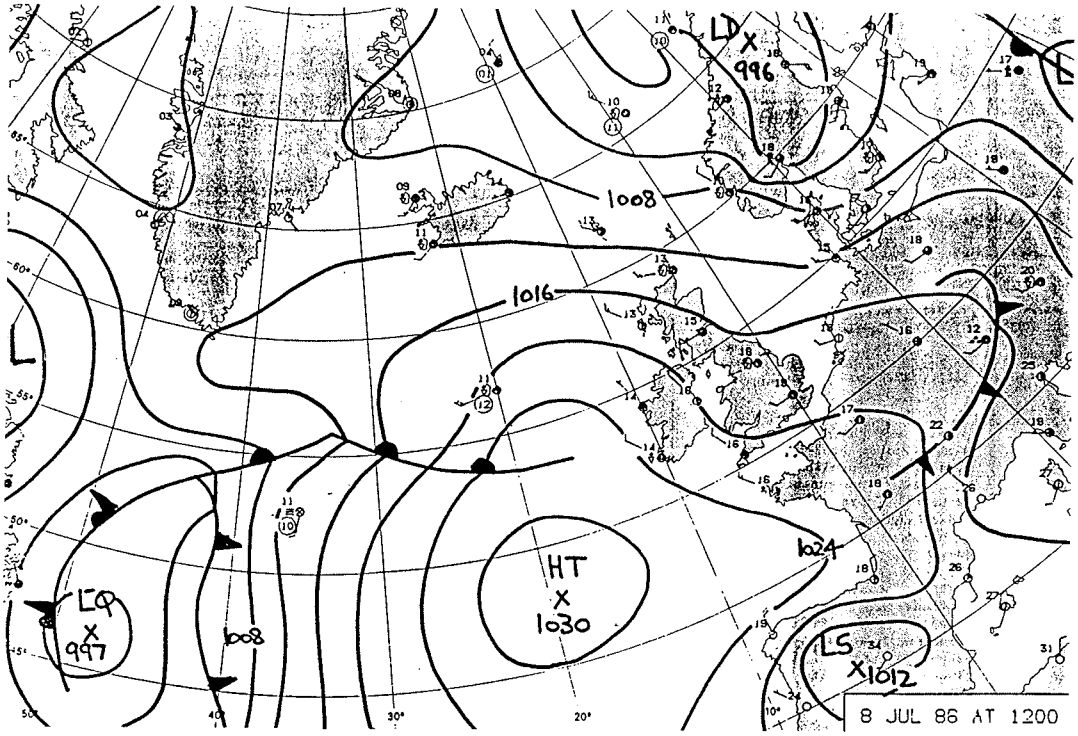

Event 4

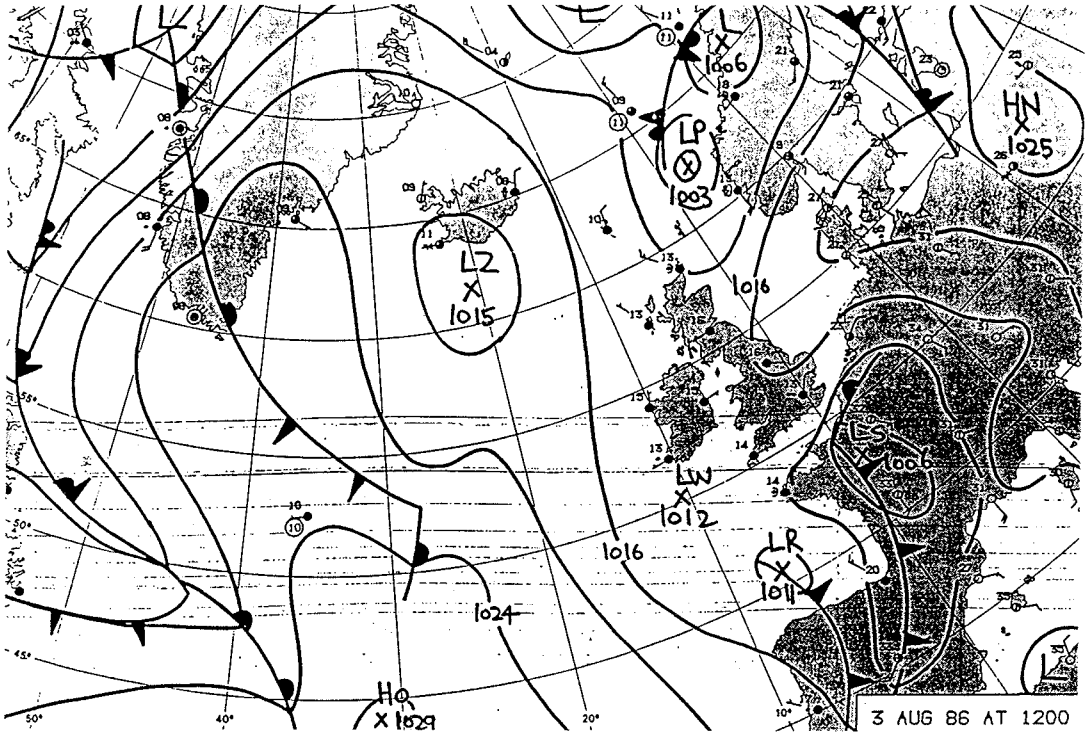

Figure II.1 Midday synoptic chart for each rainfall event

Event 5

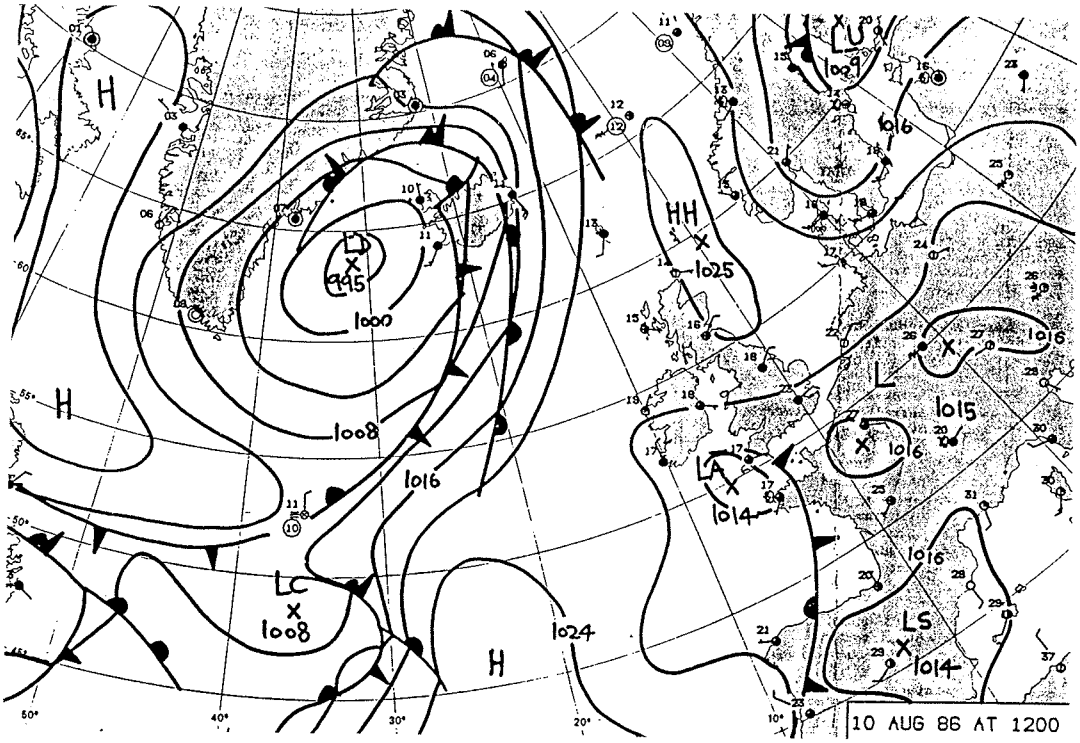

Event 6

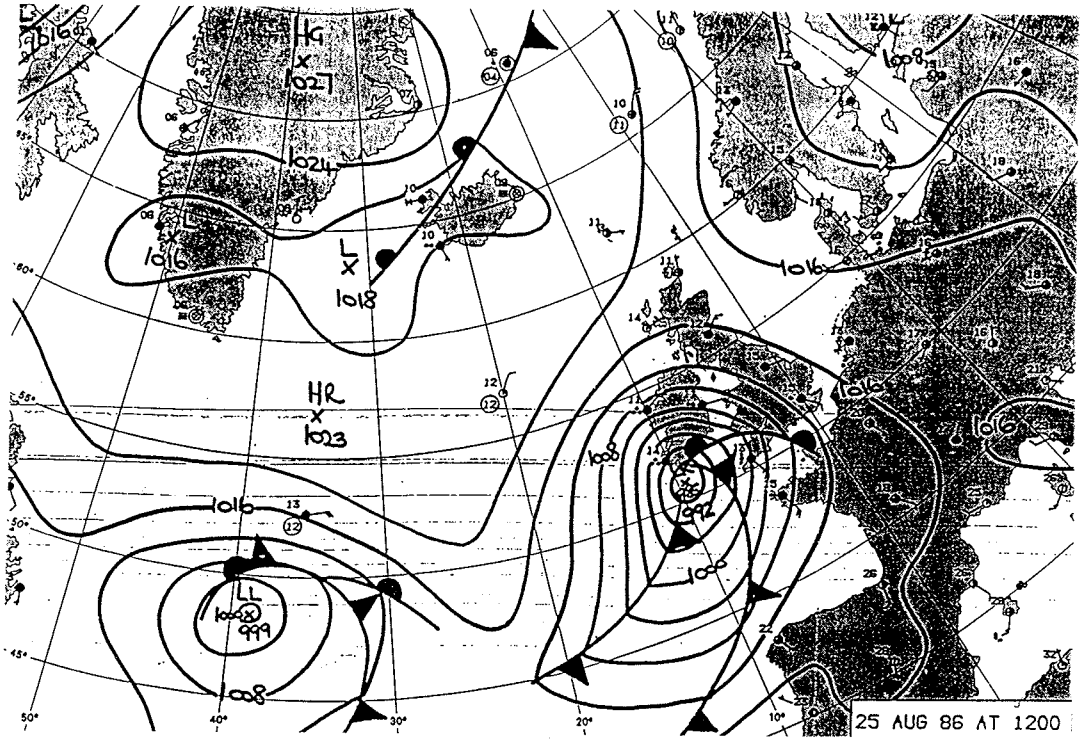

Figure II.1 Midday synoptic chart for each rainfall event

Event 7

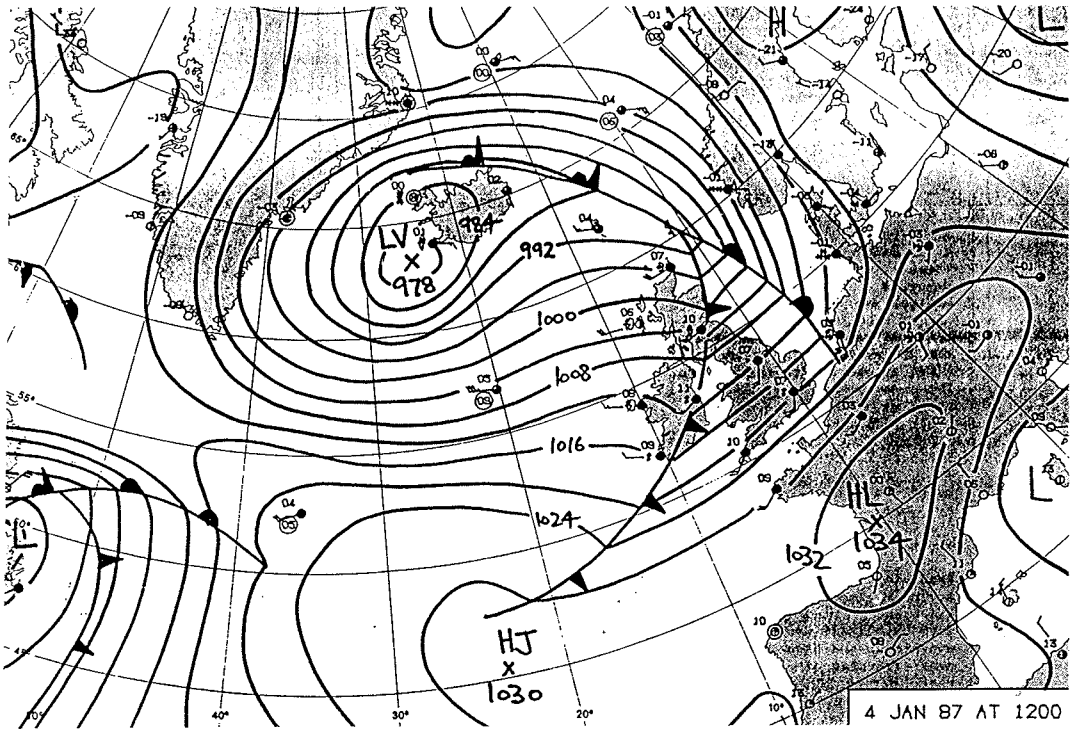

Event 8

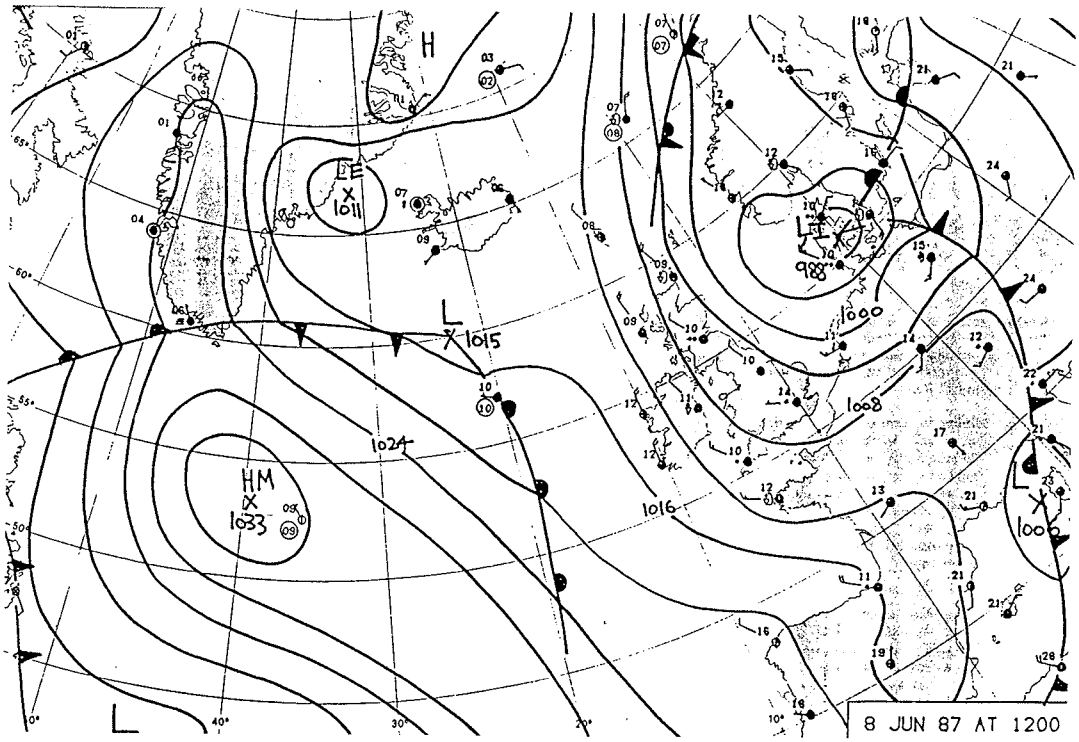

Figure II.1 Midday synoptic chart for each rainfall event

Event 9

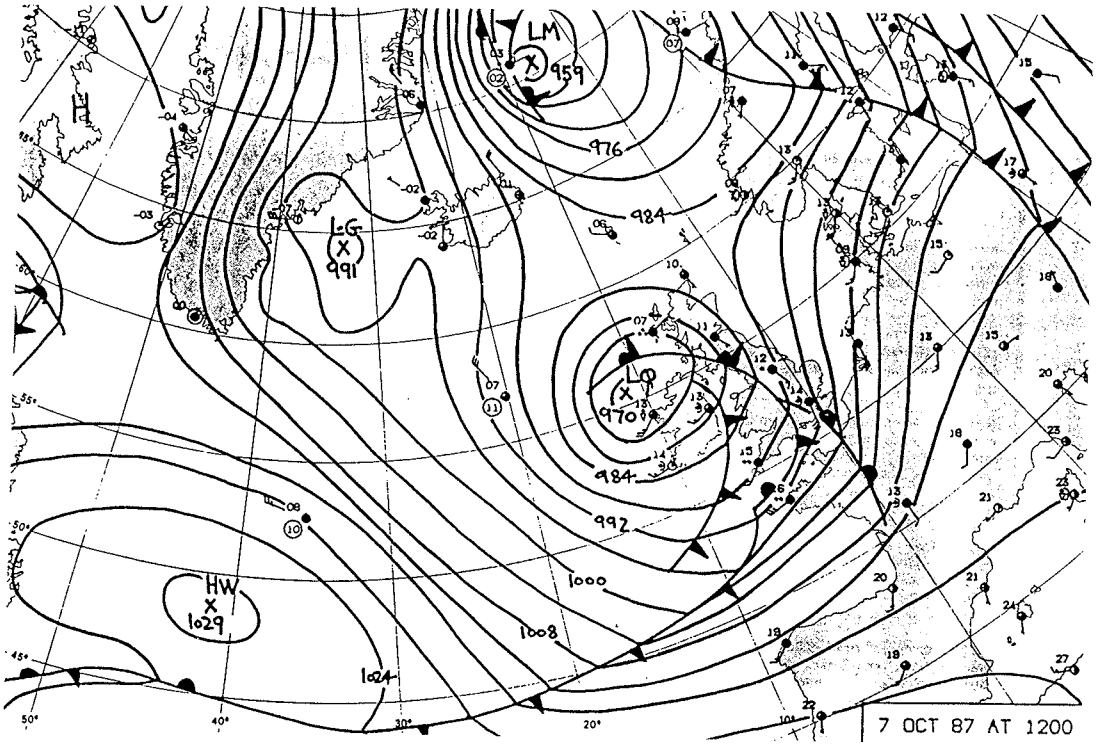

Event 10

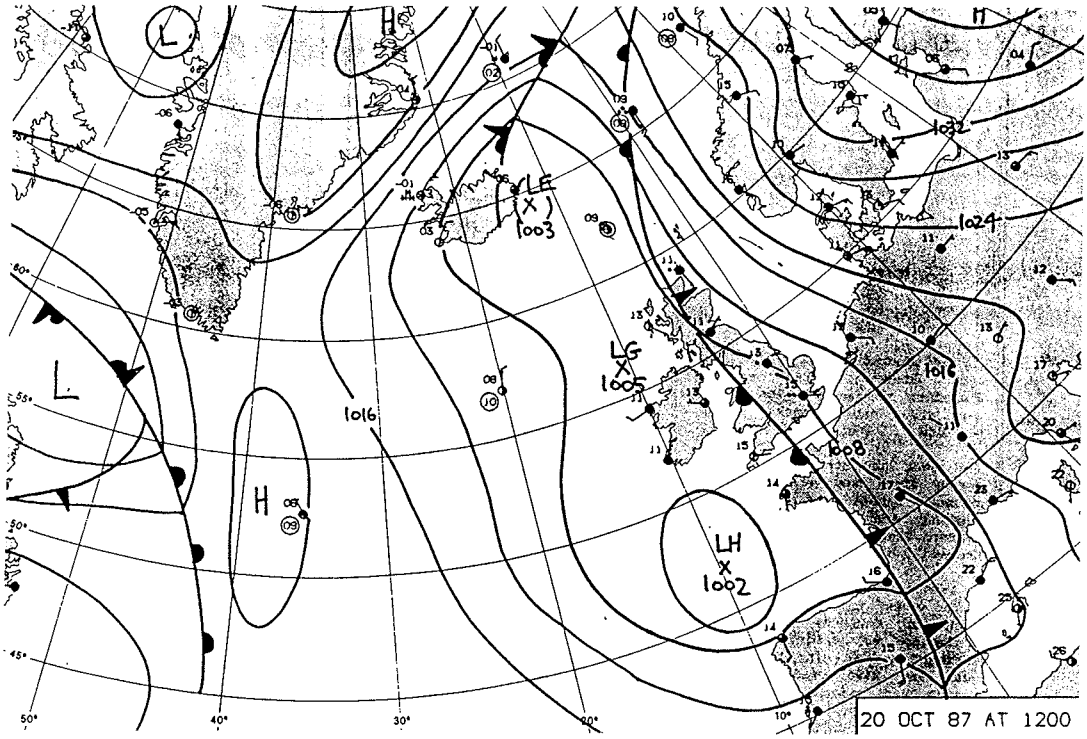

Figure II.1 Midday synoptic chart for each rainfall event

Event 11

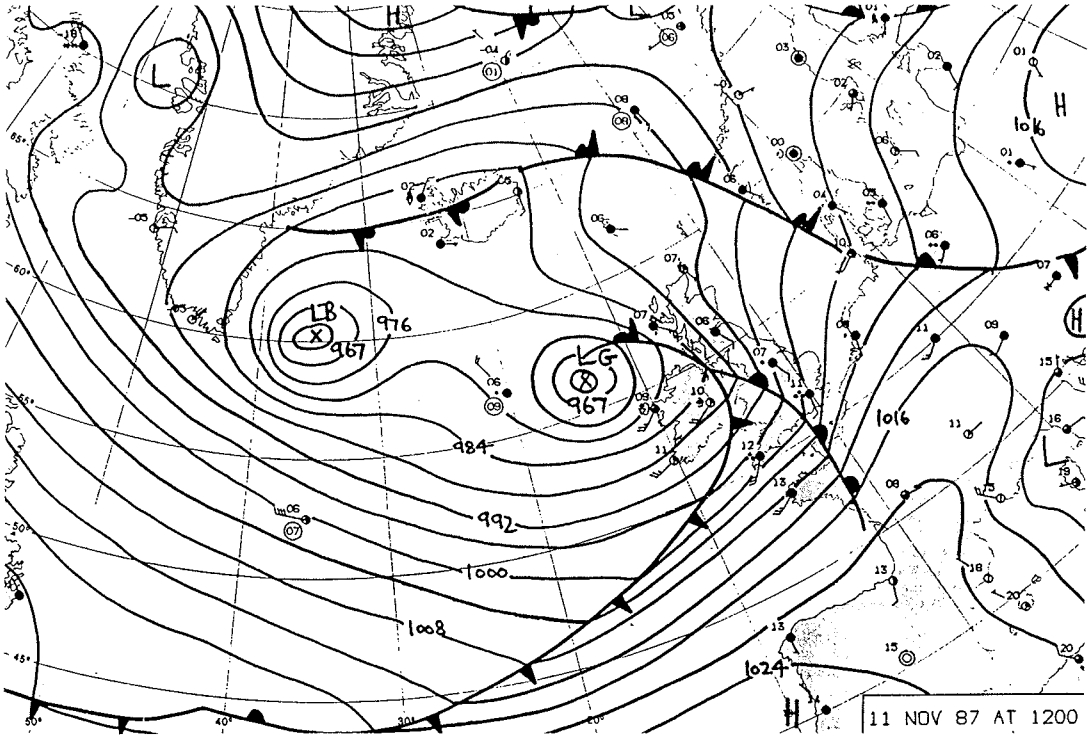

Event 12

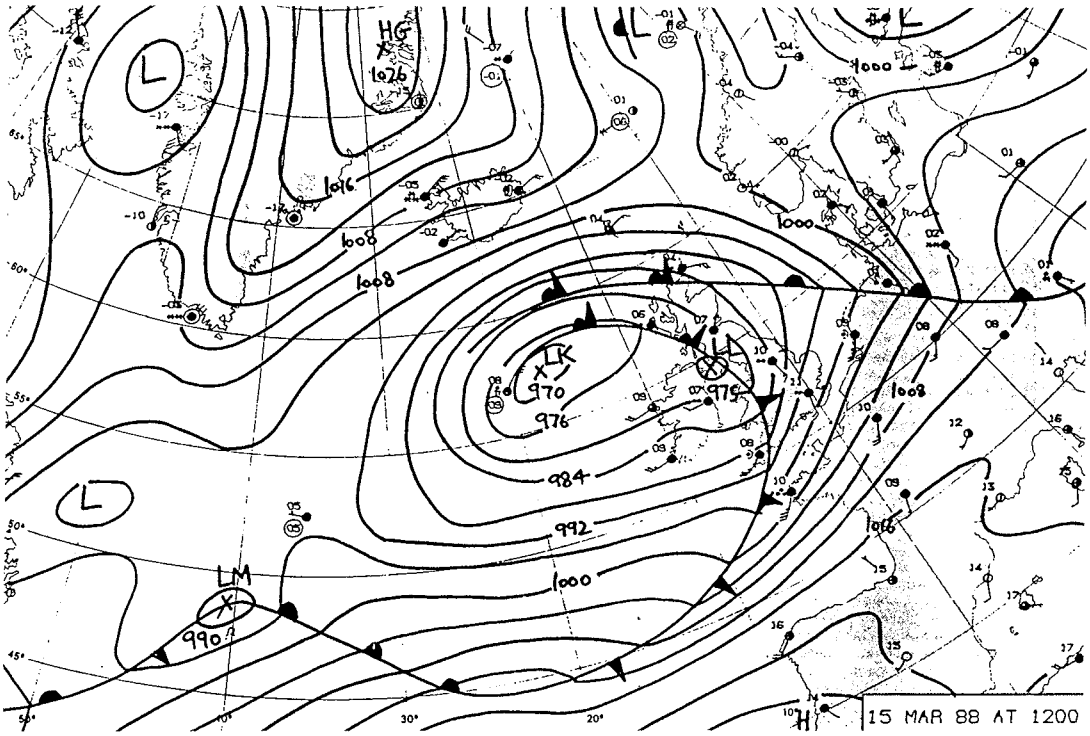

Figure II.1 Midday synoptic chart for each rainfall event

Event 13

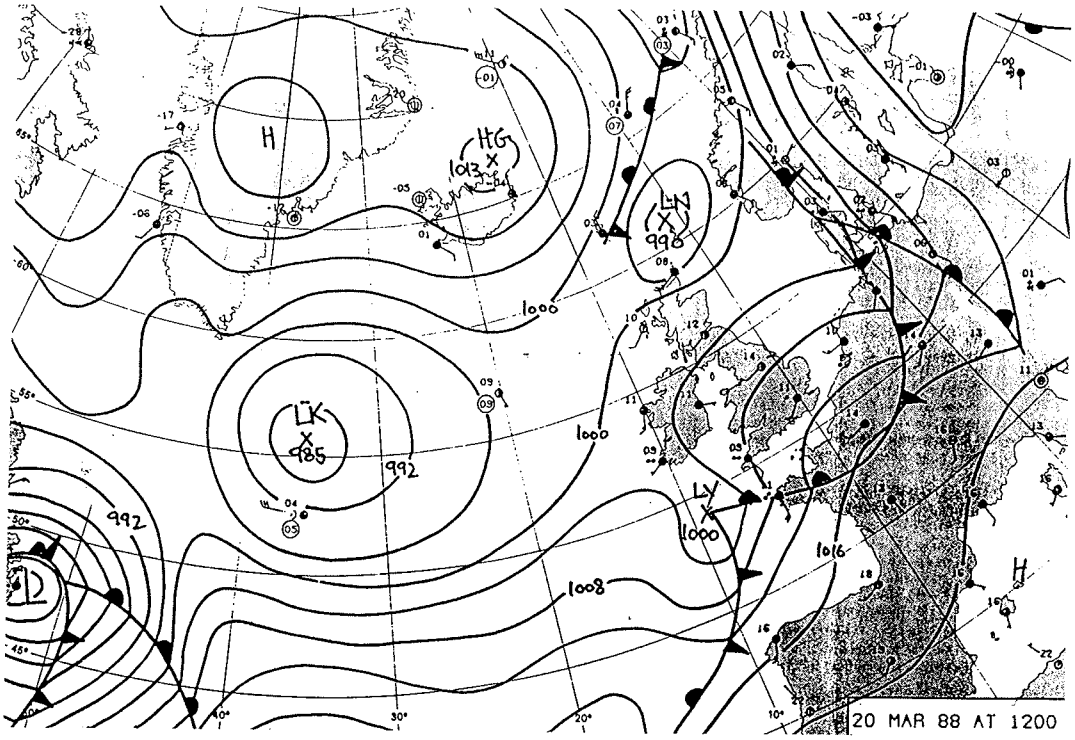

Event 14

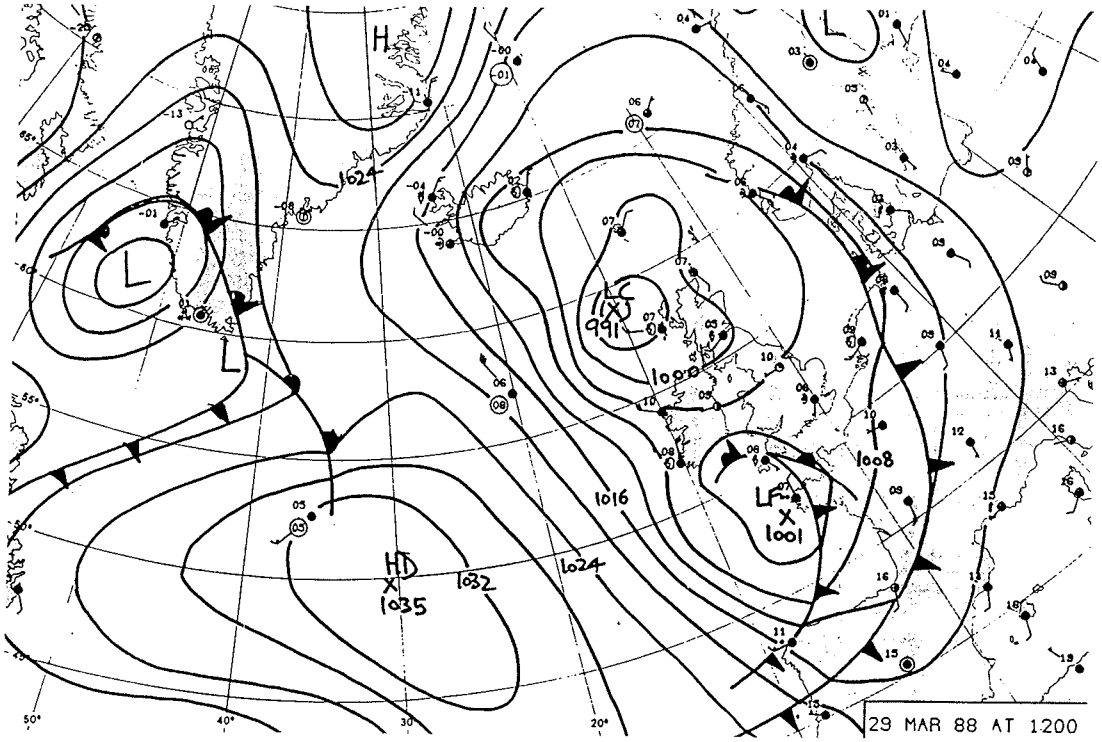

Figure II.1 Midday synoptic chart for each rainfall event

Event 15

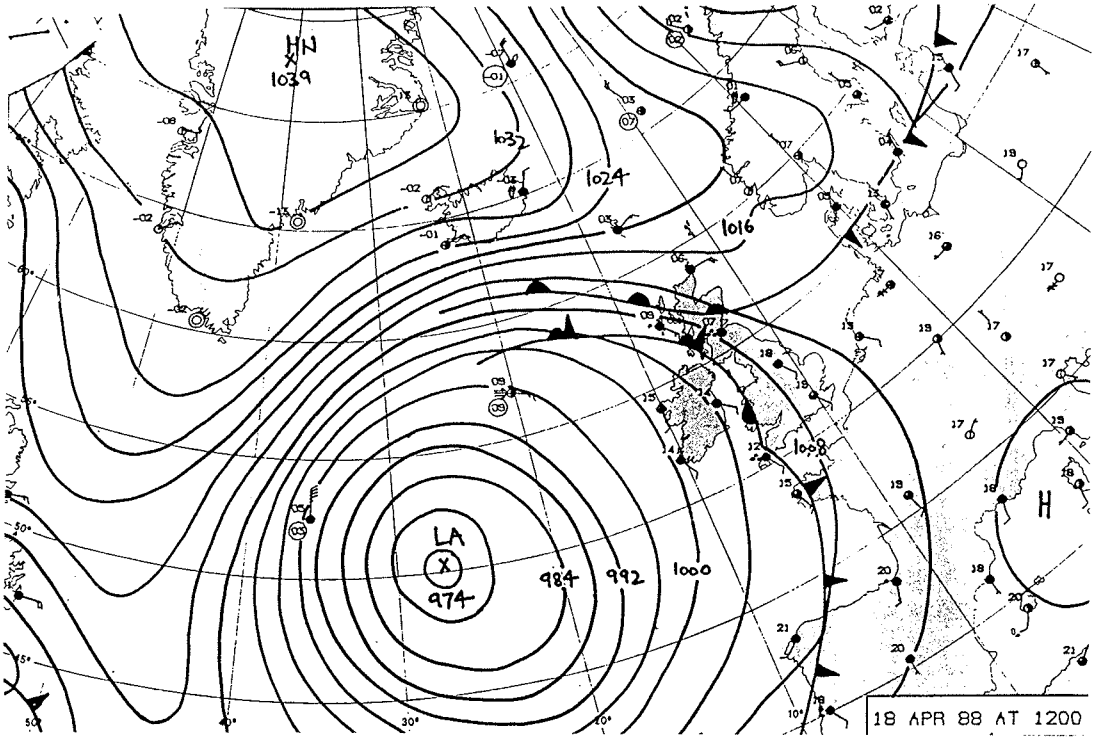

Event 16

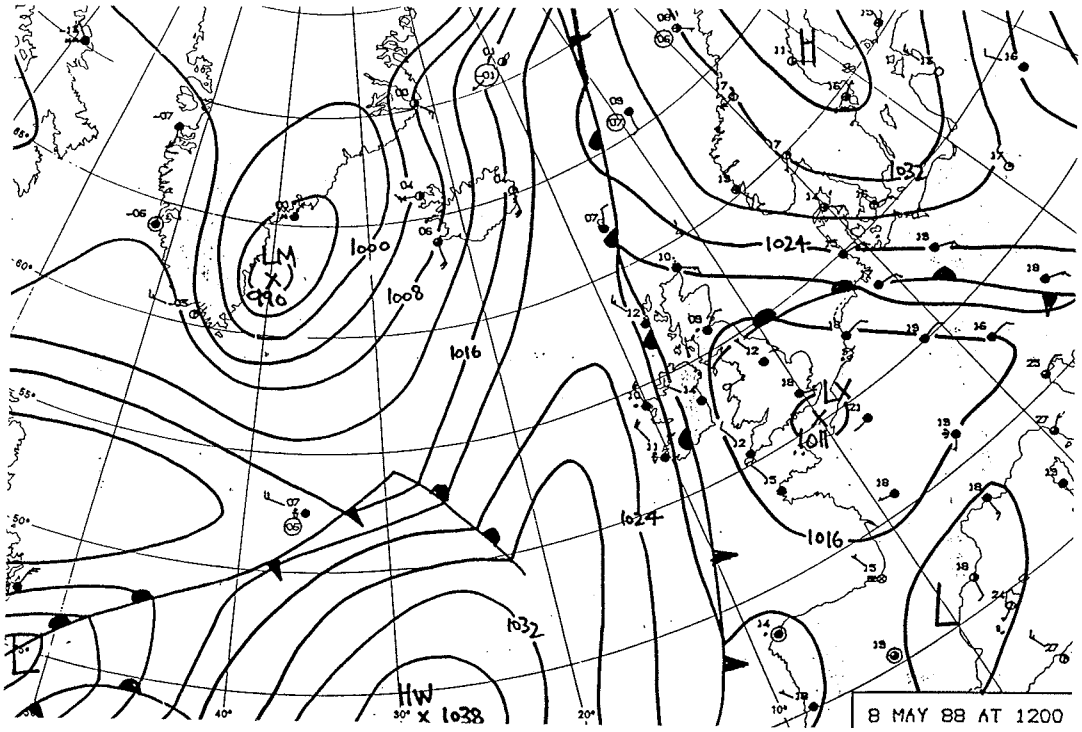

Figure II.1 Midday synoptic chart for each rainfall event

Event 17

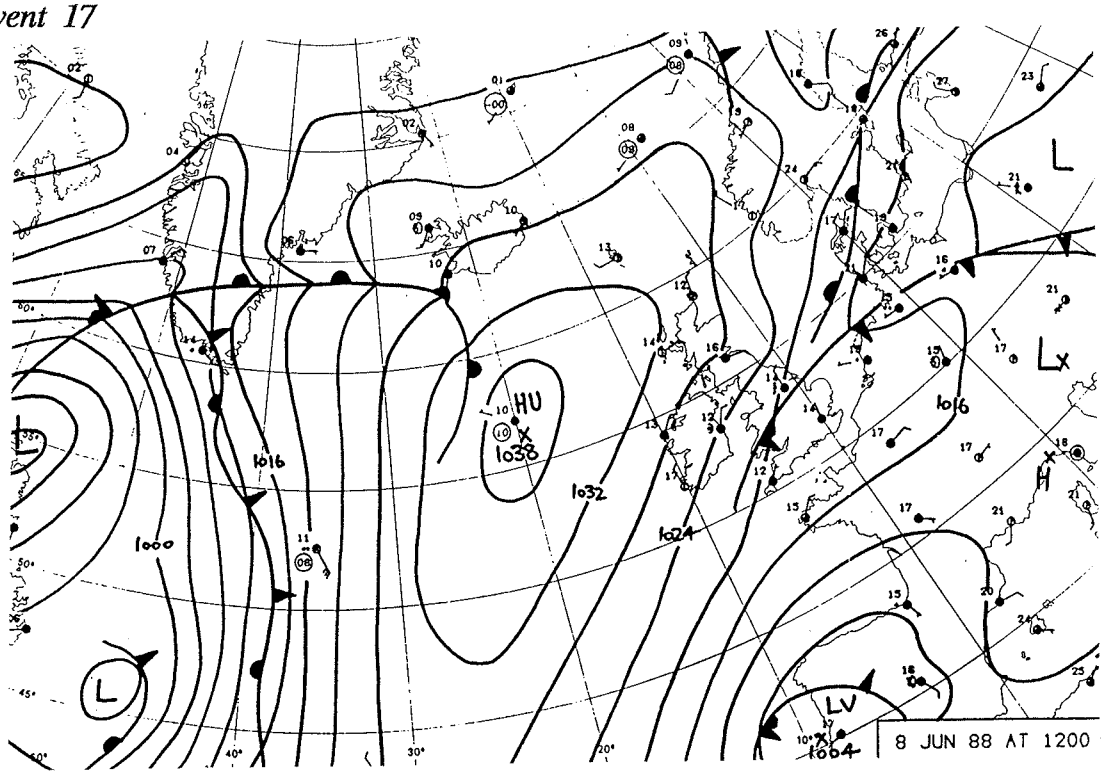

Event 18

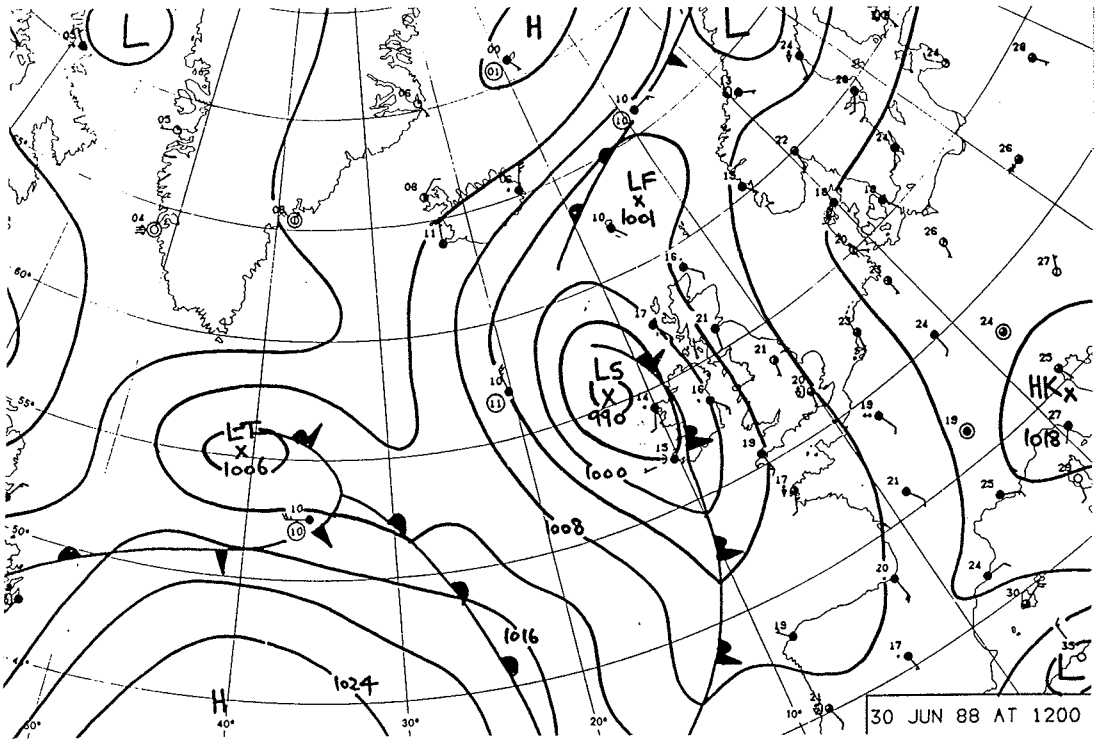

Figure II.1 Midday synoptic chart for each rainfall event

Event 19

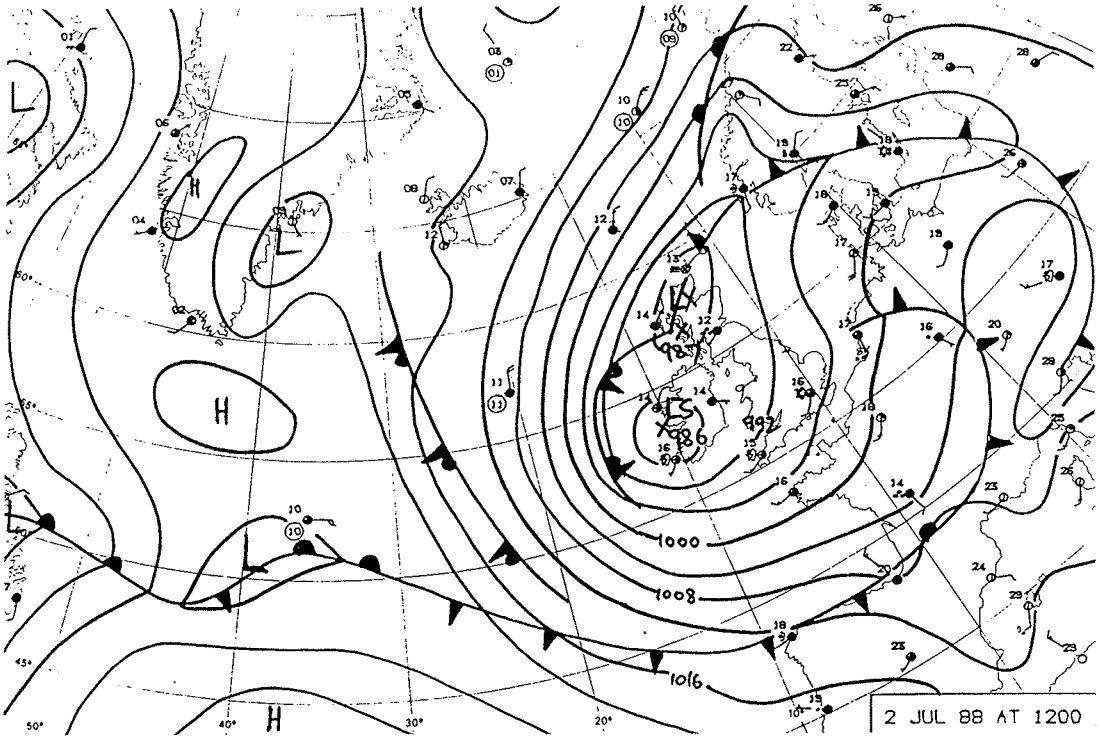

Event 20

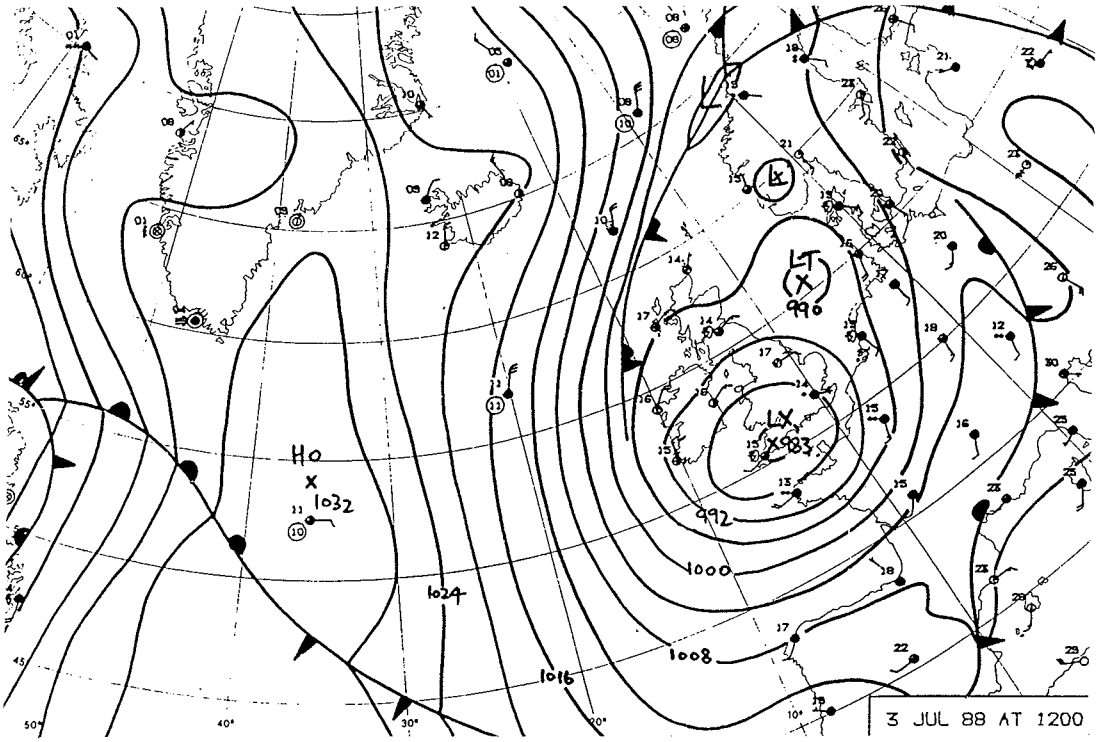

Figure II.1 Midday synoptic chart for each rainfall event

Event 21

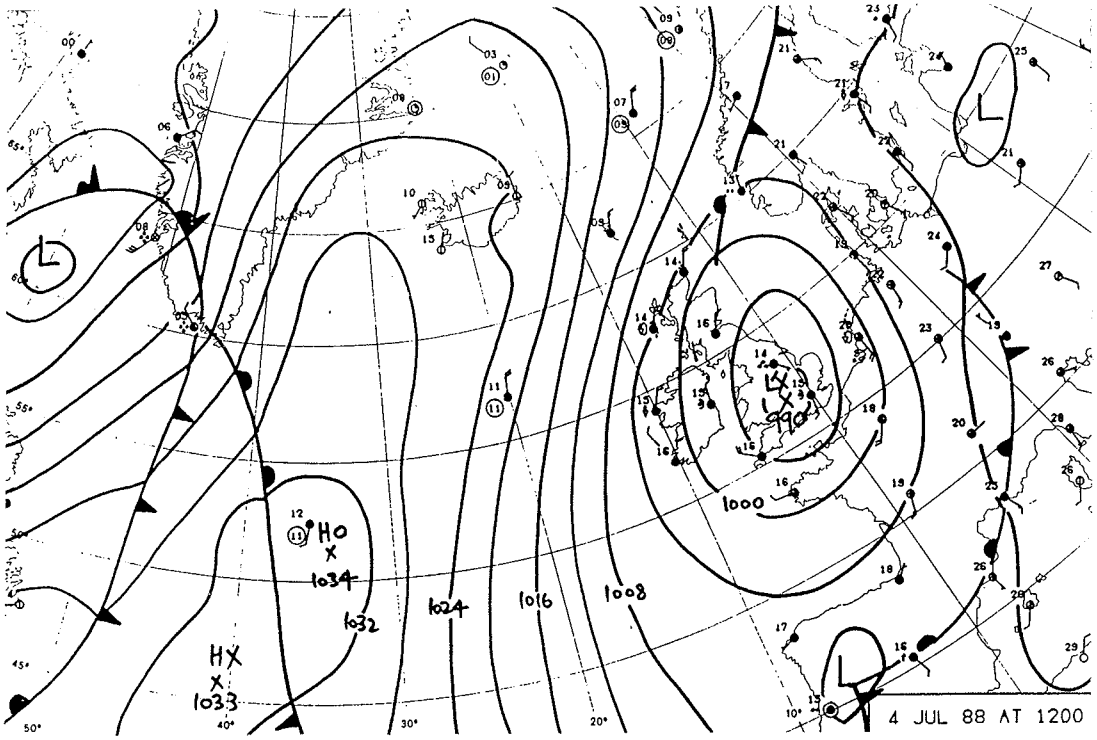

Event 22

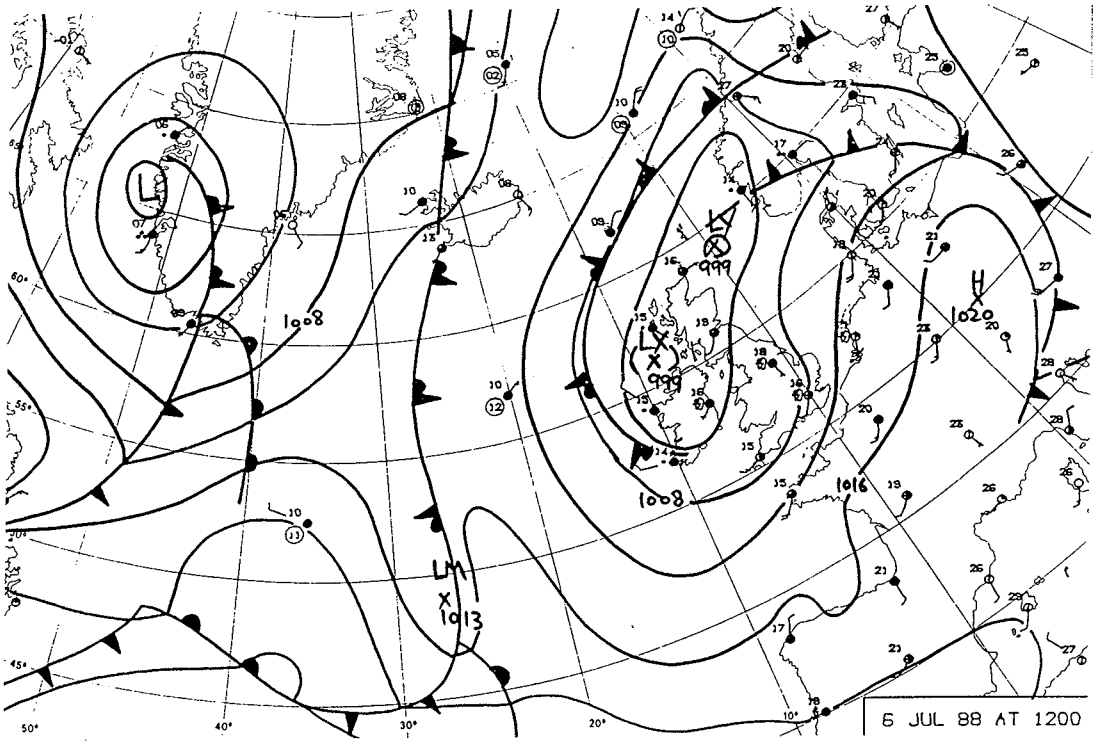

Figure II.1 Midday synoptic chart for each rainfall event

Event 23

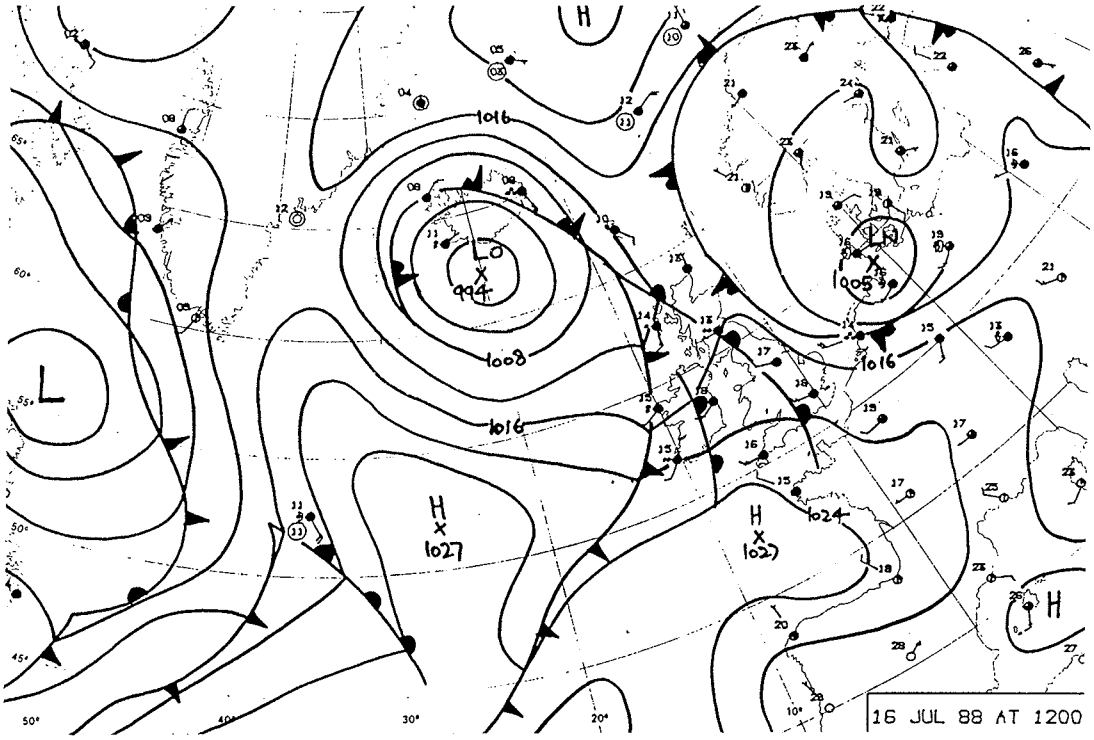

Event 24

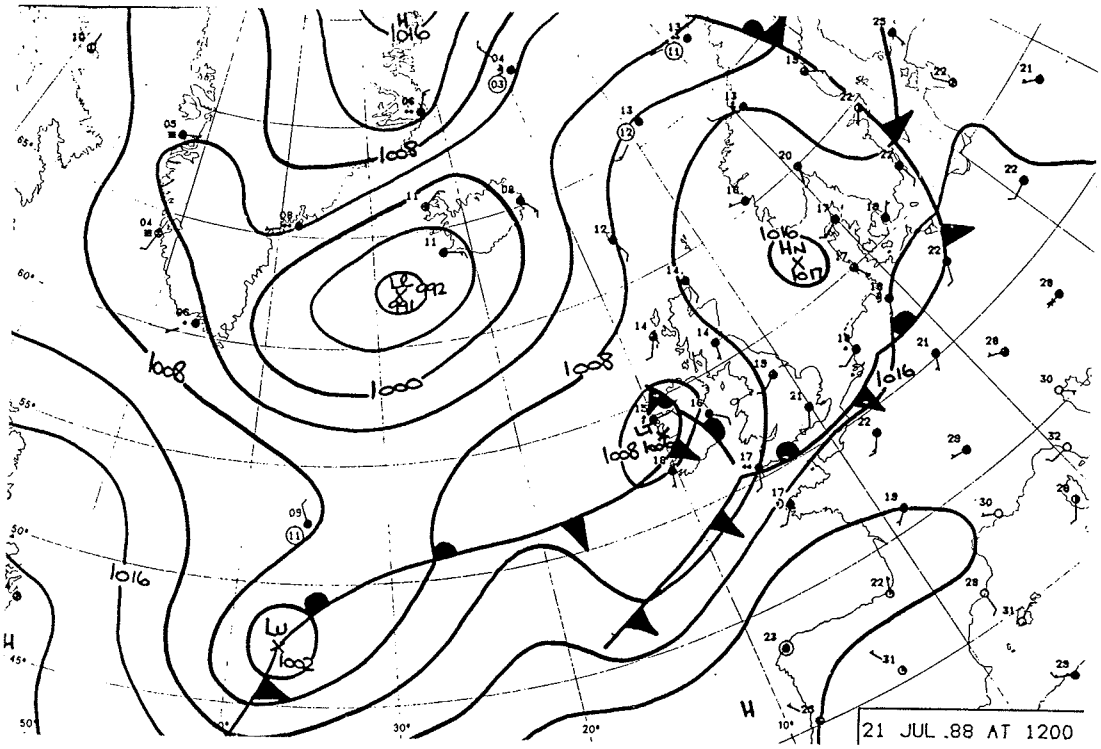

Figure II.1 Midday synoptic chart for each rainfall event

Event 25

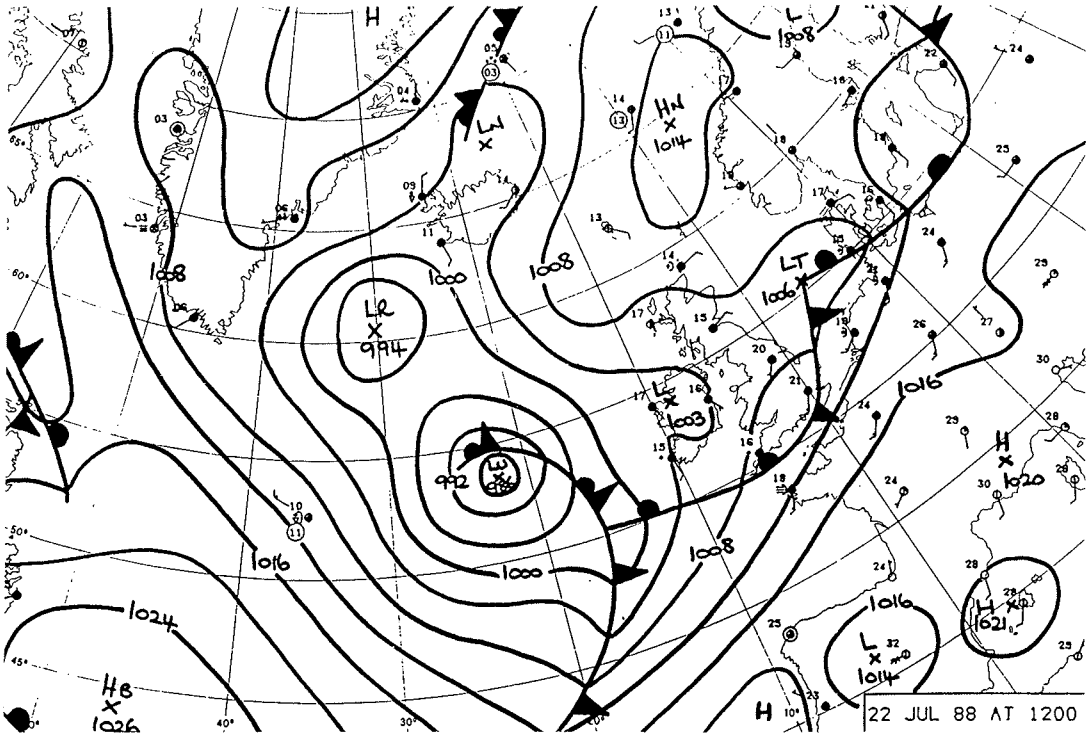

Event 26

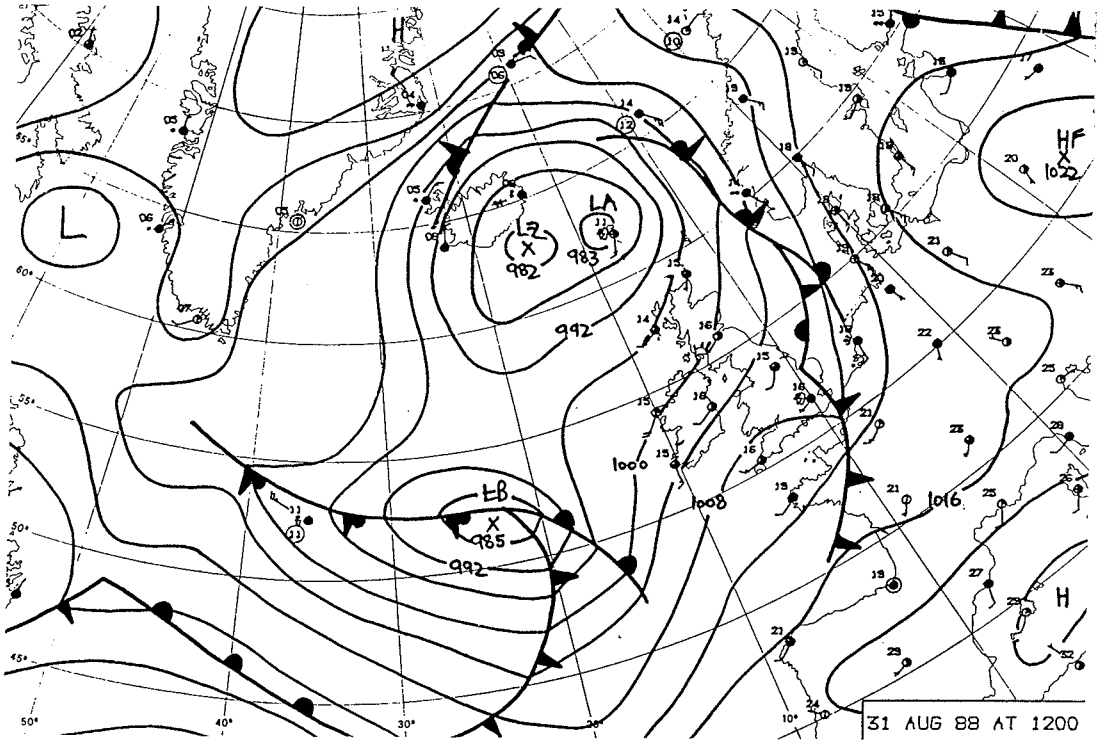

Figure II.1 Midday synoptic chart for each rainfall event

Event 27

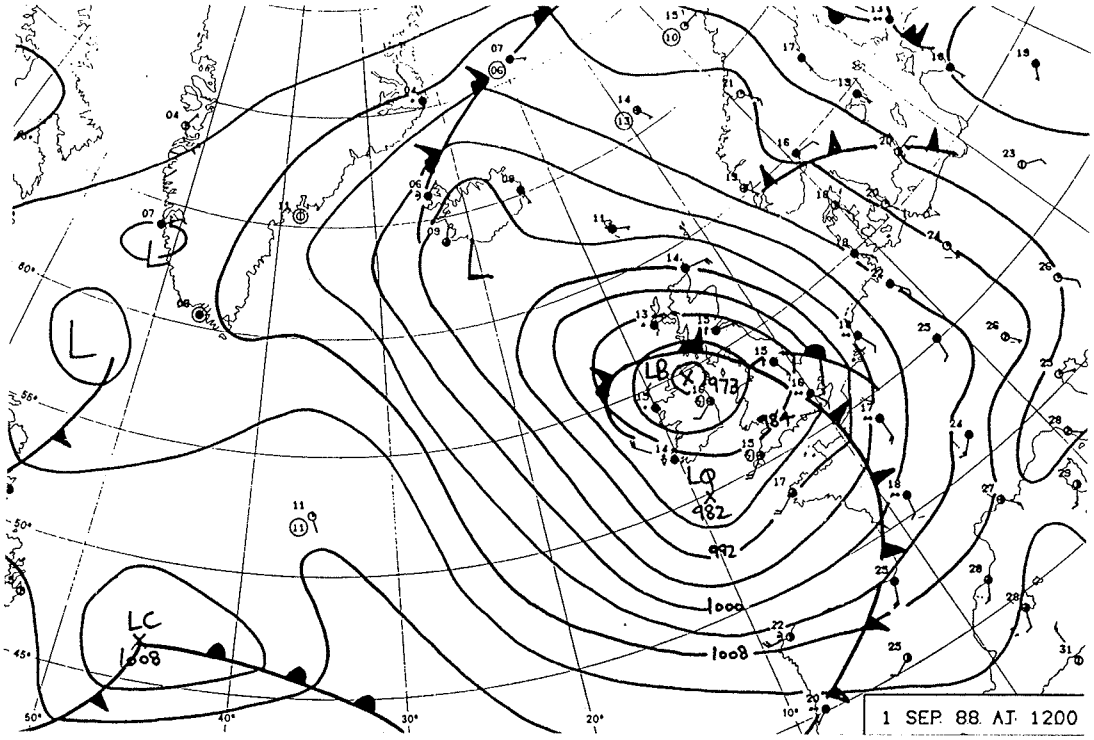

Event 28

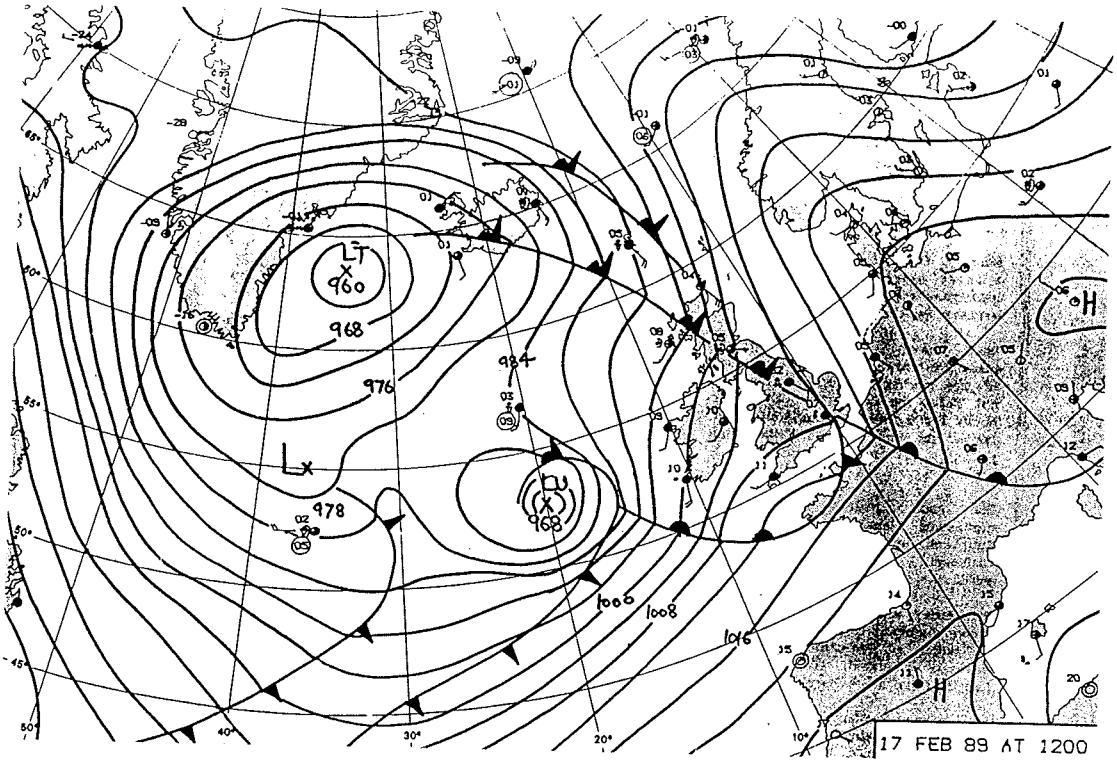

Figure II.1 Midday synoptic chart for each rainfall event

Event 29

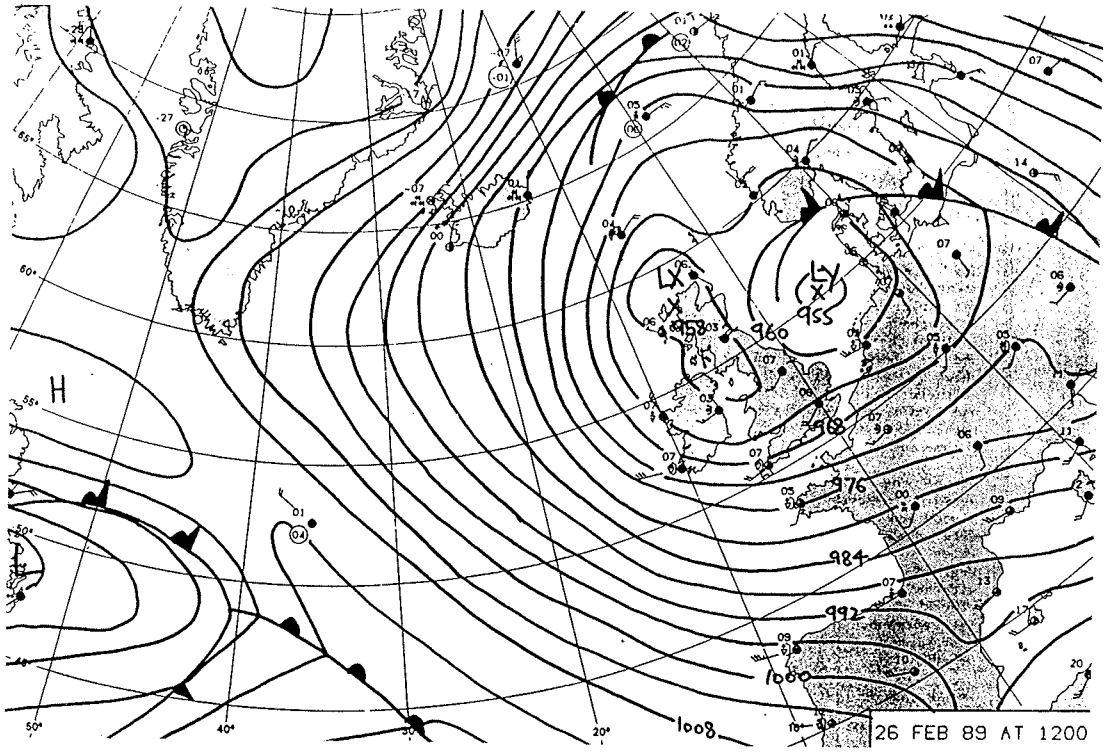

Event 30

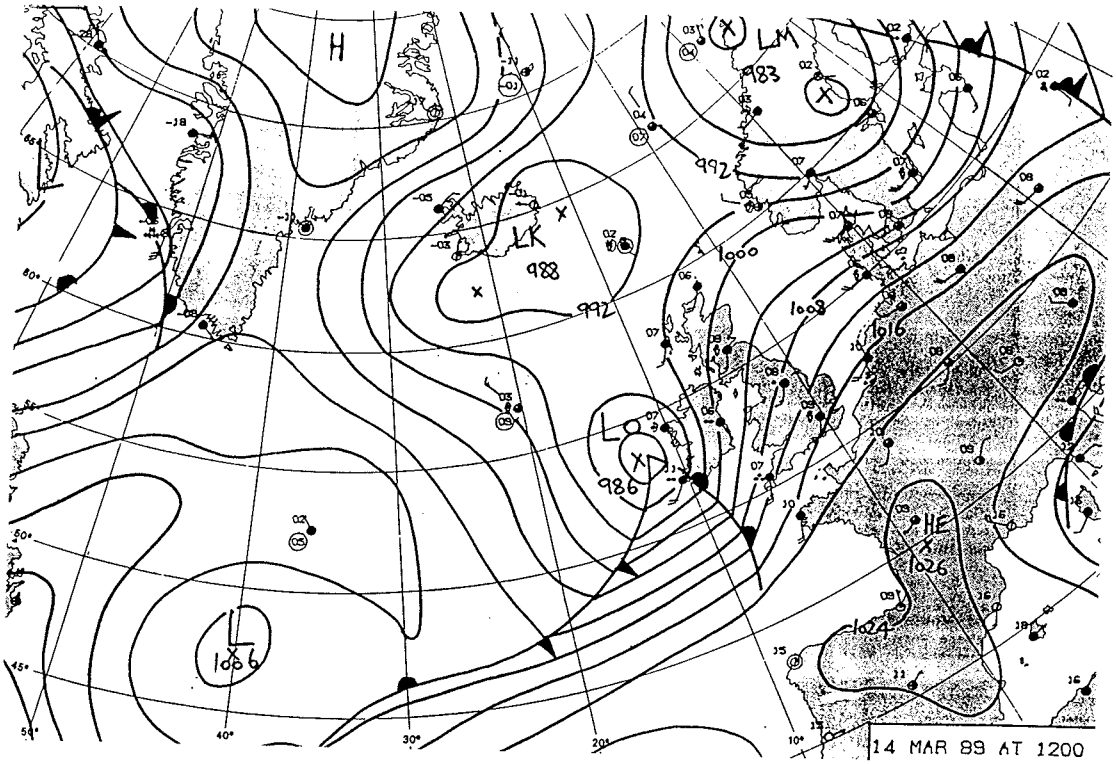

Figure II.1 Midday synoptic chart for each rainfall event

Event 31

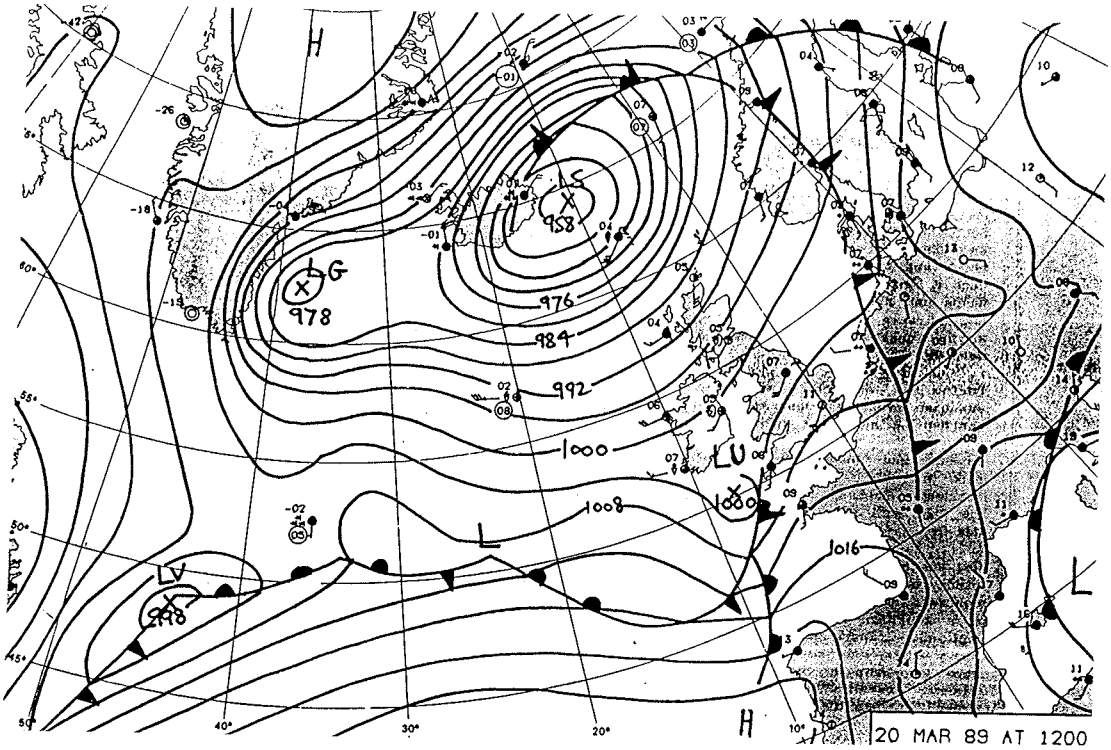

Event 32

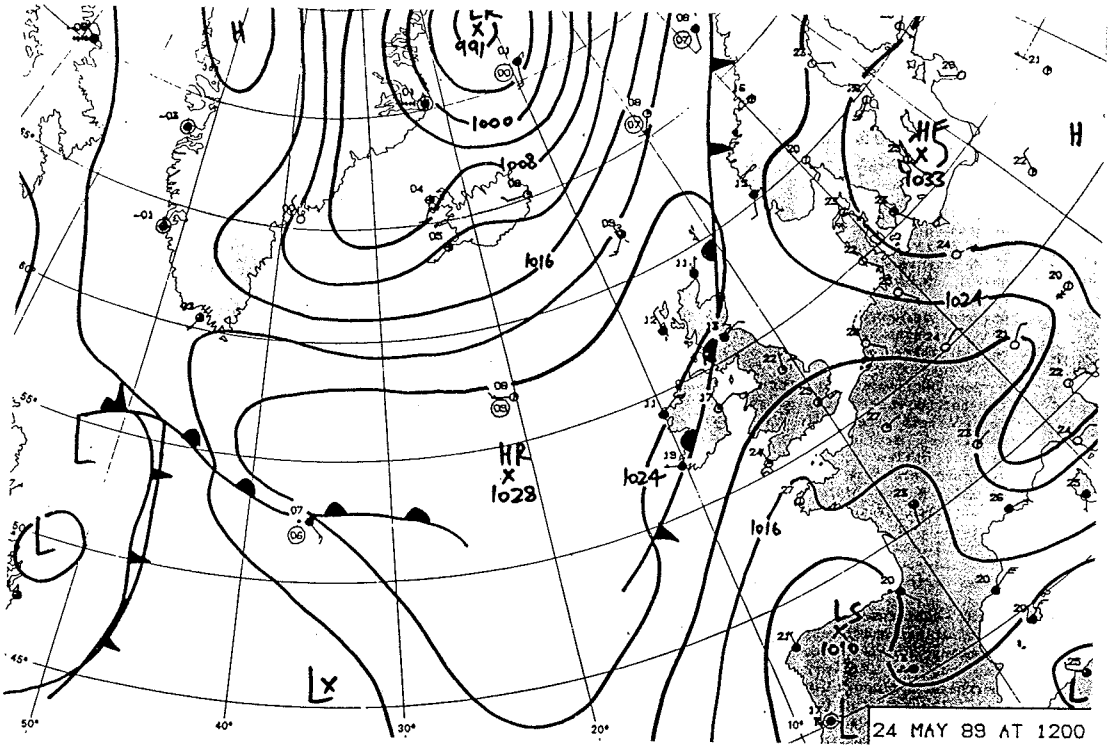

Figure II.1 Midday synoptic chart for each rainfall event

Appendix III: Review of Multiquadric Surface Fitting Techniques

III.1 INTRODUCTION

Multiquadric surface fitting has been used within the study for fitting surfaces both to calibration factors evaluated at raingauge sites and to the raingauge measurements of rainfall intensity. Several variations of the technique have been developed during the study and these are included in the following brief review of multiquadric surface fitting.

The general problem of surface fitting is to find a surface $s(\underline{x})$ which passes either exactly through, or close to, values z_i specified at N points, $\underline{x}_i$. In the present study the z_i represent the calibration factor values (or the raingauge measurements) and $\underline{x}_i = (u_i,v_i)$ the geographical locations of a set of N raingauges as expressed by their grid coordinates, u_i and v_i. Multiquadric surface fitting approaches this problem by forming the fitted surface function $s(\underline{x})$ as the sum of N functions each associated with, or centred about, one of the N locations: thus

$$s(\underline{x}) = \sum_{j=1}^{N} a_j \, g(\underline{x} - \underline{x}_j) + b \quad ,$$

where $a_1,...,a_N$ and b are parameters of the surface. The function g, the "basis function" or "distance function", also needs to be specified and a number of different types have been used within the study. Each function $g(\underline{x})$ is a function of the Euclidean measure of distance

$$d = ||\underline{x}|| = \sqrt{u^2 + v^2} \quad ,$$

or of the extended form $d = \sqrt{u^2 + v^2 + c^2} - c$, where c is a parameter. For example

cone: $g(\underline{x}) = d$

exponential: $g(\underline{x}) = \exp(-d/\ell)$

reciprocal: $g(\underline{x}) = 1/(1+d/\ell)$.

Here ℓ is an additional parameter, referred to as the scaling length. For those cases where the fitted function does not have to pass exactly through the surface fitting data, the basis function is modified to take the following values for zero distance

cone: $g(\underline{0}) = -K$

exponential: $g(\underline{0}) = 1+K$

reciprocal: $g(\underline{0}) = 1+K,$

where K is a further parameter, here referred to as the offset parameter. When this modification is used, the fitted surface formally has point discontinuities at each of the fitting points; however this problem is avoided by using the unmodified form of the basis function for surface evaluation.

For the surface fitting problem, the parameters c, ℓ and K are taken as given fixed values and it is then required to find appropriate values for the parameters $a_1,...,a_N$ and b. This is partly achieved from the set of equations resulting from imposing the condition that the fitted surface should take the values z_i at $\underline{x}_i$ for i = 1,...,N. The same equations are applied even when the final surface is not forced to go exactly through the fitting points since the offset parameter K is introduced in the above to allow this property. The equations are

$$s(\underline{x}_i) = \sum_{j=1}^{N} a_j \, g(\underline{x}_i - \underline{x}_j) + b = z_i \qquad (i = 1,...,N)$$

which when put into matrix form result in

$$\underline{G}\,\underline{a} + b\underline{1} = \underline{z} \ ,$$

where $\underline{G}$ is the (N × N) matrix with elements G_{ij} given by

$$G_{ij} = g(\underline{x}_i - \underline{x}_j) \qquad (i,j = 1,...,N) \ ,$$

$\underline{1}$ is the (N × 1) vector with unit elements and $\underline{z}$ is the vector of the "measurements" z_i (i = 1,...,N). This equation provides N constraints towards fixing the (N + 1) parameters.

III.2 FIXED VALUE AT LARGE DISTANCE TYPE

When the basis function is of the exponential or reciprocal distance type it is possible to force the fitting surface to take a given fixed value at large distances from the surface fitting points. This may be suitable for fitting a surface to rainfall intensity, when a zero value for large distances may be wanted, or for calibration factors, when zero or one may be appropriate depending on the calibration factor definition.

This approach relies on the basis function having a finite limiting value for large distances and, for both the exponential and reciprocal distance types, this limiting value is zero. Then, if b_0 is the required limiting value for the surface, this additional parameter constraint leads to $b = b_0$ and then $\underline{a}$ is given by

$$\underline{a} = \underline{G}^{-1}(\underline{z} - b_0\underline{1}).$$

The fitted surface is then completely defined.

III.3 FLATNESS AT LARGE DISTANCE TYPE

An alternative way of specifying the additional constraint necessary to define the surface fitting procedure is to impose the following requirement:

$$\underline{a}^T\underline{1} = 0.$$

This particular requirement arises in two contexts. The first of these considers the slope of the fitted surface at large distances from the fitting points and in the direction away from these points. It may be required that this slope should be zero so that the surface neither continually increases nor decreases for larger distances away from the data fitting points. When the basis function used is of the cone type, this zero-slope requirement is achieved with the above constraint. Note that the limiting surface value may well be different in different directions. For other types of basis function this constraint will in general lead to either the quickest approach to a constant value at large distances or to the least rapid increase or decrease.

A second context in which the constraint arises is for those cases where the offset parameter K is introduced. Here the fitted surface will not pass through the points z_i: the constraint

$$z_i = b + \sum_{j=1}^{N} a_j \, g(\underline{x}_i - \underline{x}_j)$$

will be satisfied for the modified function, including the offset parameter, but when the offset parameter is omitted in evaluation the surface value at $\underline{x}_i$ will be

$$z_i^* = b + \sum_{j \neq i} a_j \, g(\underline{x}_i - \underline{x}_j) + a_i\{g(\underline{0}) \pm K\}$$

where the sign depends on the particular distance basis function type. Thus

$$z_i - z_i^* = \mp K \, a_i$$

and the constraint $\underline{a}^T\underline{1} = 0$ will ensure that these "discrepancies" or "errors" will add up to zero.

If the constraint $\underline{a}^T\underline{1} = 0$ is imposed, the resulting parameters are given by

$$b = (\underline{1}^T\underline{G}^{-1}\underline{z})/\underline{1}^T\underline{G}^{-1}\underline{1}),$$

$$\underline{a} = \underline{G}^{-1}(\underline{z} - b\,\underline{1}).$$

III.4 ROUGHNESS MINIMISATION TYPE

A further way of supplying an additional constraint to complete the specification of the surface fitting procedure is to require that the quantity $\underline{a}^T\underline{a}$ should be minimised.

The above requirement may arise in two ways. Firstly, in the case where the offset modification is used so that the surface does not pass excactly through the fitting points: here, as seen in the previous section, the quantity $\underline{a}^T\underline{a}$ is directly equivalent to the sum of squares of the surface fitting "errors" and so provides a natural measure of closeness to the original data points. Secondly, where no offset parameter is introduced, the basis function $g(\underline{x})$ has, in all cases considered here, a discontinuity of slope at $\underline{x}=\underline{0}$: thus the fitted surface function will have N such discontinuities, the "size" of each being weighted by a_i for the point $\underline{x}_i$, and hence $\underline{a}^T\underline{a}$ provides a measure of the "roughness" of the surface although it measures only these slope-discontinuities.

If the quantity $\underline{a}^T\underline{a}$ is minimised, the resulting surface parameters are

$$b = (\underline{1}^T\underline{G}^{-1}\underline{G}^{-1}\underline{z})/(\underline{1}^T\underline{G}^{-1}\underline{G}^{-1}\underline{1})$$

$$\underline{a} = \underline{G}^{-1}(\underline{z} - b\underline{1}) \ .$$